GROUNDWATER MODEL OF THE UPPER GALLATIN AQUIFER AT BIG SKY, MONTANA

Kurt Zeiler, Mary Sutherland, and Ronald Breitmeyer
Ground Water Investigation Program

Front photo: Gallatin River looking north from the northern boundary of the Montana FWP Gallatin Wildlife Management Area, with outcrops of Paleozoic bedrock-forming ridges in the background on the right.
Photo by James Rose, MBMG.

GROUNDWATER MODEL OF THE UPPER GALLATIN AQUIFER AT BIG SKY, MONTANA

Kurt Zeiler, Mary Sutherland, and Ronald Breitmeyer

Montana Bureau of Mines and Geology Open-File Report 771

April 2025

https://doi.org/10.59691/FSFU2980

TABLE OF CONTENTS

Preface 1
Abstract 1
Introduction 2
  Background 2
  Objectives and Scope 3
  Project Area 3
    Area Description 3
    Climate 3
  Data Collection 3
  Data Management and Availability 6
Hydrogeological Framework 6
  Groundwater 6
  Surface Water 9
  Groundwater and Surface-Water Monitoring 9
  Conceptual Water Budget 9
    Recharge (MBR and R) 9
    SW_{in} and SW_{out} 10
    Septic effluent (Q_{se}) 11
    Alluvial Groundwater (GW_{in} and GW_{out}) 11
    Pumping Wells (PW) 12
    Evapotranspiration (ET) 12
    Springs (SPR) 15
Numerical Model Construction 15
  Model Approach 15
  Software Description 15
  Model Domain 15
  Spatial Discretization 16
  Hydraulic Parameters 16
  External Boundary Conditions 17
    Recharge (MBR and R) 17
    Alluvial Groundwater Flow (GW_{in} and GW_{out}) 17
  Internal Boundary Conditions—Sources and Sinks 17
    Surface-Water Net Gain and Loss (SW_{in} and SW_{out}) 17
    Septic Effluent Return (Q_{se}) 17
    Pumping Wells (PW) 17
    Riparian Evapotranspiration (ET) 17
    Drains (SPR) 17
Model Calibration 19
  Calibration Method 19
  Calibration Results 20
  Calibration Sensitivity Analysis 22
Simulated Water Budget 22
  Simulated Flow Zones 24
Model Evaluation 26
Current Conditions Flowpath Analyses 28
Model Scenarios 28
  Scenario 1: The Quarry Proposed Subdivision Septic System Effluent Discharge 28
  Scenario 2: Centralized Treatment Effluent Discharge Locations 32

Scenario 3: Potential Broad Additional Septic System Effluent Discharge Locations 32
Scenario 4: Reduced Future Recharge 32
Model Limitations and Recommendations 35
Conclusions 37
Acknowledgments 37
References 37
Appendix A: SWB Model/Recharge Methods 41
Appendix B: Model Groundwater-Level Calibration Information 53

FIGURES

Figure 1. The Upper Gallatin River Corridor GWIP study location map 2
Figure 2. Model area location 4
Figure 3. Subdivisions in model area 5
Figure 4. Precipitation and snow in area 6
Figure 5. Monitoring locations 7
Figure 6. Geologic setting 8
Figure 7. The mountain block recharge (MBR) catchment area 10
Figure 8. Interpolated raster elevation surface of the base of the UGA 13
Figure 9. Groundwater inflow (GW_{in}) and outflow (GW_{out}) cross sections 14
Figure 10. The model grid construction 16
Figure 11. MBR recharge to model perimeter 18
Figure 12. Groundwater flow model construction internal sources/sinks 19
Figure 13. Simulated hydraulic conductivity array 21
Figure 14. Observed vs. simulated groundwater levels 1:1 plot 22
Figure 15. Groundwater flow model water budget zones 24
Figure 16. Calibration hydrographs 26
Figure 17. The simulated potentiometric surface 27
Figure 18. The simulated UGA saturated thickness 29
Figure 19. Flowpaths simulated for existing community wastewater treatment systems 30
Figure 20. Flowpaths simulated for the proposed Quarry development 31
Figure 21. Flowpaths simulated for future centralized wastewater treatment effluent 33
Figure 22. Flowpaths simulated for locations over areas that could be hypothetically developed for residential use with additional septic systems 34
Figure 23. Simulated groundwater-level changes from long-term reduction of MBR 36

TABLES

Table 1. Measured flows and calculated gains/losses for the Gallatin River 11
Table 2. Calculation of estimated groundwater inflows to and outflows from the model domain 12
Table 3. Bulk calibration statistics for the groundwater-level targets 20
Table 4. Calibration sensitivity analysis results 23
Table 5. Conceptual vs. simulated water budget components 23
Table 6. Groundwater inflows and outflows to the model domain by water budget zone 25

PREFACE

The Ground Water Investigation Program (GWIP) at the Montana Bureau of Mines and Geology (MBMG) investigates areas prioritized by the Ground Water Assessment Steering Committee (MCA 2-15-1523). Prioritization is based on such factors as the current and anticipated growth of agriculture, industry, housing and commercial activity. Additional program information and project-ranking details are available on the MBMG GWIP website (https://mbmg.mtech.edu).

Products of the Upper Gallatin River Corridor GWIP project include:

- A groundwater-flow modeling report (this report) that presents details on model construction, groundwater flowpaths, and results of groundwater modeling scenarios for a subarea within the Upper Gallatin River Corridor study area.
- An interpretive report (Meredith and others, 2025) that presents the study scope, data and interpretations, and focuses on the hydrogeologic framework, surface-water budget, and water chemistry.
- An aquifer test report (Rose, 2022), which summarizes the results of aquifer tests performed in the study area.
- All data are available on the Ground Water Information Center database (MBMG, 2025).

ABSTRACT

The Montana Bureau of Mines and Geology Ground Water Investigation Program developed a MODFLOW-USG groundwater flow model for the alluvial Upper Gallatin Aquifer (UGA), near Big Sky, Montana. The model was designed to serve as a tool to evaluate the groundwater/surface-water interaction between the UGA and the Gallatin River and identify potential septic effluent flowpaths in the UGA. Two steady-state, snapshot model stress periods were developed to simulate flow in the UGA when groundwater levels are near their annual minima (September–October 2020) and when groundwater levels are high (May–June 2021), often associated with high-flow conditions in the Gallatin River.

The model results indicate that groundwater generally flows from south to north in the model domain and is directly interacting with the river. The model indicates the UGA relies primarily on recharge from the surrounding upland areas (mountain block recharge), and discharges primarily to the Gallatin River. Particle-tracking analyses show potential pathways of septic effluent through the UGA and potential areas of discharge to the Gallatin River, Michener Creek, and the spring ponds north of Michener Creek. The flowpath analyses may be a useful tool for future data collection or monitoring purposes. Additionally, the model and associated files are publicly available for use by others. Discussion of limitations and parameter/variable sensitivities are presented to assist in the future use of this model.

INTRODUCTION

Background

The Upper Gallatin River Corridor (UGRC) is located about 9 mi east of Big Sky Mountain Village and Big Sky Ski Resort and 2.5 mi east of Big Sky Meadow Village (fig. 1). Because of the Big Sky area's rapid growth, the Gallatin River Task Force nominated the UGRC, locally referred to as the canyon area, for a detailed hydrogeological investigation to be conducted by the Ground Water Investigation Program (GWIP). The investigation results are presented in two reports: Meredith and others (2025) describes the hydrogeologic framework and water quality of the alluvial Upper Gallatin Aquifer (UGA) and this report describes the development of a numerical flow model of the UGA.

The principal concern is the potential degradation of Gallatin River water quality associated with development. Over the past 5–10 yr, algal blooms in the Gallatin River within and downstream from the study area have occurred in late summer, suspected to be caused, at least in part, by septic effluent (and associated nutrients) loading to groundwater that flows to the river (Gardner and others, 2021).

Previous work analyzed potential septic effluent discharges to the Gallatin River as part of a broader investigation on the feasibility and necessity of centralized wastewater treatment in the UGRC (WGM, 2020). This work utilized available groundwater-elevation data and Geographic Information Systems (GIS) groundwater analysis tools to develop effluent flowpaths that could result from permitted septic systems in the area but did not identify flow through groundwater modeling.

The model described in this report was developed to evaluate the interaction between the UGA and the Gallatin River, and provides a more robust tool to evaluate the potential septic effluent flowpaths through the UGA. This report details model conceptualization, construction, operation, calibration, and sensitivity analysis of the alluvial groundwater model. Specifics on nutrient mass loading, dispersion, adsorption, transport time, and aquatic behavior of nutrients or algal growth are beyond the scope of this study. The information in this report provides the necessary foundation for modelers who may utilize and/or modify the model to address specific scenarios.

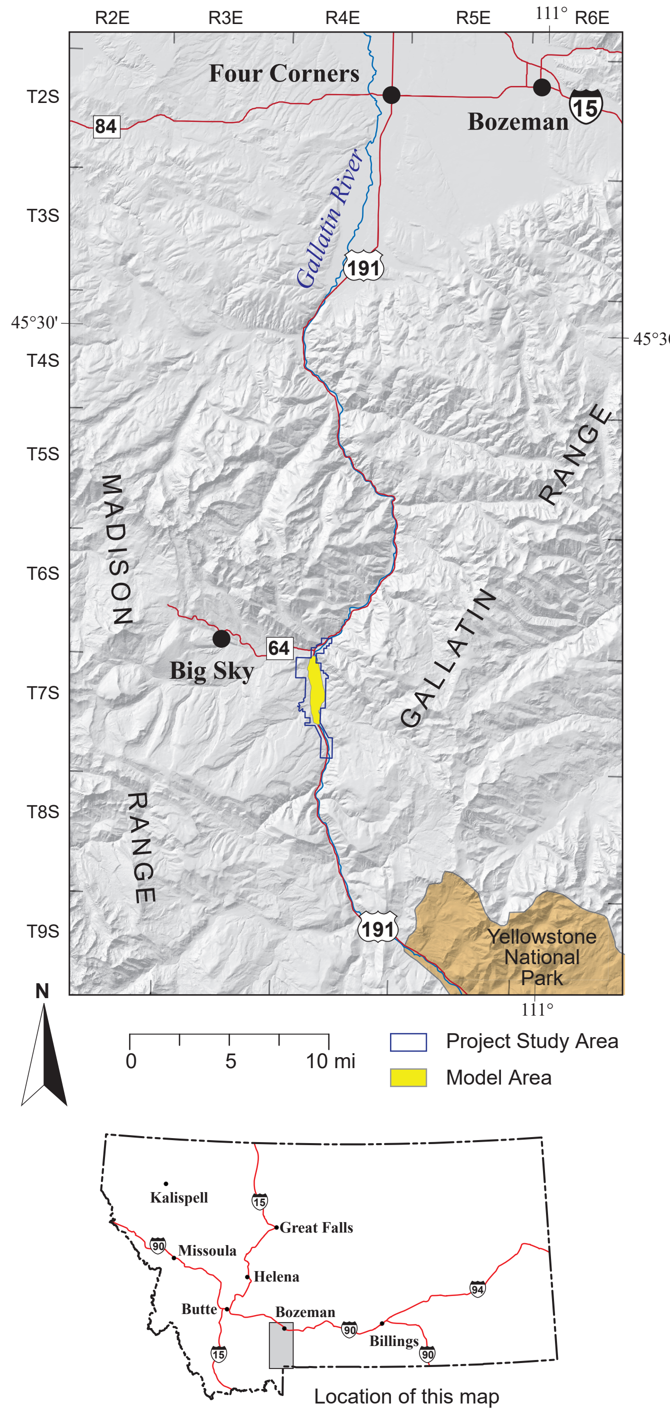

Figure 1. The Upper Gallatin River Corridor GWIP study is centered around the Gallatin River, about 9 mi east of Big Sky Mountain Village and Big Sky Ski Resort and 2.5 mi east of Big Sky Meadow Village.

Objectives and Scope

The UGA is hydrologically connected to the Gallatin River and contains septic leach fields that are potential nutrient sources to the Gallatin River.

The groundwater model was developed to:

1. Evaluate groundwater/surface-water interactions between the UGA and Gallatin River.
2. Evaluate groundwater flowpaths from current and proposed septic systems to the Gallatin River and tributaries.
3. Provide a tool to evaluate how different stresses and management scenarios may affect groundwater/surface-water interactions.

The model evaluates a low-stage period, which represents 61 days from September through October 2020, and a high-stage period, representing 61 days from May through June 2021. These stress periods were developed based on data collected from 2019 to 2021.

Project Area

The GWIP study area encompasses 5 mi^2 surrounding the Gallatin River; the modeled area covers approximately 2 mi^2 of the UGA within the study area (fig. 2). The modeled area is relatively flat. with elevation ranging from 6,000 to 6,200 ft. It is surrounded by high-relief tributary watersheds of the Madison Range to the west and the Gallatin Range to the east (fig. 1). The Gallatin River enters and exits the valley through narrow canyons of incised bedrock to the north and south, creating a wider, more developed floodplain, which is the focus of this report.

<u>Area Description</u>

The model area runs north–south, roughly parallel to Highway 191, and captures the developed and undeveloped portions of the UGRC (fig. 3). There are three tributaries to the Gallatin River within the model domain: Michener and Beaver Creeks on the west side, and Porcupine Creek on the east.

Within the model area, there are three existing and platted residential subdivisions with septic systems or individual septic tanks for each lot (fig. 3). These are the Ramshorn View Estates (referred to as Ramshorn), which includes 90 lots under 1 acre; Blackfoot Hills, which consists of 20 lots mostly over 1 acre; and San Marino, which has eight lots under 1 acre with seven acres of community space. Platted lots are not yet fully developed in all subdivisions. Big Sky Schools is a transient public water supply that accommodates approximately 450 people with a seasonal water demand. Currently, plans for the Quarry subdivision, located in the vicinity and overlying a gravel pit, are under review by Gallatin County and Montana Department of Environmental Quality (MDEQ; fig. 3). All of the existing subdivisions currently discharge wastewater effluent to the subsurface via leach-field systems (GCCHD, 2022).

<u>Climate</u>

The climate is typical of high-elevation alpine basins in southwest Montana, characterized by winter snowpack accumulation in the upper portions of watersheds, spring rains, and summer thunderstorms. Climate data used as input for the model were acquired from gridMET (Abatzoglou, 2013). The UGRC receives an average of approximately 21.6 in/yr of precipitation, primarily as winter snowfall, based on the 30-yr average of water years 1993–2022 (Abatzoglou, 2013).

Water years 2020 and 2021 (roughly the duration of this study) were compared to the 30-yr precipitation average. Precipitation over the study area during water year 2020 was 8 percent (1.7 in) below average at 19.9 in, and during water year 2021 was 16 percent (3.4 in) below average at 18.2 in (Abatzoglou, 2013; fig. 4). Snowpack water storage, characterized by the snow-water equivalent (SWE) from the Lone Mountain SNOTEL site, has a 30-yr (water years 1993–2022) median peak of 21.8 in and generally occurs in early May. In water year 2020, the peak SWE occurred 2–3 weeks earlier than average (mid-April), at 22.2 in. In water year 2021, the peak was 19.2 in, and occurred in late April. A rapid, early runoff and low precipitation in 2021 resulted in a drought year (NRCS, 2024).

Data Collection

Water levels were measured at 49 wells and stage/flow measurements were collected at 20 surface-water sites in the study area. Of these, a subset of 22 wells and 4 surface-water sites were utilized for the model calibration within the model area (fig. 5). All groundwater and most surface-water sites were professionally surveyed for both location and elevation. Details on

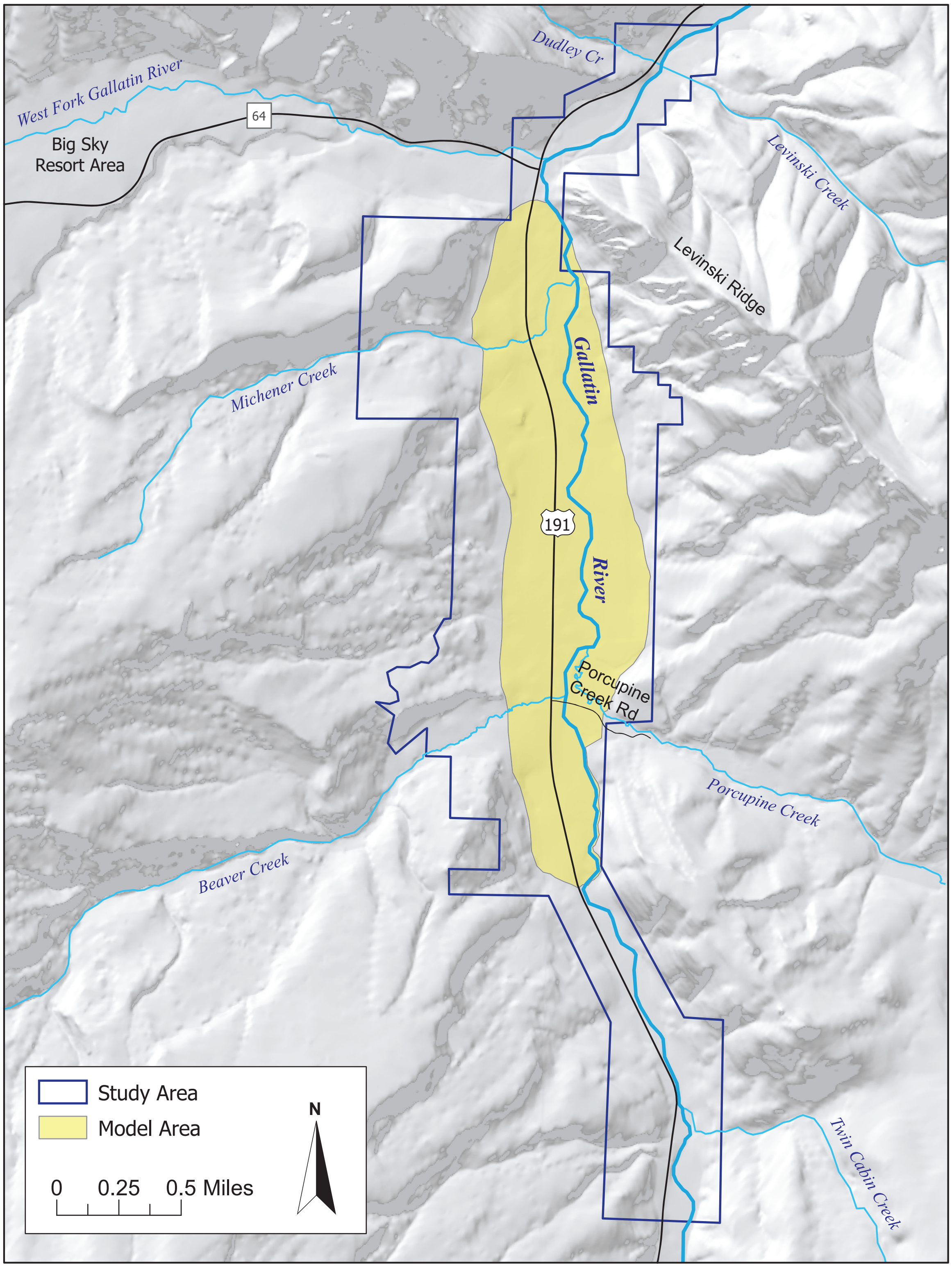

Figure 2. The model area is a subsection of the larger UGRC study area, primarily encompassing the floodplain of the Gallatin River surrounding Highway 191.

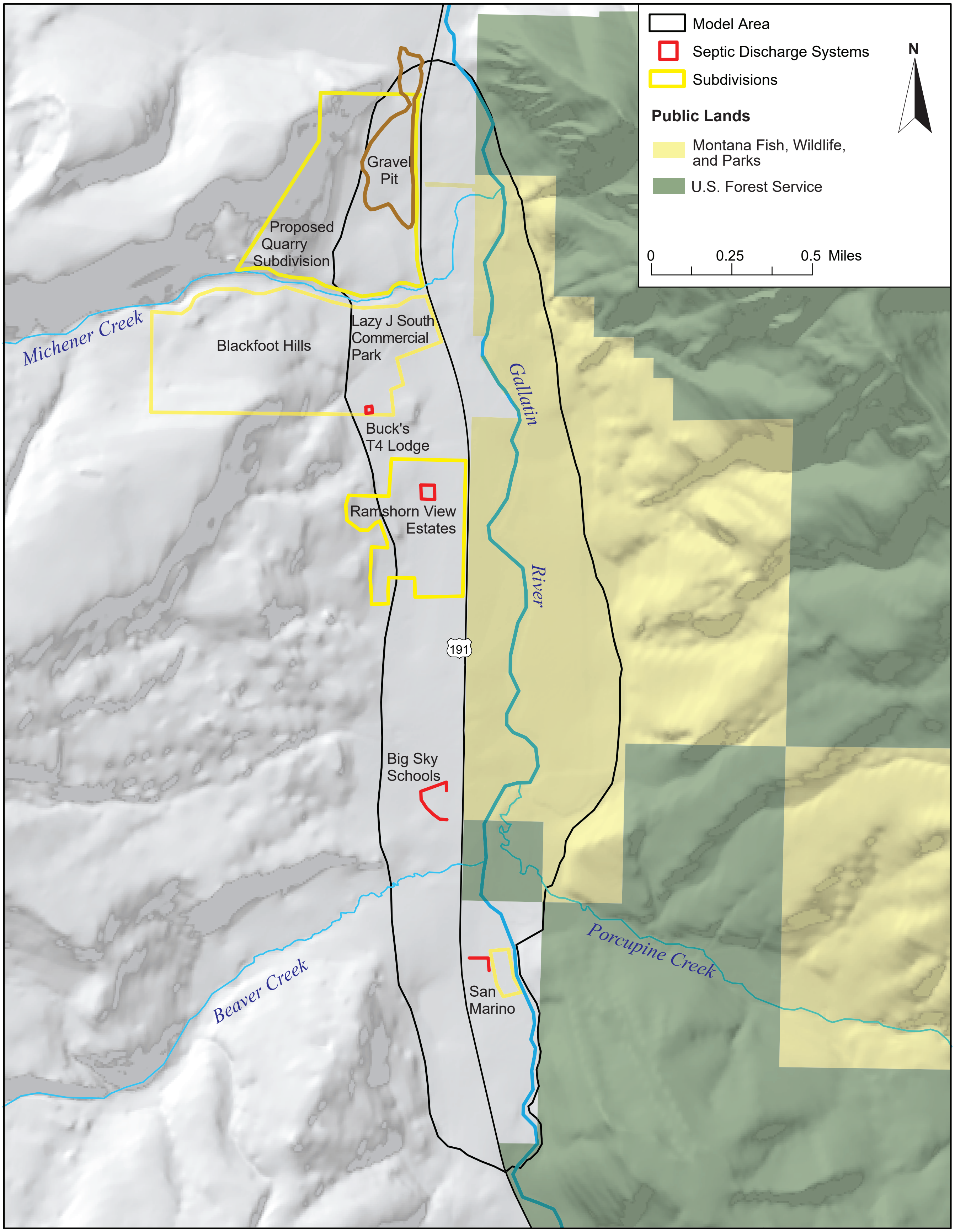

Figure 3. The model area is densely developed with subdivisions and a commercial district. All development is west of the river. East of the river is the Porcupine unit of the Gallatin Wildlife Management area.

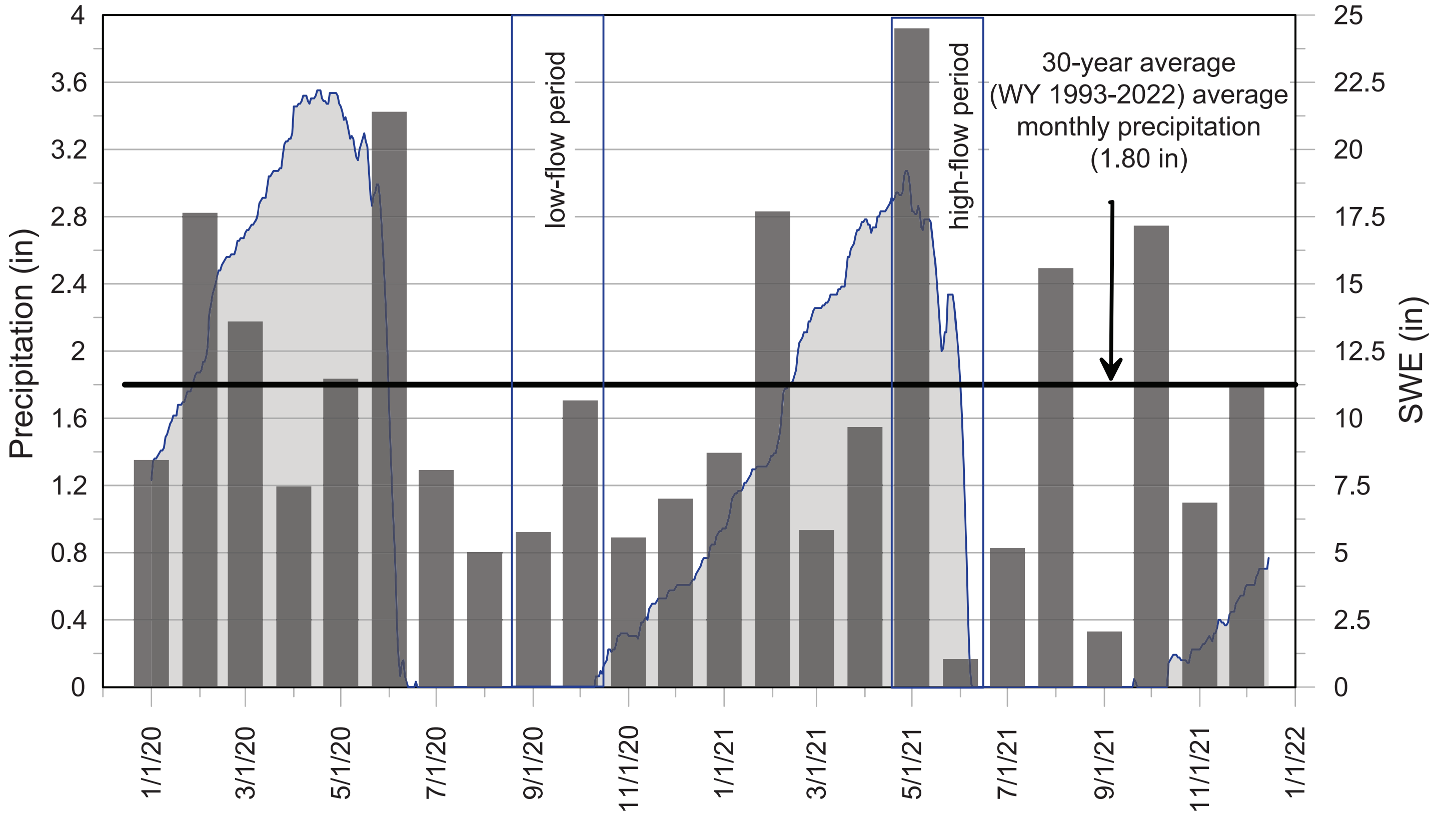

Figure 4. The low-flow period incorporated September 2020, with below-average precipitation, and October 2020, with near-average precipitation. The high-flow period includes May 2021, with above-average precipitation, and June 2021, with below-average precipitation. Water year 2020 SWE was above the 30-yr (water years 1993–2022) median of 21.8 in at the Lone Mountain SNOTEL site, while water year 2021 SWE was below the 30-yr median (NRCS, 2024). Monthly precipitation and cumulative SWE shown by the dark gray bars and blue line, respectively.

the groundwater and surface-water monitoring network are included in Meredith and others (2025). Data were collected in accordance with MBMG Standard Operating Procedures (Gotkowitz, 2023).

Data Management and Availability

Data collected for this investigation are archived in the MBMG Ground Water Information Center (GWIC) database (http://mbmggwic.mtech.edu/), and are also available on the Upper Gallatin project page within the GWIP section of the MBMG website (http://mbmg.mtech.edu/).

HYDROGEOLOGICAL FRAMEWORK

Groundwater

The unconfined UGA consists of alluvial deposits of sand, gravel, silt, clay, cobbles, and boulders incised within five different bedrock units composed of sandstone, shale, and limestone bedrock (fig. 6). The average thickness of alluvial aquifer material is approximately 35 ft, but ranges up to about 60 ft. The UGA is deepest and has the greatest saturated thickness in the central part of the valley and pinches out along the bedrock perimeter. Tributary stream valleys entering the Gallatin River valley represent higher energy depositional environments within the UGA alluvium, and as such likely include deposits of higher permeability materials. Additionally, mapped landslide and colluvial deposits as well as observed talus slopes are present at the margins of the valley and cover and may interfinger with alluvial deposits in the valley (fig. 6). The water table ranges up to 40 ft below ground surface. At the north end of the UGA, the water table is at or near the surface and a series of springs create several ponds and a marshy, riparian area.

Groundwater flows north, roughly parallel to the Gallatin River, and groundwater levels fluctuate 2–7 ft seasonally, with highest levels typically occurring in April/May from runoff and snowmelt (Meredith and others, 2025).

Results from two aquifer tests performed on the east side of the river indicate that UGA hydraulic conductivity (K) values range between 300 and 400 ft/d in this area (Rose, 2022). These are considered

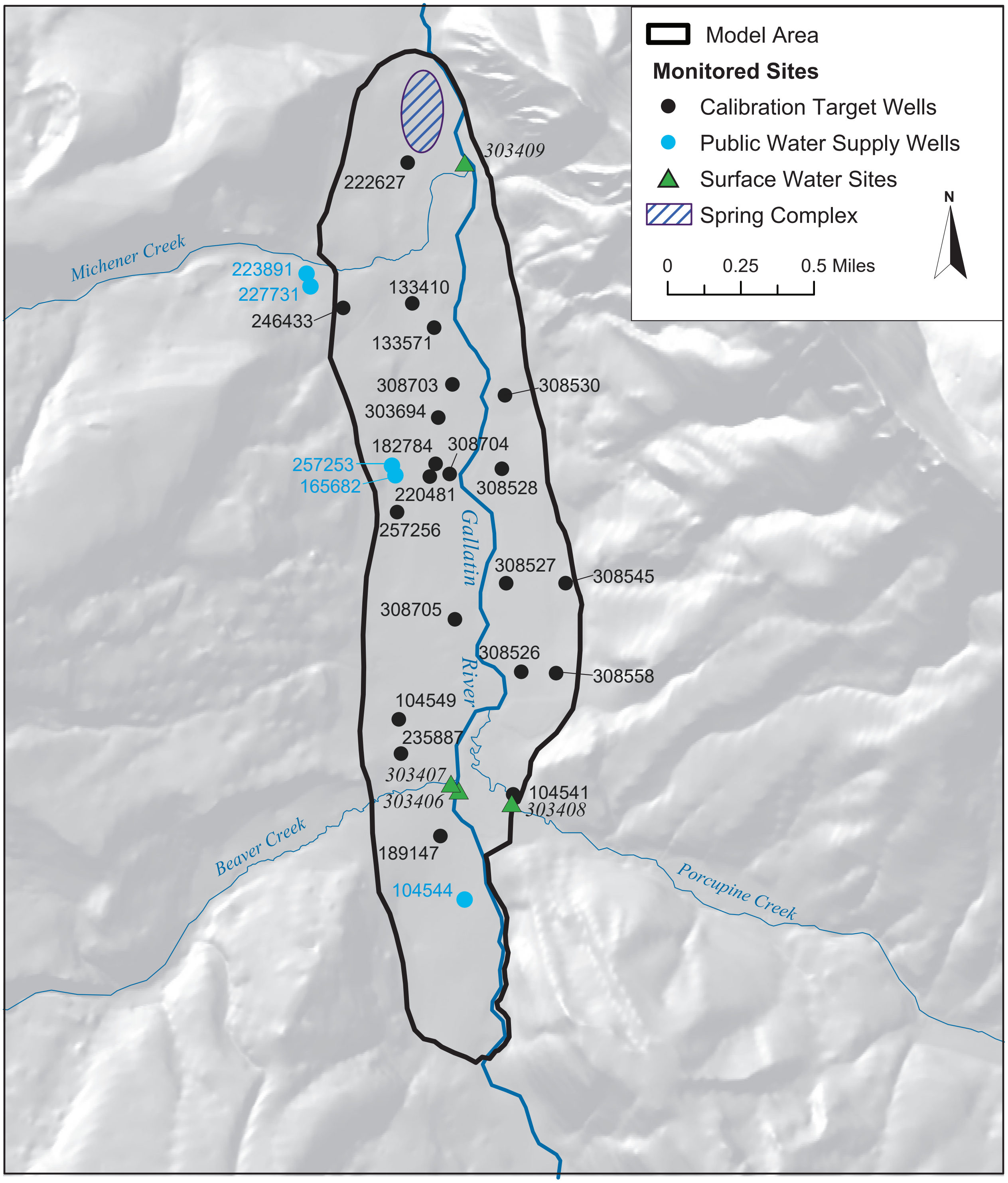

Figure 5. A total of 22 groundwater wells and 4 surface-water sites were included in calibration of the model. Also shown for reference are 5 bedrock public water supply (PWS) wells. Additional monitoring sites for the study area are included in Meredith and others (2025). East of the river is the Porcupine unit of the Gallatin Wildlife Management area.

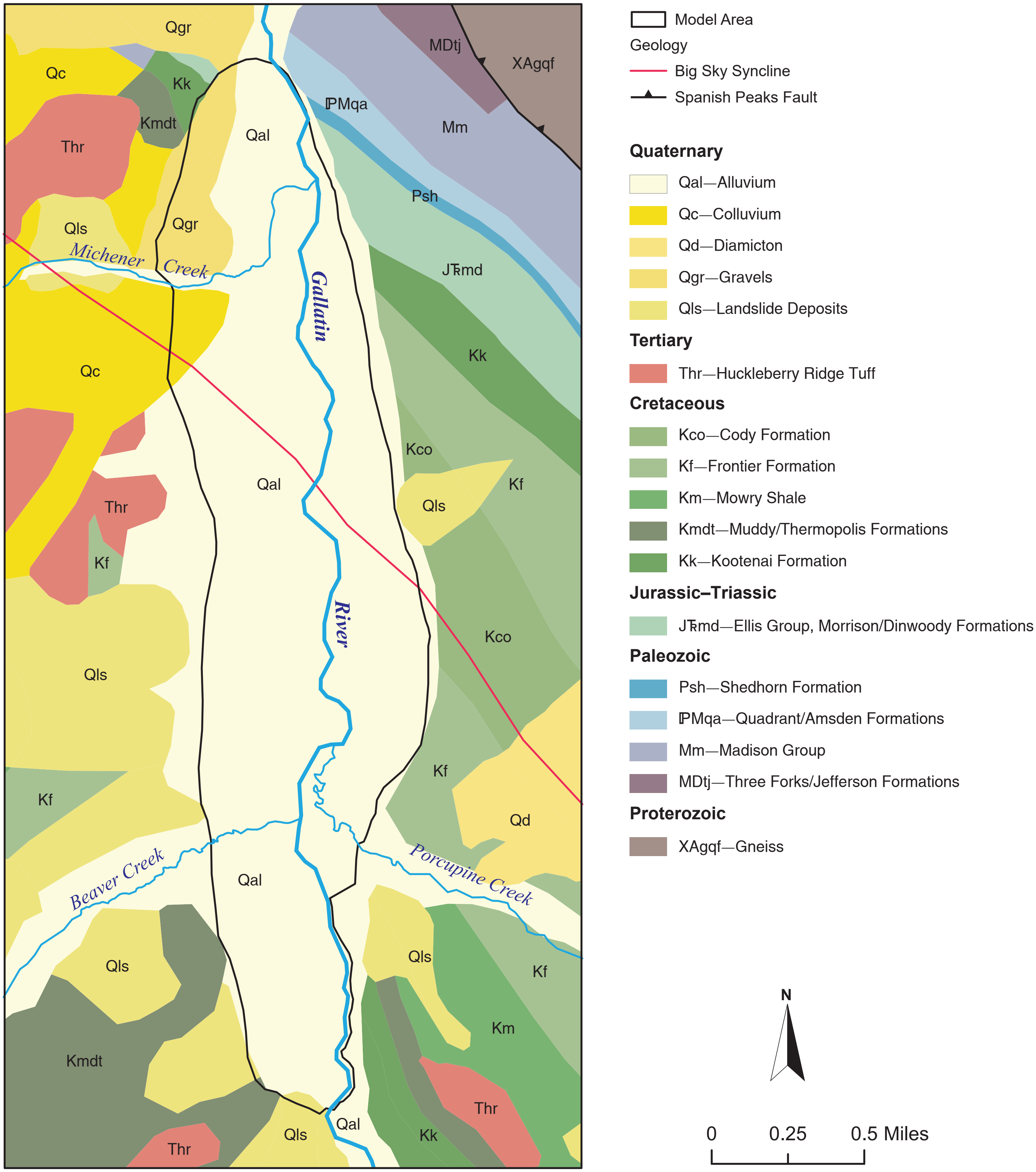

Figure 6. The model area roughly encompasses approximately 2 mi^2 of the alluvial aquifer and is bounded by impermeable bedrock of Cretaceous to Proterozoic age.

potentially low, as the discharge rates of the tests did not sufficiently stress the UGA.

Bedrock aquifers, beneath the alluvium, supply water to the Ramshorn and Blackfoot Hills subdivisions (fig. 5). Septic discharge from these subdivisions contributes minor flow to the UGA.

Surface Water

The north-flowing Gallatin River is hydrologically connected to the UGA (Meredith and others, 2025). Outside the floodplain, the tributary channels are composed of large gravel and cobbles except for Porcupine and Michener Creeks, which have sandy to muddy beds at the surface near the Gallatin River.

Surface-water stage and discharge increase rapidly in mid to late spring, in response to snowmelt and spring runoff. Flows typically peak in late May or early June depending on temperature and snowpack conditions. Flows range from less than 1 cfs in smaller tributaries to more than 3,610 cfs in the Gallatin River in 2020 (Meredith and others, 2025).

Groundwater and Surface-Water Monitoring

Stage and discharge measurements from four sites along the Gallatin River and its tributaries were used to inform the model (fig. 5); the sites were monitored from late summer 2019 through fall 2021. The surface-water measurements served two purposes: (1) to help define surface-water elevations, which the model used to simulate groundwater/surface-water interactions, and (2) to estimate stream gains/losses associated with groundwater/surface-water interactions. Rating curves were generated for Beaver Creek, Porcupine Creek, and the Gallatin River (Meredith and others, 2025).

Twenty-two wells were selected for use as model calibration targets (fig. 5). These wells were all equipped with pressure transducers to obtain hourly measurements and also measured manually at approximately monthly intervals.

Groundwater levels increase rapidly in mid to late spring, in response to snowmelt and spring runoff (Meredith and others, 2025). Flows typically peak in late May or early June, depending on temperature and snowpack conditions (Meredith and others, 2025).

Conceptual Water Budget

A conceptual water budget is grounded in the hydrologic cycle and can be represented by identifying where flow enters and leaves an aquifer. Assuming a steady-state condition, the inflows are balanced by outflows, and thus no long-term change in storage occurs. The water budget components for the UGA can be represented by the mass-balance equation below.

$$MBR + R + SW_{in} + Q_{se} + GW_{in} = SW_{out} + PW + ET + SPR + GW_{out},$$

where:

Inflows

MBR is mountain block recharge, R is areal recharge, SW_{in} is surface-water flow to groundwater, Q_{se} is inflow from septic effluent, and GW_{in} is alluvial groundwater into the model domain,

Outflows

SW_{out} is groundwater flow to surface water, PW is residential pumping wells, ET is evapotranspiration, GW_{out} is alluvial groundwater out of the model domain, and SPR is spring outflow.

The inflow and outflow components were estimated for each of the components for the low-stage period (September–October 2020), and the high-stage period (May–June 2021). Some of these flow estimates were used as input parameters for the groundwater flow model.

Recharge (MBR and R)

Mountain block recharge (MBR) refers to the movement of groundwater from a mountain block system to an adjacent lowland aquifer (Markovich and others, 2019). MBR in the study area initiates from the Gallatin Range to the east and the Madison Range to the west. Areal recharge (R, also known as diffuse recharge) is water that percolates through the unsaturated zone to the water table in response to precipitation infiltrating the soil surface (Healy, 2010). Areal recharge potentially occurs over the entire footprint of the groundwater flow model domain.

Groundwater recharge to the alluvium was estimated from the USGS Soil–Water Balance (SWB) model (Westenbroek and others, 2018), which includes both MBR from the surrounding mountain watersheds and R over the modeled area. The SWB model incorporates spatially and temporally variable datasets of climate, landscape/land-use properties, and soil properties to calculate estimates of net infiltration (i.e., potential recharge) spatially on a daily timestep using a Thornthwaite–Mather-based (Thornthwaite and Mather, 1957) water-balance approach.

The SWB model was applied over the watershed areas expected to contribute MBR to the model domain (fig. 7). The SWB net infiltration values were averaged over 2018–2023 to estimate MBR recharge at the perimeter cells, assuming MBR is relatively constant over time owing to relatively long flowpaths (up to miles) from the mountainous areas to the valley. For areal recharge (R), the SWB net infiltration values were averaged for the low-flow period (July through September 2020) and the high-flow period (March through May 2020). Additional details regarding the SWB model development and results are in appendix A.

Areal recharge (R) was calculated to be almost non-existent (0.00005 cfs) during the low-flow period when ET exceeds the precipitation rate. During the high flow period, areal recharge is larger, reaching up to 2.9 cfs.

SW_{in} and SW_{out}

Exchange between the alluvial aquifer and surface water was estimated for the Gallatin River for the low-flow period using four stream discharge measurements made in late August 2020. Gallatin River discharge near Porcupine Road Bridge (site 303406, fig. 5) was used to estimate flow at the upgradient end of the UGA for both stress periods. Measured discharge near the Wildlife Management Area (site 303409, fig. 5) was used to represent flow at the downgradient end of the UGA. Discharge measurements from Beaver Creek (303407) and Porcupine Creek (303408) were

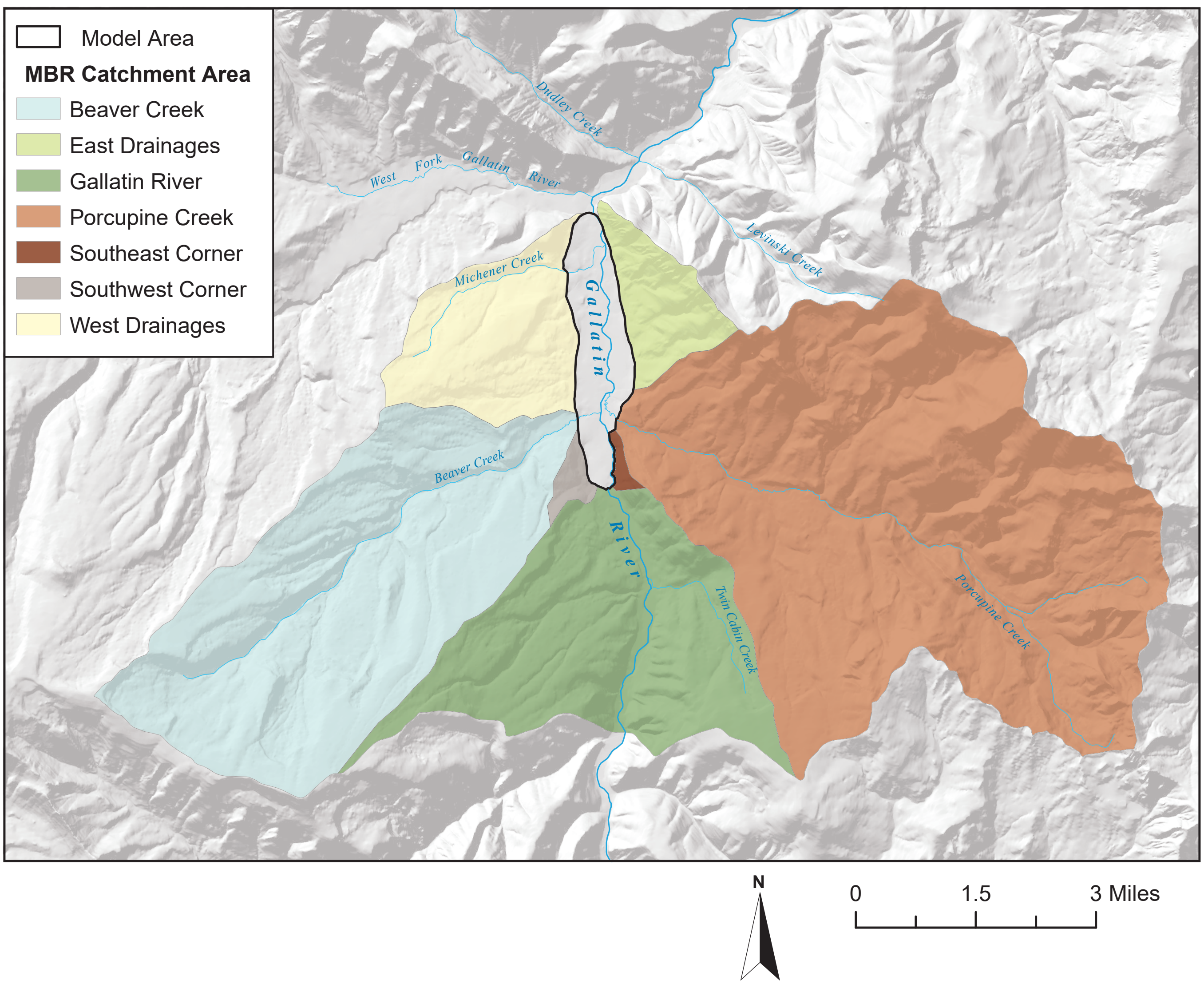

Figure 7. The mountain block recharge (MBR) catchment area for precipitation and SWE was broken into seven drainages that contributed groundwater inflow to the model area.

also accounted as upstream inflows (fig. 5). A 5 percent error in all tributary discharge measurements and a 3 percent error on Gallatin River flows was assumed (Sauer and Meyer, 1992). The measurement errors were used to calculate the root sum squared error (RSSE) that was applied to gain or loss estimates determined from individual discharge measurements.

Based on these discharge measurements, the Gallatin River gained an estimated 18.6 cfs ± 8.8 cfs between Porcupine Bridge (site 303406) and the Wildlife Management Area (site 303409; table 1).

High-stage flow measurements were less reliable due to poor channel constraints, flooding, and unsafe flow conditions. Due to these issues, synoptic stream discharge measurements at all four of these sites within the model domain were unable to be completed during the high-flow period. For these reasons, an estimate of the conceptual high-flow budget component was not calculated. Flow measurements indicated a gain between Gallatin River sites 303405 (Twin Cabins site upstream outside the model domain) and 303409 during the high-flow period; however, all other measurements fell within the margin of error, making gain-loss calculations unreliable (Meredith and others, 2025).

Synoptic flow measurements were made on Beaver Creek between sites 303416 (upstream outside the model domain) and 303407, indicating both stream gains and losses between these sites (fig. 5; Meredith and others, 2025). Synoptic flow measurements were unable to be made on Porcupine Creek due to difficult channel conditions, therefore there are no gain/loss estimates to the UGA.

Near the north end of the model domain, groundwater discharges to the surface, creating a series of spring ponds and a wetland/marsh area where the UGA thins against the underlying, low-permeability bedrock and creating an obvious surface-water gain that was not measured (spring complex shown in fig. 5).

Septic effluent (Q_{se})

Public water supply (PWS) wells draw water from the deep bedrock aquifers to supply residential subdivisions; some of this water is discharged to the UGA in the form of septic effluent. Septic discharge to the UGA was estimated for the Big Sky Schools and the San Marino, Ramshorn, and Blackfoot Hills Subdivision properties (fig. 3). Locations were based on information obtained from the Gallatin City–County Health District GIS resource website (GCCHD, 2022). PWS withdrawals were based on recorded flow data (J. Muscat, oral commun., March 8, 2021) and/or from the permitted capacity of the septic systems obtained from the Gallatin City–County Health District (GCCHD, 2022). Up to 95 percent of the pumped water is assumed to be returned as septic effluent (DNRC, 2011).

Septic discharge estimates to the UGA are:

Big Sky schools complex:	0.014 cfs
San Marino system: (GCCHD, 2022)	0.007 cfs
Ramshorn leach field system:	0.072 cfs
Blackfoot Hills Subdivision: (GCCHD, 2022)	0.028 cfs
For a total of:	**0.12 cfs**

This estimate is considered conservative, as it utilized the full permitted flow from the septic systems and does not account for non-occupancy or lower-use times of year that may occur in the area.

Alluvial Groundwater (GW_{in} and GW_{out})

Groundwater in (GW_{in}) and out (GW_{out}) is subsurface flow through the UGA underlying the Gallatin River at the south (in) and north (out) ends of model area.

Table 1. Table of measured flows and calculated gains/losses for the Gallatin River.

	Site ID	Flow (cfs)	Error (cfs)	Gains (+)/Loss (-)	RSSE
8/27/2020	303406	195	5.85		
8/26/2020	303407	1.7	0.08	18.6	8.8
8/26/2020	303408	5.8	0.29		
8/27/2020	303409	221	6.63		

Note. RSSE, root sum squared error.

The flows were calculated using the Darcy's Law flow calculation described as:

$$Q = -KiA,$$

where Q is groundwater flow rate (ft^3/d); K is hydraulic conductivity of the aquifer (ft/d); i is potentiometric head gradient (dimensionless); and A is cross-sectional area of the aquifer (ft^2). Final Q values were converted from units of ft^3/d to cfs.

Aquifer hydraulic conductivity (K) values were assumed to range from 100 to 700 ft/d. No wells with groundwater-level data are available near and both upgradient and downgradient of the north and south ends of the model domain (fig. 5). As such, the range of groundwater gradient (i) values was estimated from lidar data and surveyed elevations of the Gallatin River at the upstream and downstream ends of the model domain, with the assumption that alluvial groundwater is well connected to the river. These data produced an average gradient between 0.005 and 0.007, and these values were used for the low and high budget estimates, respectively. This range of gradients agrees with gradients apparent in the potentiometric surface map developed by Meredith and others (2025). A raster GIS dataset for the base of the aquifer was developed from drillers' logs. The cross-sectional areas of the UGA were estimated at the upstream and downstream ends of the aquifer by calculating the areas between the vertical profiles of the raster surface at each end and water-table elevations (figs. 8, 9). During the low-flow period, the calculated area for the upstream alluvium was 6,550 ft^2, and the downstream alluvial area was 18,500 ft^2. For the high-flow period, a 1 ft increase in water level was assumed, resulting in an upstream area of 7,140 ft^2 and a downstream area of 19,340 ft^2.

Applying Darcy's Law, the estimated low-flow upstream GW_{in} is between 0.04 and 0.37 cfs and the downstream GW_{out} is between 0.11 and 1.05 cfs (table 2). At high flow the estimated upstream GW_{in} is between 0.04 and 0.40 cfs, and GW_{out} is between 0.11 and 1.10 cfs.

Pumping Wells (PW)

Most water withdrawn from the UGA by domestic wells is returned through septic systems. Records from GWIC indicate that there are 55 domestic alluvial-aquifer wells in the model area. Similar to the PWS wells, up to 95 percent of pumped water is assumed to be returned as septic effluent (DNRC, 2011).

Evapotranspiration (ET)

Evapotranspiration (ET) was calculated for riparian areas using OpenET (Melton and others, 2021). These areas include the floodplain and marsh areas where groundwater is shallow or at the surface. Vegetation in the riparian areas includes grasses and willows in the southern part of the model area.

The riparian areas overlying the UGA were interpreted from aerial photography to include approximately 400 acres along the Gallatin River, Porcupine Creek, and Beaver Creek and surrounding the wetland marsh areas at the north end of the study area.

Table 2. Calculation of estimated groundwater inflows to and outflows from the model domain.

Low-Flow Model—GW_{in} (Upstream)			Low-Flow Model—GW_{out} (Downstream)		
	Low Estimate	High Estimate		Low Estimate	High Estimate
i	-0.005	-0.007	i	-0.005	-0.007
A (ft^2)	6,550	6,550	A (ft^2)	18,500	18,500
K (ft/d)	100	700	K (ft/d)	100	700
Q (cfs)	0.04	0.37	Q (cfs)	0.11	1.05

High Flow Model—GW_{in} (Upstream)			High Flow Model—GW_{out} (Downstream)		
	Low Estimate	High Estimate		Low Estimate	High Estimate
i	-0.005	-0.007	i	-0.005	-0.007
A (ft^2)	7,140	7,140	A (ft^2)	19,340	19,340
K (ft/d)	100	700	K (ft/d)	100	700
Q (cfs)	0.04	0.40	Q (cfs)	0.11	1.10

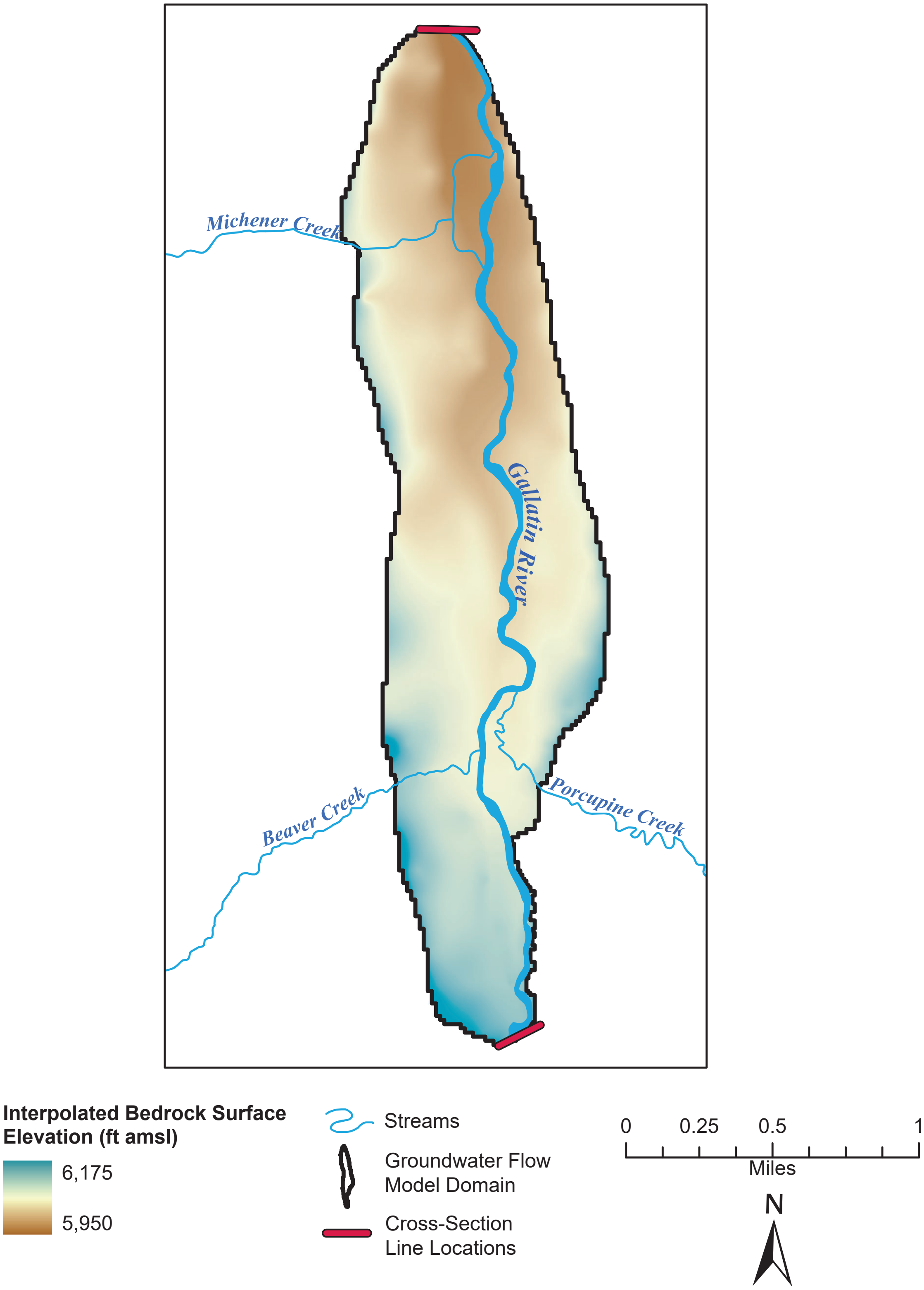

Figure 8. Interpolated raster elevation surface of the base of the UGA. The elevation of the bedrock surface becomes shallower to the north of the model area.

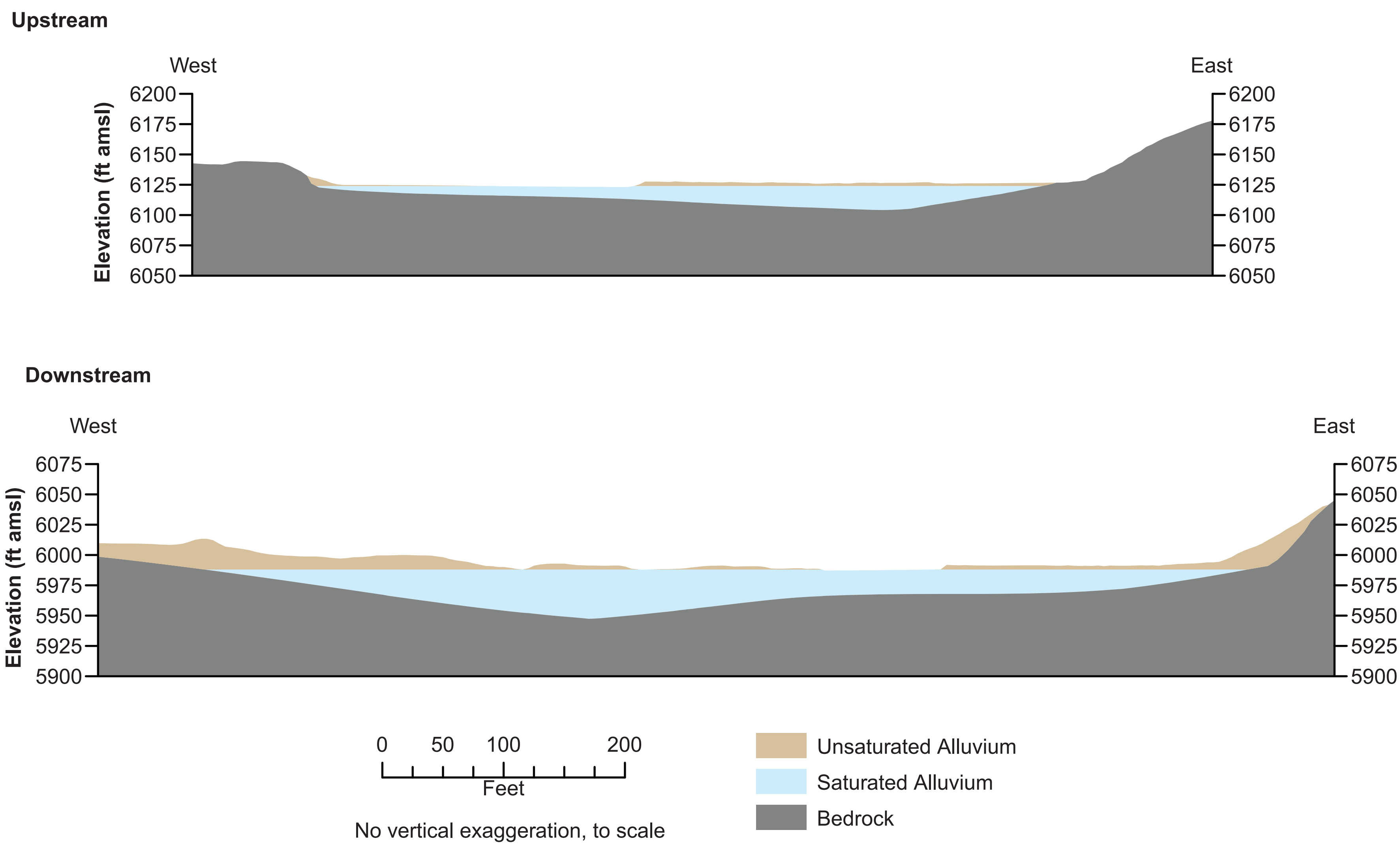

Figure 9. Groundwater inflow (GW_{in}) and outflow (GW_{out}) were calculated by the cross section of alluvial area between the groundwater surface and the bedrock base of the aquifer at the inflow and outflow of the Gallatin River. Cross sections are drawn to scale.

OpenET aggregates the average of six ET models (Melton and others, 2021) to estimate actual ET. Actual ET in excess of precipitation is assumed to be sourced from soil zone and shallow groundwater. The precipitation (from gridMET, Abatzoglou, 2013) was subtracted from ET (from OpenET) over the 400-acre riparian area to estimate ET losses. The results indicate that an average 0.6 cfs is lost from the soil and shallow groundwater for the low-flow period and 1.1 cfs for the high-flow period. These values are used as the upper limit for ET in the conceptual water budget as they include ET from the soil zone and shallow groundwater.

Springs (SPR)

Springs discharge from the UGA into ponds and marshy areas at the north end of the model domain. The diffuse, non-channelized nature of the springs and marshes made measurements impossible. Therefore, the model was used to estimate flows based on groundwater and surface-water stages.

NUMERICAL MODEL CONSTRUCTION

Model Approach

Two steady-state stress periods were modeled to evaluate low- and high-flow regimes. The model attempts to replicate low-flow conditions in September through October 2020, and high-flow conditions in May through June 2021. Anderson and others (2015) describe this approach as a bounding successive steady-state method, in this case where the solutions for two steady-states representing the end range of conditions of low and high flow are executed successively.

The steady-state simulations used average flow rates and water-level elevations for each boundary condition, calculated as daily rates through the period of the flow regime. Low- and high-flow conditions were simulated by adjusting the head stage of the river and tributaries in the model. The numerical model was then used to simulate potential flowpaths to determine locations of groundwater discharge to surface water.

Software Description

An unstructured model grid was initially developed using Groundwater Modeling Software (GMS, version 10.4.5; Aquaveo, 2019) to be utilized with the U.S. Geological Survey (USGS) MODFLOW-USG code, version 1.5 (Panday and others, 2019). The model was refined with Groundwater Vistas version 8 [Environmental Simulations, Inc. (ESI), 2020] as a graphical user interface. Groundwater Vistas facilitates using maps, aerial images, and GIS products for groundwater modeling. Highly Parallelized Parameter Estimation Software (PEST_HP) version 18.25 was used for automated model calibration (Watermark Numerical Computing, 2024). In addition to the MODFLOW groundwater model, associated particle tracking-based flowpath analyses were conducted using mod-PATH3DU version 2.1.8 (S.S. Papadopulos and Assoc. Inc., 2024; Craig and others, 2019) to track flowpaths in the UGA from septic tank leach fields.

Model Domain

The model domain was defined by approximating the alluvial valley fill (Qal, fig. 6). This results in the eastern and western edges of the model domain occurring at or near the break in slope forming the valley floor. At the south end, the model domain extends to a pinch-point in the Gallatin River, where the river enters the model area through a narrow bedrock canyon comprised of Kootenai (Kk), Muddy, and Thermopolis Formations (Kmdt; fig. 6) and the UGA is thin (<10 ft). At the north end, the model boundary approximates where the UGA shallows against nearly vertically dipping outcrops of the Quadrant and Amsden Formations (ⱣMqa), Madison Group (Mm), and Three Forks and Jefferson Formations (MDtj; fig. 6).

The UGA is represented as a single-layer, two-dimensional model with varying elevations for the top and bottom of each individual model cell. The upper surface of the model is defined by the average elevation for each model grid cell from lidar data collected for the USGS (NV5 Geospatial, 2021, 2024). The bottom surface of the model is defined by the average elevation of each model grid cell from the raster dataset of the bottom of the alluvium (fig. 8).

Spatial Discretization

MODFLOW-USG's unstructured grid capability provided flexibility in grid spacing refinement, which focused the resolution of cells around surface water. The grid has a total of 17,995 cells that are approximately square in map or plan view (fig. 10). Unrefined cells had an initial target size of 100 ft on each side. The grid dimensions were adjusted to fit the geometry of the model domain and any polygon or line features defining items such as rivers and model domain boundaries. The resulting grid for the UGA has an unrefined cell size of approximately 74 ft. Refined cells in the Gallatin River are approximately 40 ft and refined cells in the tributary stream areas are 9.3 ft. The single-layer grid has a variable cell thickness ranging between 1 and 78 ft, reflective of unconsolidated deposits that constitute the UGA. No cells were permitted to have a thickness of less than 1 ft to prevent numerical instability.

The model uses North American Datum 1983 coordinates with a Montana State Plane projection in international feet. The vertical datum is NAVD88. Grid rotation was not required since flow is estimated to be predominantly in the south-to-north direction, conforming to the accepted model grid orientation (Anderson and others, 2015).

Hydraulic Parameters

Four areas, or zones, with different hydraulic conductivity were initially delineated based on different hydrogeologic conditions within the model domain. The first zone is the alluvium in the valley/floodplain. The second is a wedge of colluvium deposited within the alluvium expected to have lower K values (fig. 6). The third and fourth zones are areas expected to have higher permeability materials, including coarser alluvial deposits from the Porcupine and Beaver Creek drainages. Prior to model calibration with PEST_HP, each zone was assigned an initial K value based on preliminary manual model calibration testing and literature values for the observed geological materials (Fetter, 2010). An initial K value of 300 ft/d was applied to the alluvium with an allowable range of 0.3 to 800 ft/d. The colluvium was assigned an initial K value of 30 ft/d with an allowable range of 0.3 to 300 ft/d. The coarser Porcupine and Beaver Creek deposits were assigned an initial K value of 1,000 ft/d with an allowable range of 0.3 to 2,500 ft/d, and the east valley margin was assigned an initial K value of 800 ft/d with

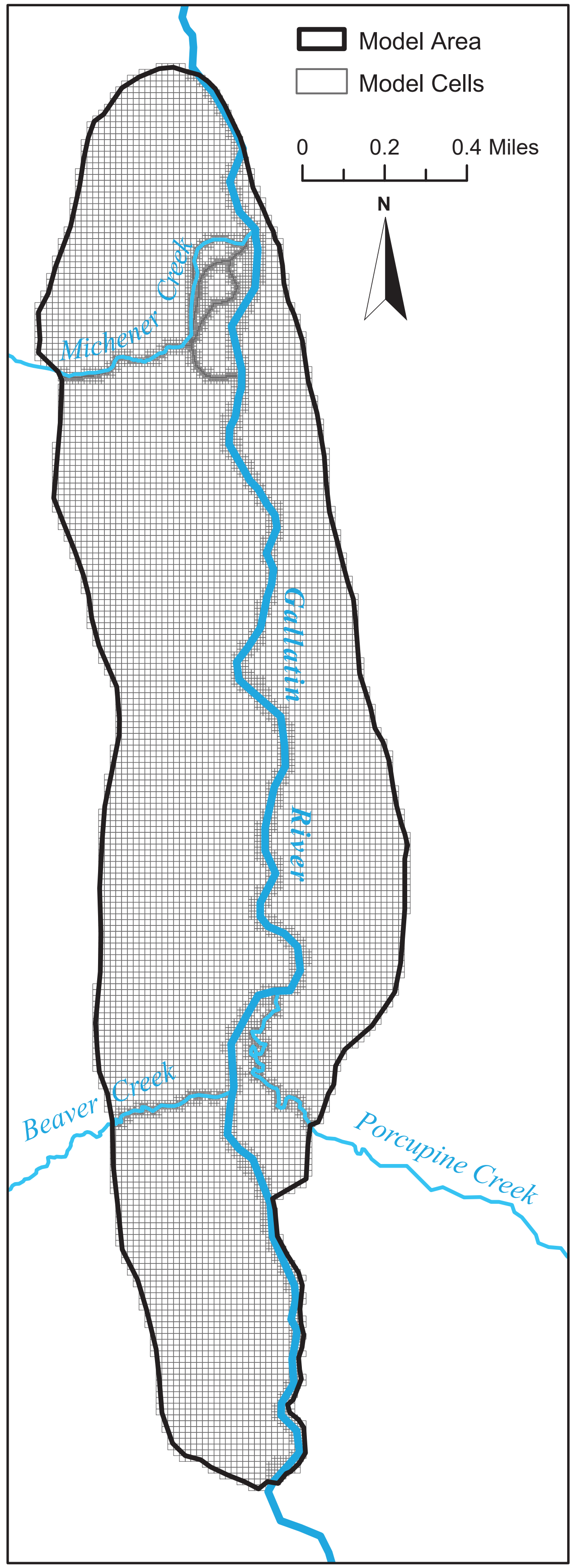

Figure 10. The model grid construction consisted of finer cells around surface water in order to better represent the groundwater/surface-water interaction.

an allowable range of 0.3 to 2,500 ft/d. Note that the wide range of values for these zones was chosen to allow the parameter estimation process a wider latitude. PEST_HP then optimized the K values for each zone to the calibration targets, as described in the calibration section below. Because the model is steady-state, aquifer storage parameters such as specific yield and specific storage are not necessary as inputs.

External Boundary Conditions

Recharge (MBR and R)

The east and west perimeters of the model were designated as recharge boundaries to represent inflow from MBR using the RCH package. A value of 17.3 cfs was assigned for MBR recharge during both the low- and high-flow periods, assuming MBR is relatively constant over time. This falls within the conceptual range of inflow from snowmelt and precipitation to potential recharge in the MBR catchment areas (fig. 7). These inflows are calculated in the water budget through MBR accumulated in the catchment area outside the model and inflowing to the valley floor. The RCH package was also used to apply recharge from precipitation (R) to the model domain surface area. Areal recharge (R) during the low-flow stress period was minimal, with only 0.00005 cfs simulated as reaching the UGA; for the high-flow period R was much higher, 1.4 cfs, corresponding to the period of maximum snowmelt and precipitation.

Alluvial Groundwater Flow (GW_{in} and GW_{out})

General head boundaries (GHB Package) to the north and south (fig. 11) were used to approximate the alluvial inflow and outflow. Flows across these boundaries are calculated in the water budget as GW_{in} and GW_{out}.

Internal Boundary Conditions—Sources and Sinks

Sources and sinks are shown in figure 12 and details of the simulated flows are described below.

Surface-Water Net Gain and Loss (SW_{in} and SW_{out})

Aquifer gains and losses from surface water were simulated using the MODFLOW RIV Package. The RIV Package represents a head-dependent boundary condition that compares the model-computed groundwater level in a RIV cell to the user-input value of surface-water stage for the cell. The model computes flow between the UGA and the river using the conductance value and the difference in the surface-water stage and simulated groundwater level. The cell conductance is a user-estimated term incorporating the streambed hydraulic conductivity, thickness, and area within the model cell. If the computed groundwater level exceeds the surface-water stage, groundwater discharges to surface water. If the computed groundwater level is below the surface-water stage, surface water is lost to the UGA. Input stage values for the RIV Package model cells were developed by averaging the land-surface elevation from the lidar datasets (NV5 Geospatial, 2021, 2024).

Septic Effluent Return (Q_{se})

Inflows from the septic effluent were modeled using the MODFLOW WEL package to inject water at the location of the septic leach fields. A total of 0.12 cfs was applied to the model as septic return flows sourced from the bedrock aquifers.

Pumping Wells (PW)

Domestic and PWS withdrawals accounted for less than 0.3 percent of the overall conceptual water budget; this estimated value is likely a conservatively high amount due to the seasonal nature of water demand. Groundwater withdrawals are not expected to alter the model for two reasons: (1) the alluvial wells are low flow, serving only a single residence for an unknown portion of the year with an uncertain flow rate, and (2) the consumed volume is minimal compared to the amount of groundwater flowing through the model area. Therefore, the pumping well component of the water budget is assumed to be a net zero inflow or outflow with respect to groundwater flow and volume and was not included in the numerical model.

Riparian Evapotranspiration (ET)

Riparian uptake was simulated with the MODFLOW EVT Package. The ET surface in the package was set by the lidar-based DEM surface elevation (NV5 Geospatial, 2021, 2024) with a 3-ft extinction to replicate the rooting depth of the riparian grasses and applied to 400 acres near surface water (fig. 12).

Drains (SPR)

Michener Creek and the marshy areas surrounding the springs at the north end of the model were represented with the MODFLOW Drain (DRN) Package. The DRN Package is similar to the RIV cells in that it represents a head-dependent boundary condition, but

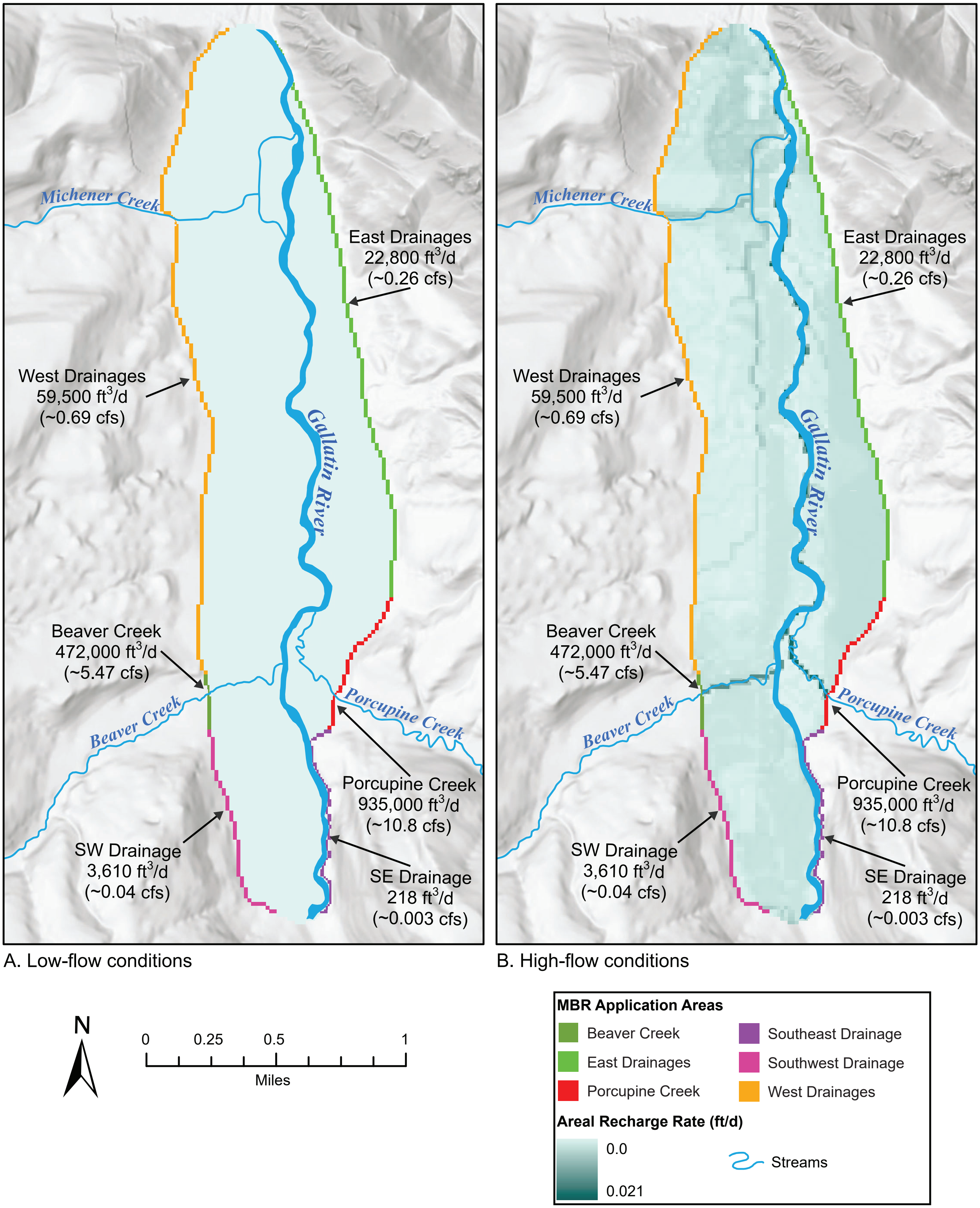

Figure 11. Recharge inputs for both mountain block recharge (MBR) and areal recharge for low- (A) and high-flow (B) conditions.

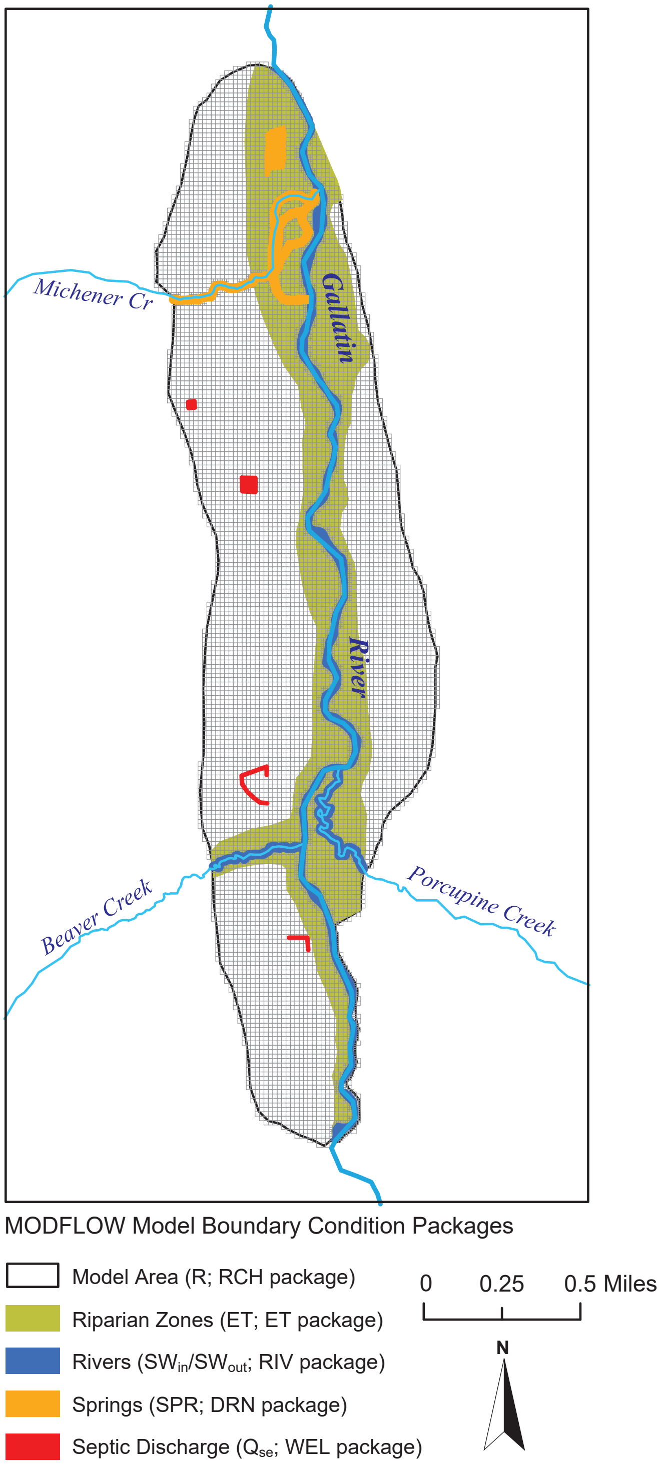

Figure 12. Groundwater flow model construction of internal model boundary conditions that introduce or remove water from the aquifer.

one that only allows flow out of the UGA to surface water. Input stage values for the DRN Package cells were developed by averaging the land-surface elevation from the lidar datasets (NV5 Geospatial, 2021, 2024).

MODEL CALIBRATION

Groundwater model calibration is most commonly performed through "history matching," in which model input parameters are adjusted to produce outputs that match actual field measurements (Anderson and others, 2015). Model calibration is a necessary step to ensure the groundwater system is properly characterized.

Calibration Method

The model was calibrated using PEST_HP, an inverse modeling or parameter estimation tool (Watermark Numerical Computing, 2024). PEST_HP varies the model input parameters with the goal of matching model-simulated values to real-world observed or estimated values. A calibration "residual" is the difference in the simulated value from the observed/estimated target value, calculated as the observed value minus the simulated value, such that a positive residual value indicates the simulated value is too low and a negative residual value indicates the simulated value is too high. Weights are applied to the residuals for each target, with the values of each weight designed to reflect measurement error/uncertainty, the relative importance of matching a target to the overall modeling purpose, or attempting to balance the error contributions of different measurement types with different measurement units, or some combination of these reasons (Anderson and others, 2015). PEST_HP successively adjusts model input parameter values and calculates the model goodness of fit for each parameter change using the sum of squared errors of the weighted calibration residual values.

To calibrate this model, PEST_HP varied K values within the expected geologic constraints until the model replicated observed groundwater-level calibration targets. The net streamflow gain to the Gallatin River from the UGA was also used to optimize calibration during the low-flow stress period, using the estimated streamflow gain of 18.6 cfs ± 8.8 cfs between Porcupine Bridge (site 303406, fig 5) and the Wildlife Management Area (site 303409, fig. 5). The goals of the calibration exercise were to have the root mean squared error (RMSE) of the groundwater-level target residuals be 5 percent or less of the overall range of the target observed groundwater levels (i.e., a scaled groundwater-level RMSE error of less than 5 percent), and to have the simulated streamflow gain value be within the estimated error of 8.8 cfs.

Average groundwater levels at 22 observation wells during the low- and high-flow periods were used as calibration targets for both stress periods, resulting in 44 total groundwater-level targets. Groundwater-level calibration targets were weighted equally for each well to prevent location bias toward individual wells. The streamflow-gain target was weighted differently because the MODFLOW model simulated flow in units of cubic feet per day (ft^3/d), which is numerically much larger than the groundwater levels in units of feet. For example, the estimated 8.8 cfs error in the streamflow gain is 760,320 ft^3/d. As such, the streamflow gain target was weighted in PEST_HP to make a 760,320 ft^3/d residual equivalent to a 2-ft residual at a groundwater-level target.

Calibration Results

Initial hydraulic conductivity values were assigned in PEST_HP at 432 randomly positioned points in the model, and interpolation between those points created a calibrated K-value array across the model domain (fig. 13). This array presents a probabilistic representation of the UGA permeability distribution that reflects the best match of simulated to estimated heads at calibration targets without overfitting.

Hydraulic conductivity estimates calibrated with PEST_HP ranged from 10.8 ft/d to 2,500 ft/d; the lower K values correspond to the colluvium (K zone 2), which is consistent with published ranges of K values for the material types found in the UGA (Fetter, 2010; Domenico and Schwartz, 1990). The range of values is considered reasonable given the variability in alluvial deposits (Boggs, 2001; Fetter, 2010).

Analysis of how well a model simulates observed conditions is based partially on statistics related to model residuals (the difference between simulated and observed groundwater levels). Standard calibration statistics include the average residual, absolute average residual, RMSE (which gives greater weight to larger residuals), and the scaled RMSE (RMSE divided by the total range of target groundwater levels, a measure of how well the model simulates groundwater flow gradients). Table 3 shows the bulk calibration statistics for the groundwater-level targets following calibration. The RMSE for the 44 groundwater-level calibration targets was 1.20 ft, which when scaled by the range in target values of 90.42 ft results in a scaled RMSE value of 1.3 percent, suggesting the calibration closely matches observed field measurements. The slightly positive residual mean (0.40 ft) indicates that on average, there is minimal bias where the model slightly underestimates groundwater levels, and the absolute residual mean suggests that the groundwater flow solution is typically within 0.91 ft of the observed values. Figure 14 presents a scatter plot comparing the simulated and observed groundwater-level elevations; the values generally fall near the 1:1 line and the minimum and maximum residuals fall within ± 3.2 feet. This indicates the model was able to simulate the full observed range of groundwater-level elevations with reasonable accuracy.

The simulated Gallatin River net gain for the low-flow period was 15.8 cfs; this falls within the expected range of 9.7 to 27.4 cfs, suggesting the modeled streamflow gains are reasonably accurate.

Although no single set of statistical criteria exist that quantify a well-calibrated model (Anderson and others, 2015), the groundwater-level calibration statistics and the modeled streamflow gain indicate the model is well-calibrated with regard to the model objectives. Further, the outcome of the PEST_HP calibration exercise met the goals of a scaled RMSE

Table 3. Bulk calibration statistics for the groundwater-level targets.

RMS Error (ft)	1.20
Scaled RMSE (%)	1.3%
Residual Mean (ft)	0.41
Absolute Residual Mean (ft)	0.91
Scaled Absolute Residual Mean (%)	1.0%
Residual Standard Deviation (ft)	1.12
Scaled Residual Std. Deviation (%)	1.2%
Sum of Squares (ft^2)	63.1
Min. Residual (ft)	-2.26
Max. Residual (ft)	3.18
Number of Observations	44
Range in Observations (ft)	90.42

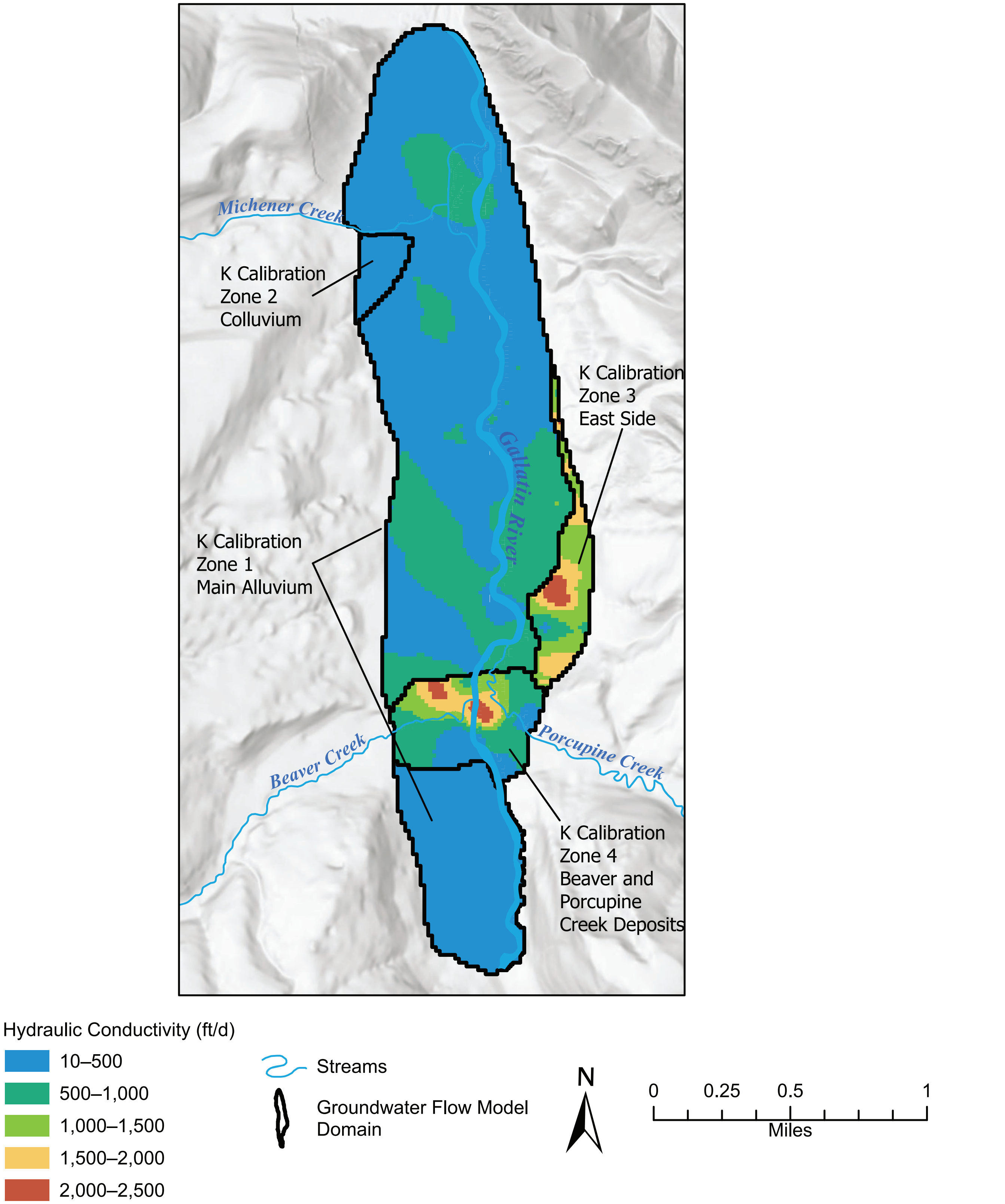

Figure 13. The automated parameter estimation process utilized pilot points to determine the calibrated model's hydraulic conductivity array within the alluvial aquifer. The final hydraulic conductivity (HK) array fell between 10 and 2,500 ft/d.

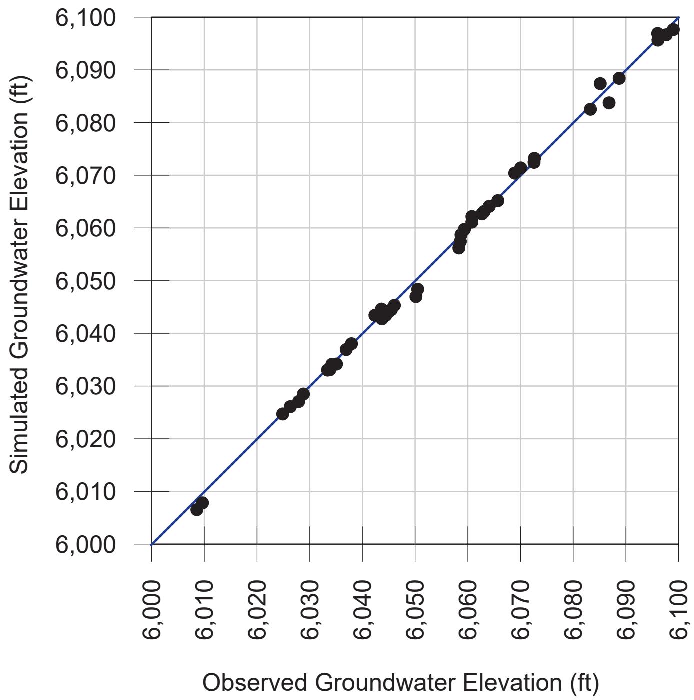

Figure 14. Measured versus simulated groundwater elevations compared closely in the model, indicating the model closely replicates measured conditions with a RMSE of 1.2 ft or 1.3% of the vertical model surface.

of less than 5 percent for the groundwater-level targets and low-flow streamflow gain simulated value within the estimated measurement error of the low-flow streamflow gain value.

Calibration Sensitivity Analysis

A limited sensitivity analysis was conducted to test how changes in K, recharge, and ET affect the model results. The selected input parameters were varied to determine how much they altered the RMSE of the simulated vs. measured groundwater levels and the percentage change in simulated streamflow gains to the Gallatin River during the low-flow period. Table 4 summarizes how each parameter varied relative to the low-stage model and the effect of that change on the model.

The results indicate the RMSE is primarily affected by alterations to the K field. Holding the K in each K calibration zone constant to the geometric mean of K distribution created the most significant increase in error, both in RMSE and in decreasing the calculated gains. The Beaver and Porcupine Creek deposits area (K calibration zone 4, fig. 13) was the most sensitive to scaling the conductivity, causing more than 10 percent change to the simulated gains from the river. Alternately, the small wedge of colluvium (K calibration zone 2, fig. 13) showed the least sensitivity, with scaling the conductivity having no discernible effect on the calibration.

Decreasing recharge by 25 percent has a greater impact on the calibration than increasing recharge. Altering recharge changed the simulated gains, suggesting the surface-water gains are dependent on recharge to groundwater. Altering ET by 50 percent had a minimal impact, with higher ET causing greater error. Decreased ET did not alter the RMSE and minimally (0.2 percent) altered the simulated gains.

The model is relatively insensitive to changes in ET and most sensitive to changes in the K value distribution. Therefore, any changes to the hydraulic conductivity or recharge distributions should be expected to significantly alter the model output.

SIMULATED WATER BUDGET

Table 5 shows the conceptual and modeled water budget values for the entire model domain. Ranges for the conceptual budget are included where appropriate. The groundwater recharge (MBR and R) and septic effluent returns (Q_{se}) were represented as specified flow boundaries (using the RCH and WEL Packages) so the modeled flow rates faithfully represent the specified input flow rates.

The simulated Gallatin River streamflow gain (Net SW_{out} - SW_{in}) was 17.3 cfs in the low-flow period and 18.4 in the high-flow period. These values fall within the range of the conceptual water budget estimates. However, some cells simulated a streamflow gain and some a streamflow loss, similar to real-world conditions. The simulated ET values were close to the low range of conceptually estimated ET values. The numerical model simulates ET only from phreatic water (saturated groundwater), whereas the conceptual model includes ET from phreatic water and the soil zone. The simulated values for ET were 0.1 cfs in the low-flow model and 0.2 cfs in the high-flow model. Given the lack of vadose water being simulated in the groundwater model, the values are within the range of the conceptual water budget estimates that included ET from both unsaturated soils and groundwater, and these simulated values are thus considered a reasonable approximation of ET consumption directly from saturated groundwater.

Table 4. Calibration sensitivity analysis results.

Sensitivity Parameter Altered from Calibrated Model	Root Mean Squared Error (RMSE) Head (ft)	Streamflow Gain Low-Flow Period Percent Change (%)
Calibrated model (baseline)	1.20	0.0%
Constant K in each zone GEOMEAN[a] of K values	3.91	-22.5%
K scaled down by GSD[b], zone 1	1.41	0.4%
K scaled up by GSD[b], zone 1	1.46	-2.1%
K scaled down by GSD[b], zone 2	1.20	0.0%
K scaled up by GSD[b], zone 2	1.20	0.0%
K scaled down by GSD[b], zone 3	1.22	-0.1%
K scaled up by GSD[b], zone 3	1.21	0.1%
K scaled down by GSD[b], zone 4	1.73	-11.3%
K scaled up by GSD[b], zone 4	1.61	17.9%
High ET (increase by 50%)	1.20	-0.4%
Low ET (decrease by 50%)	1.20	0.2%
High recharge (increase by 25%)	1.37	18.7%
Low recharge (decrease by 25%)	1.54	-18.7%

[a]GEOMEAN, geometric mean.

[b]GSD, geometric standard deviation.

Table 5. Conceptual vs. simulated water budget components.

Low-Flow	Conceptual			Simulated	High-Flow	Conceptual			Simulated
INFLOW					INFLOW				
Budget Component	Low		High		Budget Component	Low		High	
MBR (cfs)	13.0	–	21.6	17.3	MBR (cfs)	13.0	–	21.6	17.3
R (cfs)	–	–	0.0[b]	0.0	R (cfs)	–	–	2.9	1.4
Q_{se} (cfs)	–	–	0.1	0.1	Q_{se} (cfs)	–	–	0.1	0.1
GW_{in} (cfs)	0.0[b]	–	0.4	0.1	GW_{in} (cfs)	0.0[b]	–	0.4	0.1
OUTFLOW					OUTFLOW				
SW_{out} - SW_{in} Net (cfs)[a]	14.2	–	23.0	17.2	SW_{out} - SW_{in} Net (cfs)[a]	N/A	–	N/A	18.4
PW (cfs)	–	–	0.0[b]	–	PW (cfs)	–	–	0.0[b]	–
ET (cfs)	–	–	0.6[c]	0.1	ET (cfs)	–	–	1.1[c]	0.2
SPR (cfs)	N/A	–	N/A	0.0[b]	SPR (cfs)	N/A	–	N/A	0.1
GW_{out} (cfs)	0.1	–	1.0	0.2	GW_{out} (cfs)	0.1	–	1.1	0.2

[a]Conceptual flows are as a net for the reach; simulated flows are calculated across individual model cells.

[b]Calculated/measured amount exceeds the significance of the units.

[c]ET estimates include ET from both unsaturated soil and saturated groundwater.

The model simulated the groundwater discharge to Michener Creek and the spring ponds to be 0.1 cfs during the low-flow period and 0.2 cfs during the high-flow period.

For both the low- and high-flow periods, the simulated alluvial groundwater flow into the model from the south (GW_{in}) was 0.1 cfs and the alluvial groundwater flow out of the model to the north was 0.2 cfs.

Simulated Flow Zones

Based on the water budget results, six zones were identified that provide further detail on net streamflow gains and losses in different areas of the model (fig. 15). The zoned budget approach simplifies post-processing of the model results and allows for comparison to field-collected data. Each zone was defined around specific areas of interest. Budget zone 1 includes the UGA between Beaver and Porcupine Creeks to the south and Michener Creek to the north. Budget zones 2 and 3 are defined by the riparian area surrounding Beaver and Porcupine Creeks, respectively. Budget zone 4 includes the portion of the UGA north of Michener Creek. Budget zone 5 includes the area between the Gallatin River and Porcupine Creek. Budget zone 6 is the area south of Beaver Creek.

Both stress periods simulated net streamflow gains (groundwater discharging to surface water with positive values of SW_{out} - SW_{in}) and net stream loss (surface water discharging to groundwater with negative values of SW_{out} - SW_{in}; table 6). The central alluvium (budget zone 1) exhibited the greatest simulated net streamflow gains, while the zone between Porcupine Creek and the Gallatin River (budget zone 5) and north alluvium (budget zone 4) were also simulated to provide net discharge groundwater to surface streams. The zones for Beaver Creek (budget zone 2), Porcupine Creek (budget zone 3), and the south alluvium (budget zone 6) were all simulated to have small net values of stream loss, i.e., negative values of SW_{out} - SW_{in}.

For both stress periods, the model simulated gaining conditions on the Gallatin River over most of the model domain (zones 1, 4, and 5); minor losing conditions were simulated in the southern part of the model domain (zone 6) and along Beaver and Porcupine creeks (zones 2 and 3). The modeled streamflow gains and losses (SW_{out} - SW_{in}) for each budget zone and stress period are summarized in table 6.

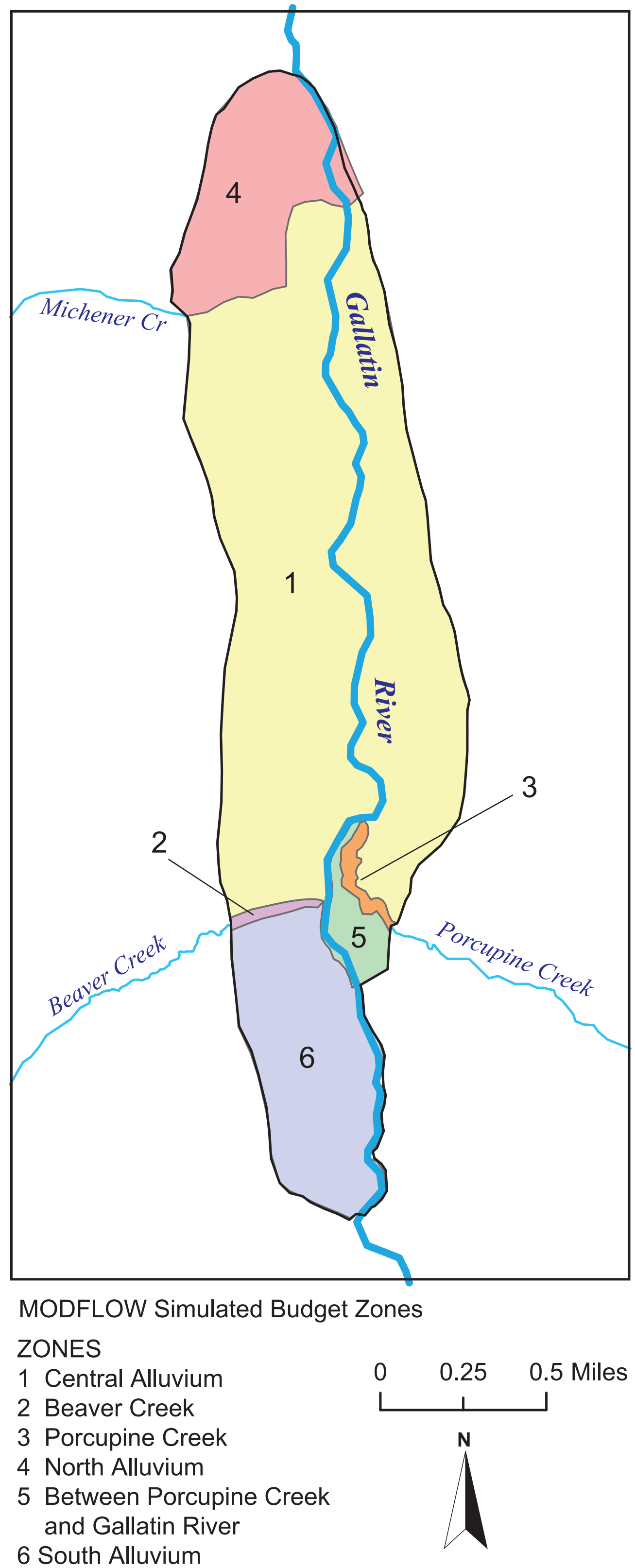

Figure 15. Groundwater flow model construction of the six simulated zones for summarizing output water balances.

Table 6. Groundwater inflows and outflows to the model domain by water budget zone.

A. Low-Flow Period

	Budget Zone (Zone Number)	Central Alluvium (1)	Beaver Creek (2)	Porcupine Creek (3)	North Alluvium (4)	Between Porcupine Creek and Gallatin River (5)	South Alluvium (6)	Totals
Inflow	Q_{se} (cfs)	0.1	0.0	0.0	0.0	0.0	0.0	0.1
	GW_{in} (cfs)	0.0	0.0	0.0	0.0	0.0	0.1	0.1
	MBR (cfs)	9.7	0.4	0.7	0.2	2.4	3.8	17.3
	R (cfs)	0.0	0.0	0.0	0.0	0.0	0.0	0.0
	From Other Zones (cfs)	10.7	6.1	7.3	0.8	8.6	2.6	36.1
	Total Inflow (cfs)	20.6	6.6	8.0	1.1	11.0	6.5	53.6
Outflow	SPR (cfs)	0.0	0.0	0.0	0.0	0.0	0.0	0.0
	SW_{out} - SW_{in} Net (cfs)[a]	13.1	-0.3	-0.5	0.8	4.7	-0.6	17.2
	ET (cfs)	0.1	0.0	0.0	0.0	0.0	0.0	0.1
	GW_{out} (cfs)	0.0	0.0	0.0	0.2	0.0	0.0	0.2
	To Other Zones (cfs)	7.4	6.9	8.5	0.1	6.2	7.0	36.1
	Total Out (cfs)	20.6	6.6	8.0	1.1	11.0	6.5	53.6

B. High-Flow Period

	Budget Zone (Zone Number)	Central Alluvium (1)	Beaver Creek (2)	Porcupine Creek (3)	North Alluvium (4)	Between Porcupine Creek and Gallatin River (5)	South Alluvium (6)	Totals
Inflow	Q_{se} (cfs)	0.1	0.0	0.0	0.0	0.0	0.0	0.1
	GW_{in} (cfs)	0.0	0.0	0.0	0.0	0.0	0.1	0.1
	MBR (cfs)	9.7	0.4	0.7	0.2	2.4	3.8	17.3
	R (cfs)	0.9	0.0	0.0	0.2	0.0	0.2	1.4
	From Other Zones (cfs)	11.0	6.2	7.3	0.9	8.7	2.6	36.7
	Total Inflow (cfs)	21.8	6.6	8.0	1.3	11.1	6.7	55.6
Outflow	SPR (cfs)	0.0	0.0	0.0	0.0	0.0	0.0	0.1
	SW_{out} - SW_{in} Net (cfs)[a]	14.2	-0.4	-0.6	0.9	4.8	-0.5	18.4
	ET (cfs)	0.2	0.0	0.0	0.0	0.0	0.0	0.2
	GW_{out} (cfs)	0.0	0.0	0.0	0.2	0.0	0.0	0.2
	To Other Zones (cfs)	7.4	7.0	8.6	0.2	6.3	7.2	36.7
	Total Out (cfs)	21.8	6.6	8.0	1.3	11.1	6.7	55.6

[a]Conceptual flows are as a net for the reach; simulated flows are calculated across individual model cells.

MODEL EVALUATION

The modeling approach presented herein is intended to bound the observed range conditions between a low-flow and high-flow period. The simulated groundwater levels (heads) represent the average condition for each stress period (flow regime).

The simulated groundwater levels across the model had a scaled RMSE of 1.3 percent, well within the acceptable margin of error of less than 5 percent. Both stress periods reproduce the observed water levels within acceptable calibration error. The simulated Gallatin River flow gains in the central alluvial section reflect the measured gains, and the model closely represents other conceptually calculated inputs and outputs, including GW_{out} and GW_{in}, ET, and SPR (table 5). The model also replicated the marshy areas, showing groundwater near the surface (flooded cells) in those areas.

The simulated low- and high-period groundwater levels were compared to actual groundwater measurements. Figure 16 shows time-series groundwater-elevation data from two wells, and the simulated groundwater elevations at the well locations. The average simulated groundwater level during each period match the observed groundwater levels (note the increases between the low- and high-flow periods). Appendix B provides similar calibration hydrographs for all 22 calibration observation wells as well as a table of simulated, target, and residual values at the wells for both model stress periods.

Figure 17 presents maps of the simulated potentiometric surfaces for both the low- and high-flow periods that show similar north–south alluvial groundwater flow within the valley. The potentiometric surfaces also indicate where the model simulates discharge to the Gallatin River with steeper gradients toward the river, and where the model simulates minor stream

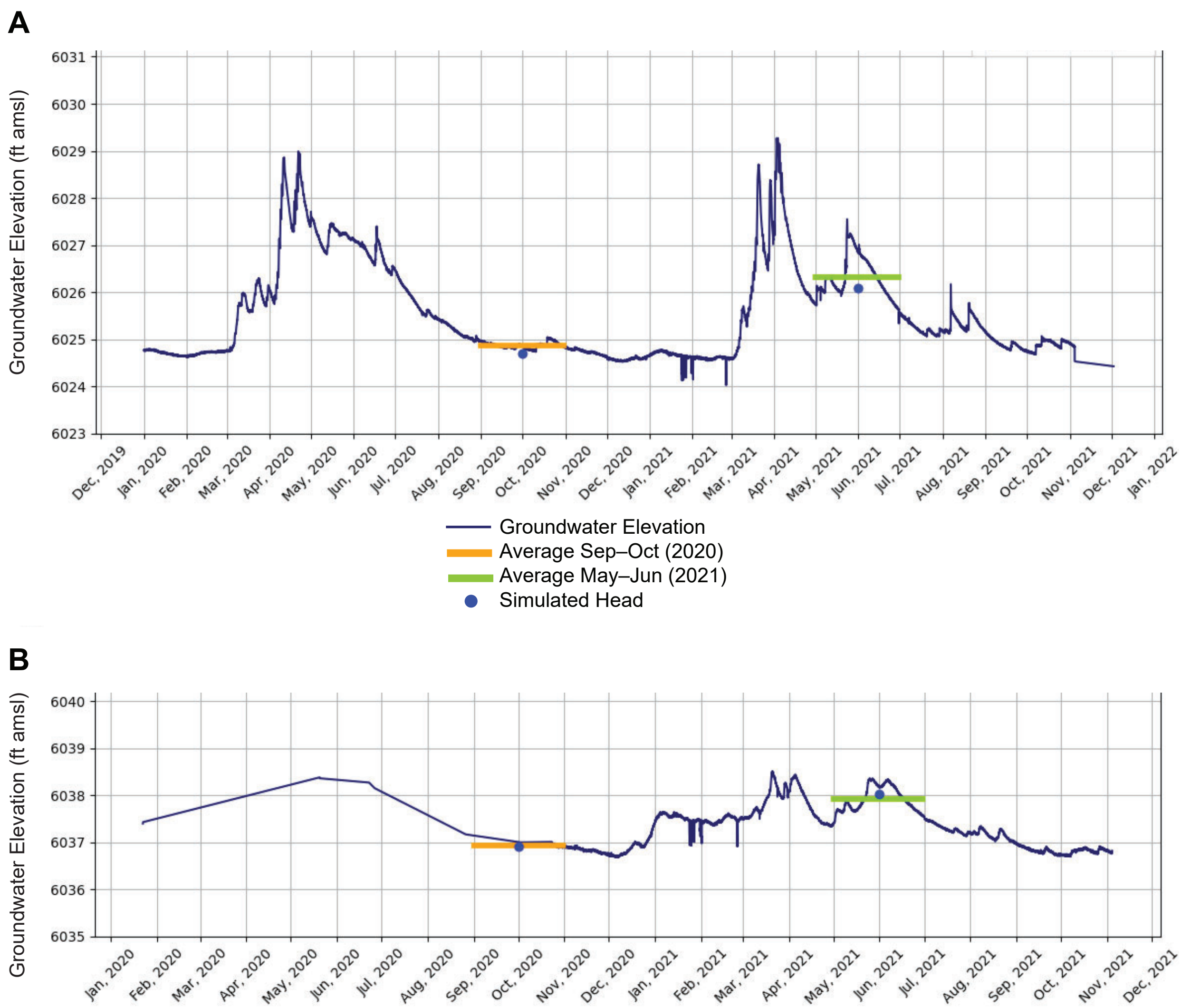

Figure 16. Sample well locations showing measured groundwater elevations and average low- and high-flow period groundwater elevations compared to simulated groundwater elevations after model calibration.

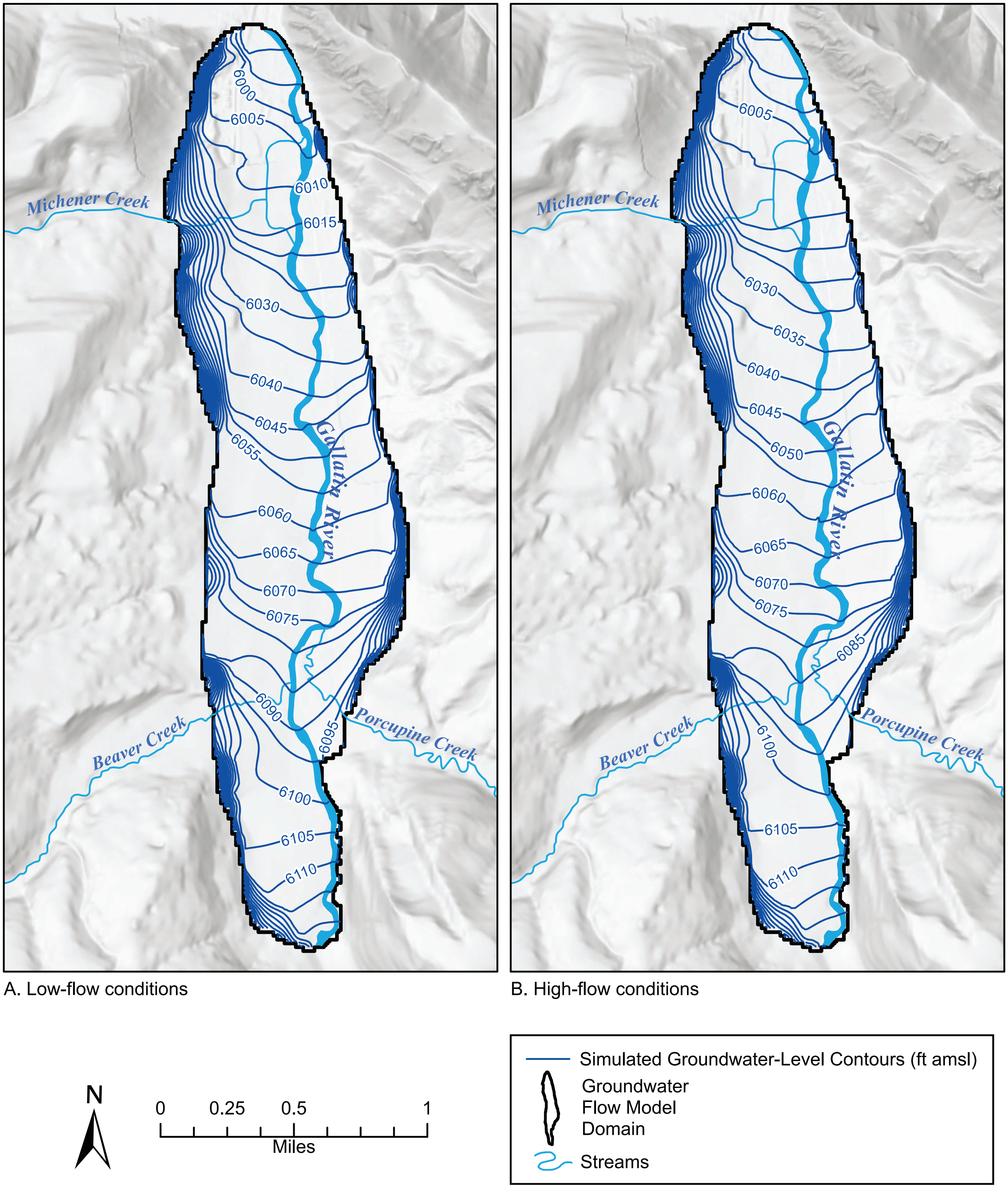

Figure 17. The simulated potentiometric surface for both the (A) low- and (B) high-flow conditions.

loss from the river to groundwater where the gradient is away from the river. Figure 18 presents maps of the simulated saturated thickness of the UGA for both the low- and high-flow periods that show the saturated thickness is least near the valley margins and greatest in the center of the valley and beneath the Gallatin River. Note that the simulated saturated thicknesses are similar between the low- and high-flow periods.

The overall results indicate that the model reasonably reproduces the aquifer behavior and groundwater/surface-water interactions. Additional field-measured streamflow values to estimate gain and loss in the Gallatin River would be required for more certain verification of the model.

CURRENT CONDITIONS FLOWPATH ANALYSES

The calibrated model was used to assess groundwater flowpaths from existing septic systems using forward particle tracking methods. Particle tracking is a form of post-processing that delineates groundwater flowpaths by tracking the movement of imaginary particles through the simulated groundwater flow field (Anderson and others, 2015). Particle tracking does not simulate solute concentrations, nor account for phenomena like dilution and dispersion that may attenuate solute concentrations in groundwater. However, these attenuation processes are more likely with longer flowpaths, and less likely with shorter flowpaths. Particle tracking was performed with the code mod-PATH3DU that is designed specifically for use with MODFLOW-USG flow models with unstructured grids (S.S. Papadopulos and Assoc. Inc., 2024; Craig and others, 2019).

Particles were introduced to model cells containing existing septic systems, and tracked as they moved through the UGA to their ultimate discharge point on the Gallatin River; this was done for both the low- and the high-flow conditions (fig. 19). For both conditions, the Blackfoot Hills effluent flowpaths were simulated to travel beneath Michener Creek and discharge to the Gallatin River near the downstream end of the model domain, with flowpath lengths ranging from approximately 1.1 to 1.2 mi. In the high-flow condition, however, some simulated flowpaths discharged to the spring ponds north of Michener Creek, with flowpath lengths ranging from approximately 0.8 to 0.9 mi. In the low-flow condition, the Ramshorn subdivision effluent flowpaths were simulated to discharge to the Gallatin River both upstream of Michener Creek (approximately 0.4- to 0.5-mi flowpath lengths) and near the downstream end of the model domain (approximately 1.3-mi length flowpaths). However, in the high-flow condition, the flowpaths were simulated to discharge to the Gallatin River upstream of Michener Creek (approximately 0.4- to 0.5-mi flowpath lengths) and to Michener Creek itself (approximately 0.7- to 0.8-mi flowpath lengths) rather than traveling beneath the creek to the Gallatin River further downstream. In both the low- and high-flow conditions, the Big Sky Schools effluent flowpaths were simulated to discharge to the Gallatin River, with flowpath lengths ranging from approximately 0.9 to 1.4 mi. In both the low- and high-flow conditions, the San Marino effluent flowpaths were simulated to discharge to the Gallatin River, with flowpath lengths ranging from approximately 0.1 to 0.2 mi.

MODEL SCENARIOS

Four potential future condition scenarios were simulated for the low-flow and high-flow stress periods. For the first three scenarios, particle-tracking methods as described above were used to assess flowpaths from potential nutrient sources. For each analysis, septic effluent discharge locations and flow rates were adjusted based on the assumptions described below, then forward particle tracking was performed using mod-PATH3DU. The fourth scenario was related to water supply and the potential future reduction of recharge to the UGA within the model domain.

Scenario 1: The Quarry Proposed Subdivision Septic System Effluent Discharge

The Quarry is a proposed subdivision in the northwestern part of the groundwater flow model domain (fig. 20). The proposed locations and maximum septic discharge rates were obtained by digitizing maps provided in the Final Environmental Assessment (EA) document for Phase 1 (MDEQ, 2023), and the Draft EA document for Phase 2 (MDEQ, 2024).

To simulate the effect of septic discharge, additional inflow was added to the groundwater flow model at the proposed septic locations. Some proposed septic locations are located up the western hillslope from the alluvial deposits and thus outside the model domain. The flows from these septic systems were added to the nearby perimeter model cells. Initial particle locations

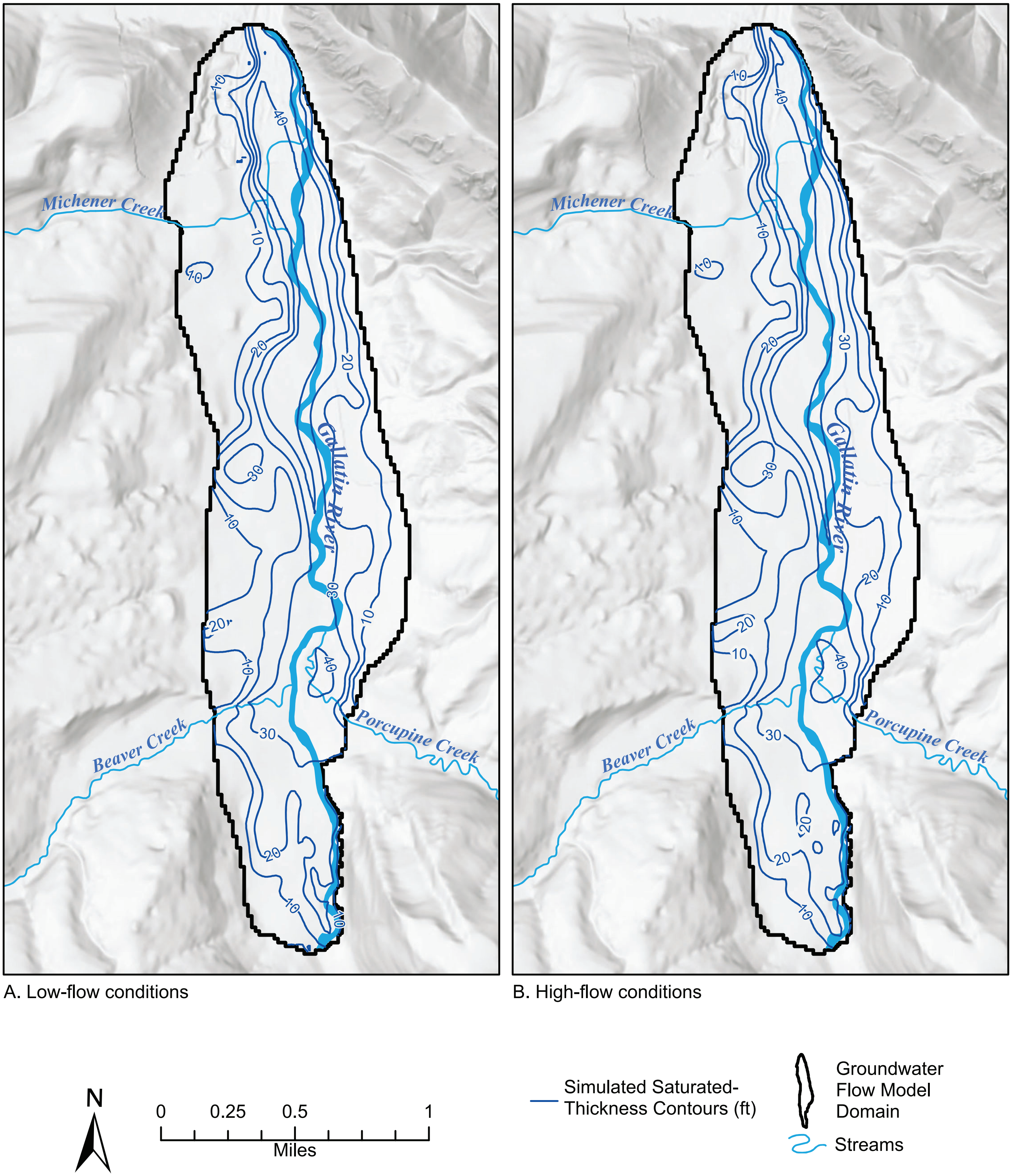

Figure 18. The simulated UGA saturated thickness for both the (A) low- and (B) high-flow conditions.

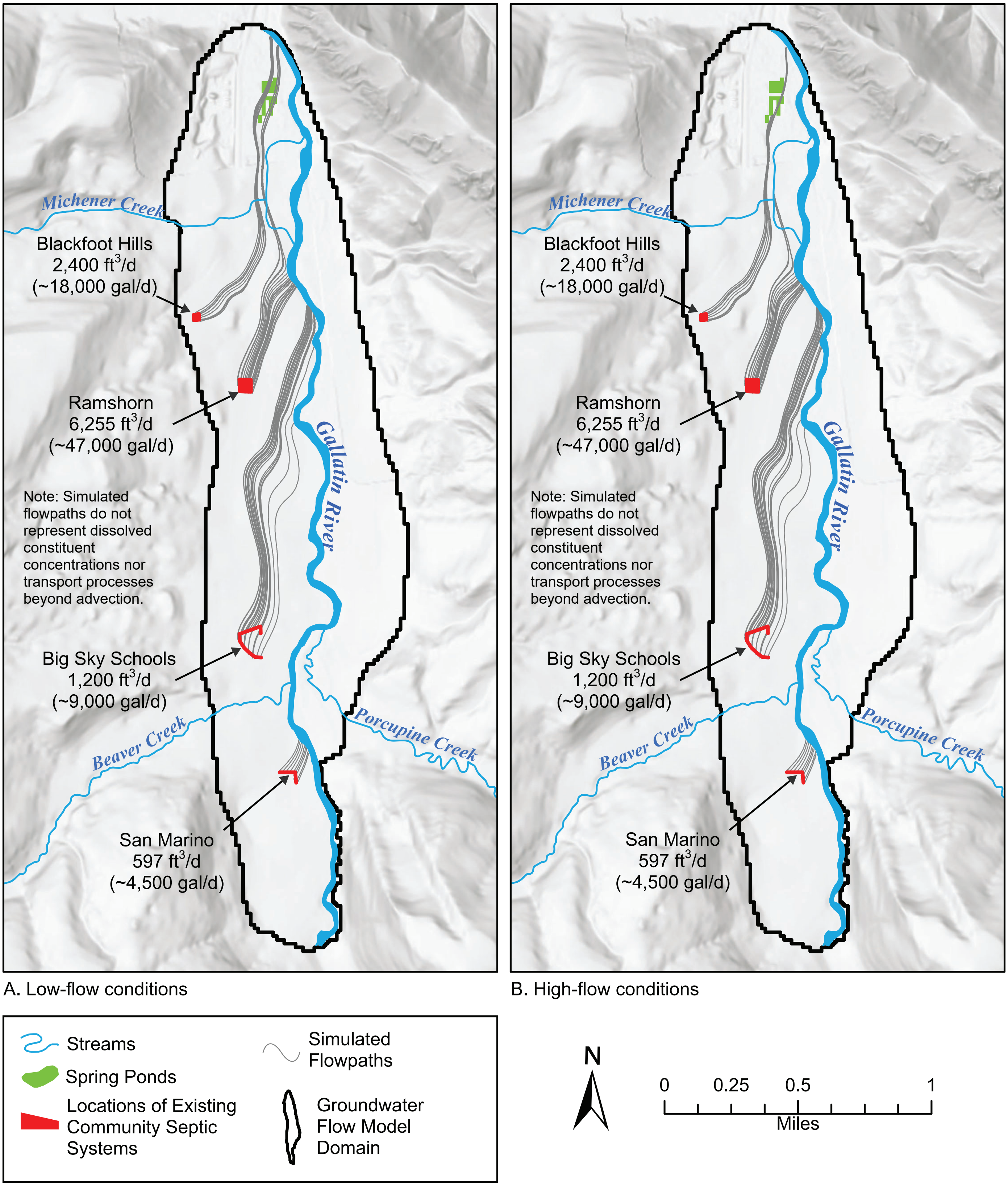

Figure 19. Flowpaths simulated for existing community wastewater treatment systems that contribute effluent discharge to groundwater for low- (A) and high-flow (B) conditions.

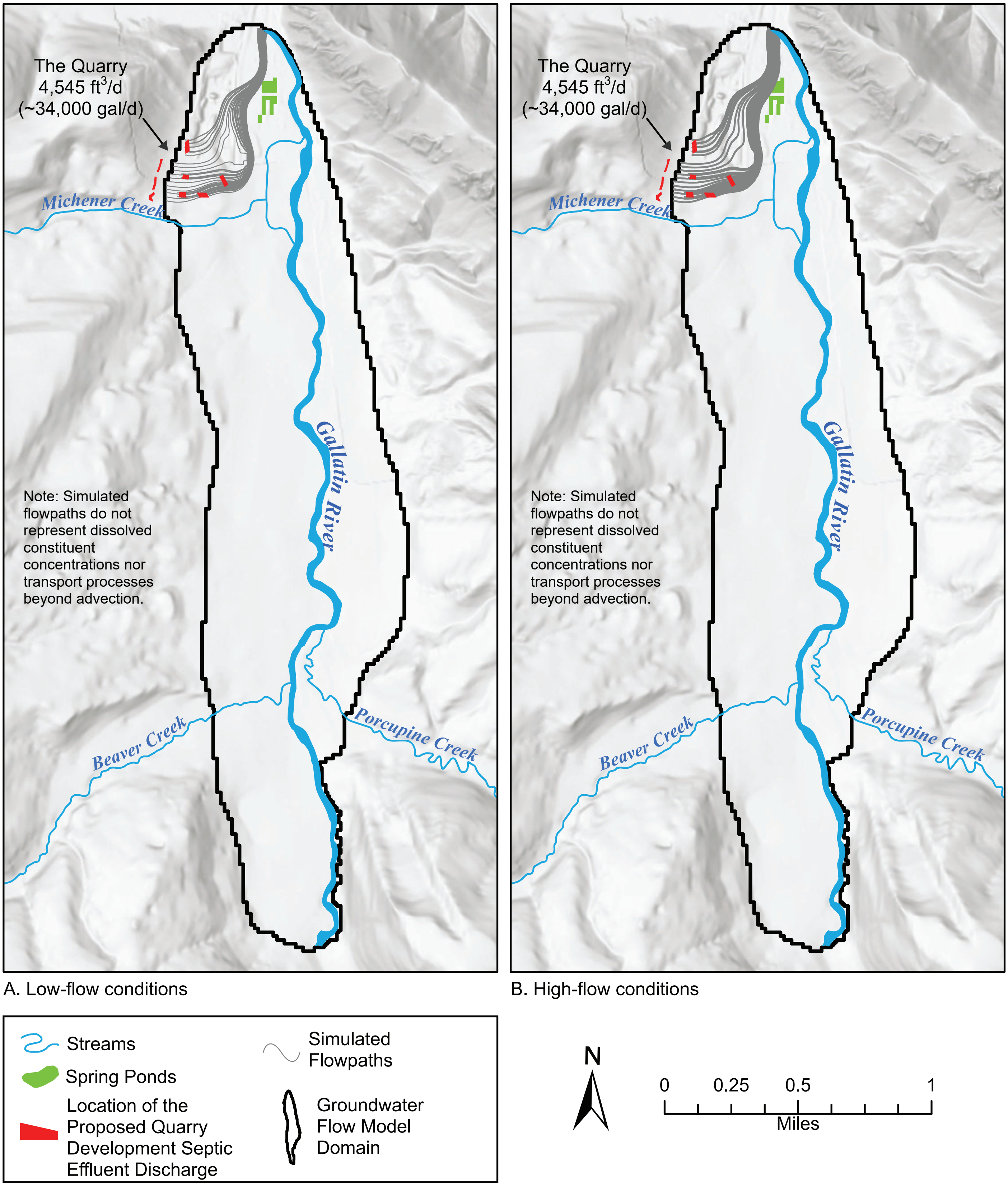

Figure 20. Flowpaths simulated for the proposed Quarry development that would discharge septic system effluent to groundwater for low- (A) and high-flow (B) conditions.

were placed at the centers of each cell with added septic discharge. Figure 20 shows the simulated particle track flowpaths; in both the low- and high-flow conditions, the simulated Quarry septic effluent flowpaths traveled approximately 0.5 to 0.9 mi to the Gallatin River.

Scenario 2: Centralized Treatment Effluent Discharge Locations

A project is currently being studied to reduce septic effluent loading to the alluvial groundwater in the Gallatin Canyon area. The project focuses on building out infrastructure to pipe raw wastewater from the canyon to an expanded Big Sky County Water and Sewer District (BSCWSD) Water Resource Recovery Facility (WRRF) treatment plant. Treated water would then return to multiple groundwater disposal locations in the Canyon Area (BSCWSD, 2024). The returned disposal water would be treated to Class A-1 standards, a higher treatment level than the currently permitted wastewater disposal occurring in the canyon area. Preliminary disposal locations of WRRF-treated effluent and flow rates ranges were obtained from WGM Group (Michelle Pond, written commun., January 6, 2025).

Discharge from the proposed disposal locations was modeled using the maximum anticipated discharge rates. Some proposed disposal locations in the vicinity of the proposed Quarry subdivision were also located up the western hillslope outside the model domain, and flows from these locations were placed in the nearby model cells at the perimeter of the model domain. Initial particle locations were placed at the centers of each cell with added treated water discharges.

Figure 21 shows the simulated particle track flowpaths for the low- and high-flow conditions. The simulated flowpaths from the proposed Quarry location to the Gallatin River ranged from approximately 0.5 to 0.9 mi. During high-flow conditions, some flowpaths traveled to the spring ponds, with flowpath lengths ranging from approximately 0.4 to 0.6 mi. Simulated flowpaths from the proposed Lazy J location traveled to Michener Creek, the spring ponds, and the Gallatin River under the low-and high-flow conditions; flowpath lengths ranged from approximately 0.7 to 0.9 mi for Michener Creek and the spring ponds and range from approximately 1.0 to 1.2 mi for the Gallatin River. Simulated flowpaths from the proposed Ramshorn location under the low-and high-flow conditions traveled to the Gallatin River, with flowpath lengths ranging from 0.4 to 1.2 mi. Simulated flowpaths from the proposed Ophir School (of the Big Sky Schools) location under the low-and high-flow conditions traveled to the Gallatin River, with flowpath lengths ranging from 0.8 to 1.1 mi. Simulated flowpaths from the proposed Newberry location under the low- and high-flow conditions traveled to the Gallatin River, with flowpath lengths ranging from 0.9 to 1.4 mi.

Scenario 3: Potential Broad Additional Septic System Effluent Discharge Locations

This scenario assumes no centralized wastewater treatment and that future residential development occurs over broad areas of privately owned lands using septic systems for wastewater disposal. The potential development locations and estimates of septic effluent flows were obtained from WGM Group (Abby Indreland Hunt, written commun., December 27, 2024).

The simulated flows assumed the maximum estimated septic effluent rates prorated by area for each cell included within the footprint of the potentially developed tracts. For lands outside the groundwater flow model domain, the estimated septic effluent flows were equally distributed to the perimeter model cells adjacent to the tract. Initial particle locations were placed at the centers of each cell with added broadly dispersed septic effluent flows.

Figure 22 shows the simulated discharge locations for low- and high-flow period conditions. Because this scenario involves so many initial hypothetical particle locations, showing the flowpaths is difficult and impractical. The results for low- and high-flow conditions show discharge locations at Michener Creek, the spring ponds, and broadly along the Gallatin River, with simulated lengths ranging from nearly zero (where particles are released very near these receiving waterbodies) to approximately 1.6 mi.

Scenario 4: Reduced Future Recharge

Drought conditions are an expected feature of Montana's current and future climate. As described above, groundwater recharge to the alluvium in the valley is primarily sourced from snowmelt in the surrounding mountains. Future drought conditions may reduce and/or shift precipitation from snow to rain, resulting in more runoff and less groundwater recharge.

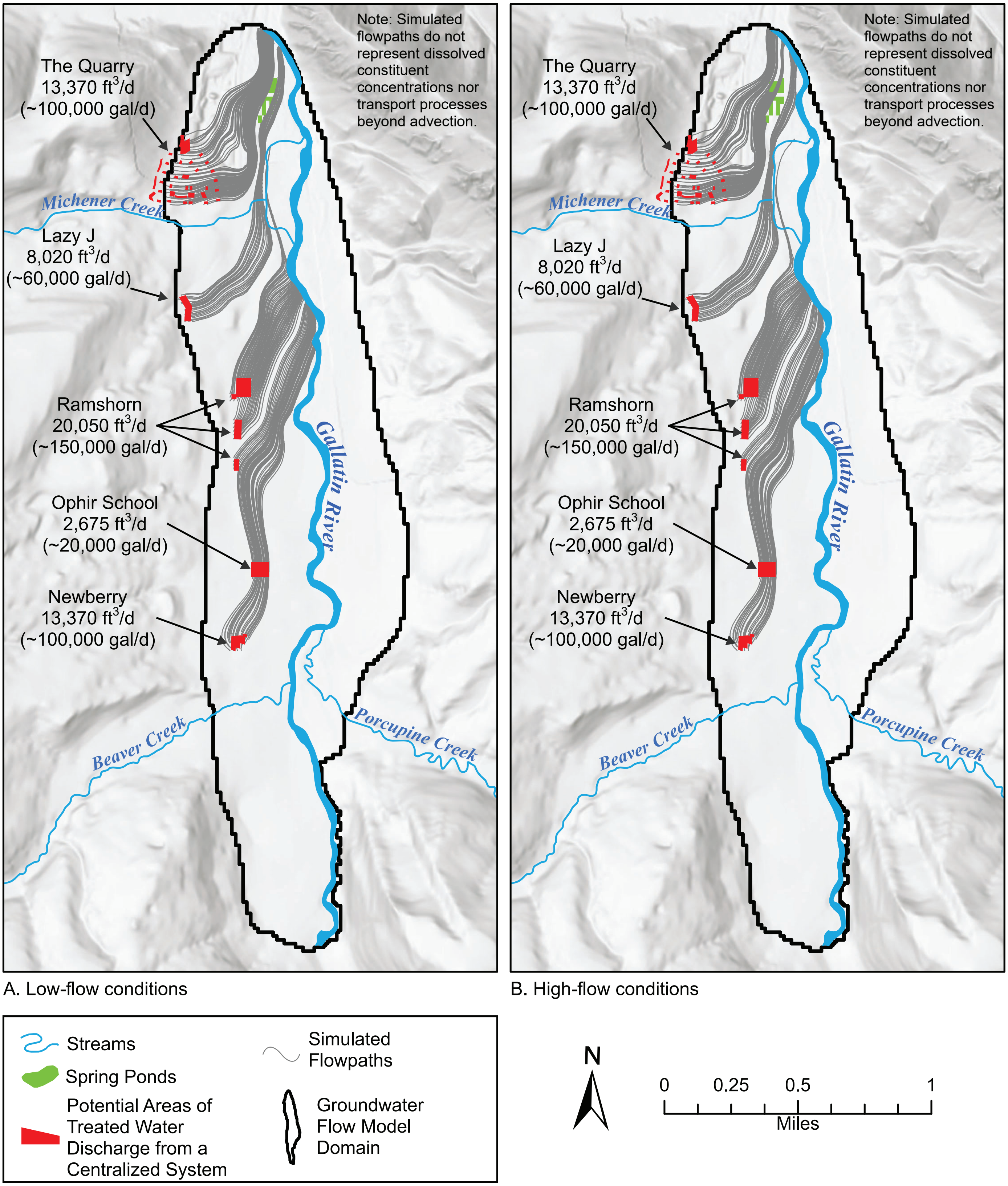

Figure 21. Flowpaths simulated for future centralized wastewater treatment effluent being discharged to groundwater from preliminary design locations (Michelle Pond, written commun., January 6, 2025) for low- (A) and high-flow (B) conditions.

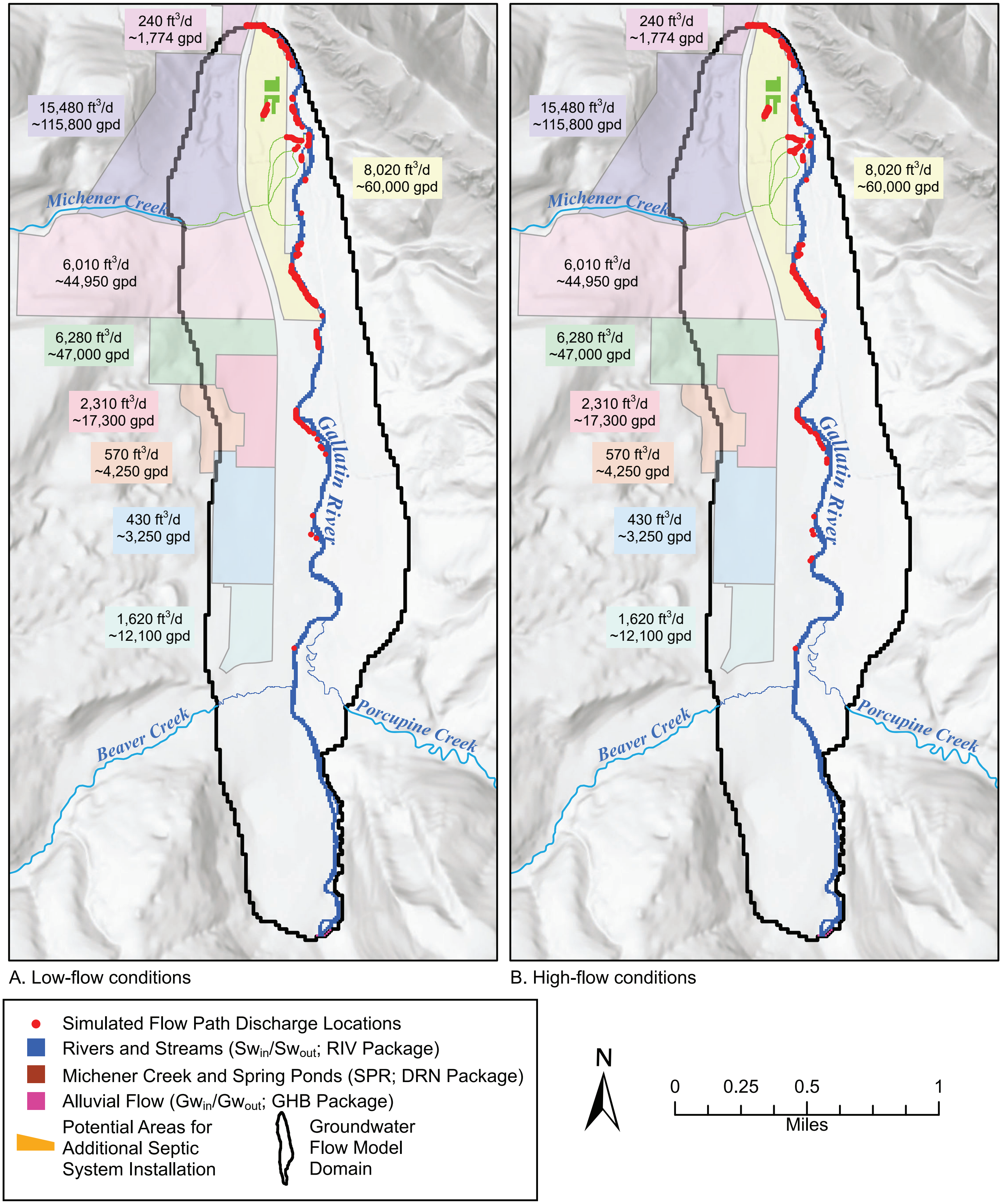

Figure 22. Flowpaths simulated for locations over areas that could be hypothetically developed for residential use with additional septic systems (Abby Indreland Hunt, written commun., December 27, 2024) that would potentially discharge effluent to groundwater for low- (A) and high-flow (B) conditions.

To assess the potential impacts of reduced snowpack on groundwater recharge, the simulated MBR rates were reduced in the low- and high-flow steady-state model stress periods.

Peak water-year snow-water equivalent (SWE) data were retrieved for Lone Mountain SNOTEL station (SNOTEL ID 590; USDA NRCS, 2024). The lowest recorded peak SWE was 13.8 in for water year 1993–1994, 64.5 percent of the median peak SWE of 21.4 in. Based on this percentage calculation, a value of 65 percent of the estimated MBR (i.e., a 35 percent reduction) was selected for a predictive simulation of the reduction of long-term groundwater recharge resulting from a potential future reduction in snowpack.

To simulate reductions in snowmelt recharge, the MBR value was reduced 35 percent. Additionally, areal recharge (R) to the alluvium was set to zero to replicate drought conditions. For the low-flow period, areal recharge was already minimal, but for the high-flow period, the 35 percent reduction in MBR combined with elimination of R represented a total recharge reduction of approximately 40 percent.

Nearly 100% of the reduction in recharge was reflected in a decrease in simulated net groundwater discharge to surface water, primarily the Gallatin River. Alluvial groundwater flow in and out of the model domain and riparian ET were simulated to be minimally impacted, with changes well under one percent of the overall model budget. Figure 23 depicts the simulated changes in groundwater levels resulting from the reductions in recharge. The maximum decrease in groundwater levels due to the reduced recharge was approximately 4.1 ft for the low-flow period and 4.6 ft for the high-flow period. The greatest groundwater-level reductions were simulated in the vicinities of Beaver and Porcupine Creeks, where the greatest recharge rates of MBR were estimated to occur.

MODEL LIMITATIONS AND RECOMMENDATIONS

The groundwater model described in this report was developed to evaluate flow directions and path lengths and groundwater/surface-water interactions between the Gallatin River and the UGA. The model reasonably reproduced observed field conditions consistent with the low- and high-flow periods of calibration.

Because groundwater flow models are simplified representations of complex natural systems and are constructed with assumptions, there are limitations in their use and interpretations. The model utilizes the river (RIV) package to simulate groundwater discharge to and from surface water, not surface water flows themselves. This method was appropriate for this investigation, but if in-stream flows were to be considered, the stream-flow-routing (SFR) package would be more suitable. Additionally, only steady-state conditions were considered, which matched field measurements, but cannot replicate storage or changes over time. The model simulates low-frequency stresses with long-term effects that can be represented by differences between low and high conditions. To evaluate shorter timescale and/or higher frequency stresses, a transient model would need to be developed from the steady-state model presented here.

Particle tracking was utilized to simulate flowpaths from the septic leach fields and other potential future wastewater discharge locations, but not mass transport. A combined groundwater flow and mass-transport model that accounts for dilution and dispersion, such as MODFLOW-USG Transport (Panday, 2024) or MODFLOW 6 (Langevin and others, 2024; minimum version 6.2.0 required), would be required to simulate actual mass loading from the septic systems to the Gallatin River. Additional water-quality data obtained along flowpaths would be required for this type of modeling. The path line analyses presented here show where additional data could be collected to inform a more complex transport simulation.

This model has several potential future uses, such as assessing the conversion of individual septic systems to community sewer systems for existing subdivisions, or determining future septic discharge flowpaths. The model may also serve as a useful baseline for developing a more complex mass-transport model to assess the fate and transport of septic or other contamination through the UGA. With additional streamflow information, the model could be modified to assess in-stream flows using the streamflow-routing (SFR) Package.

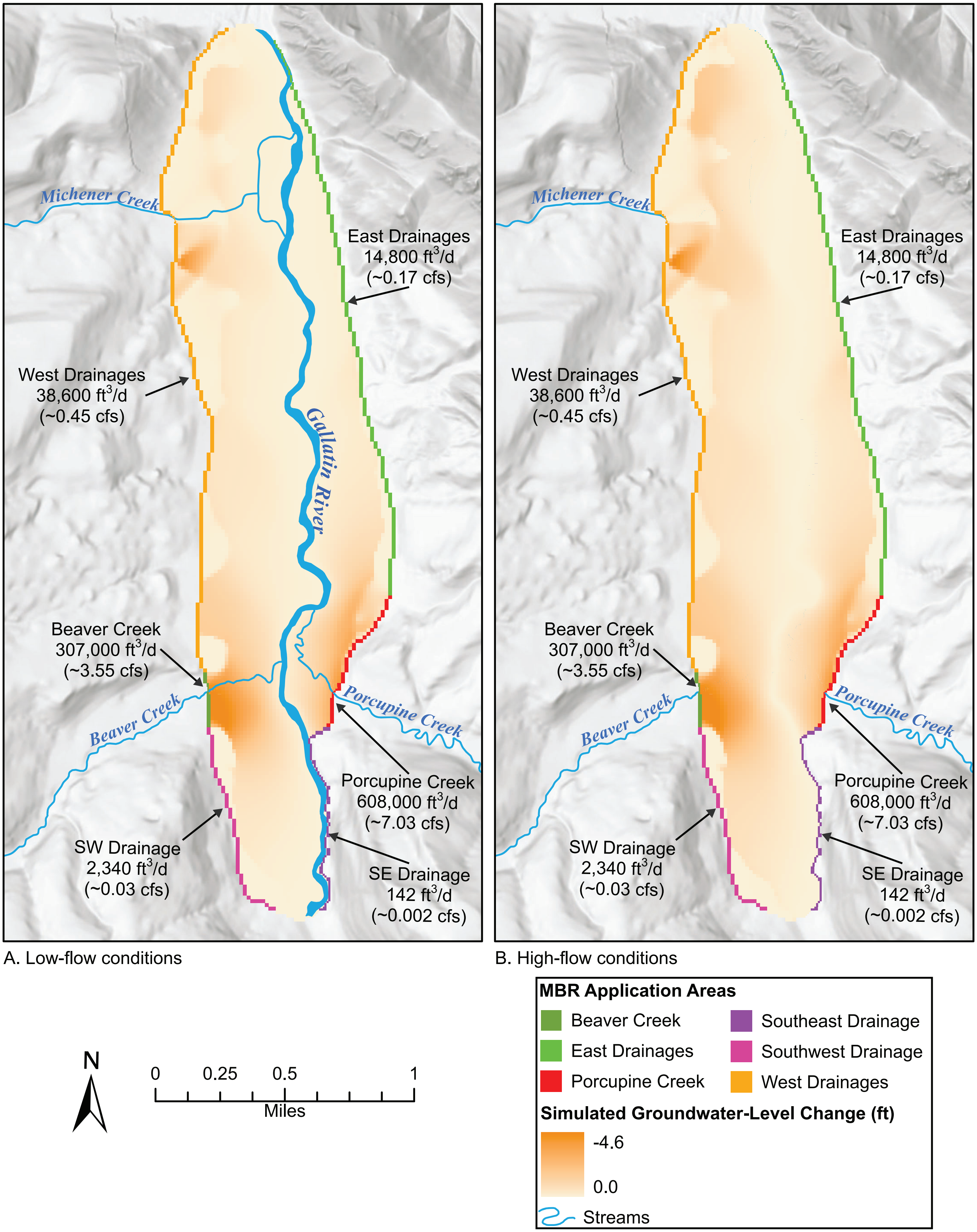

Figure 23. Simulated groundwater-level changes from long-term reduction of MBR by 35% from the base MBR estimates and elimination of areal recharge for low- (A) and high-flow (B) conditions.

CONCLUSIONS

Groundwater flow and groundwater/surface water interaction in the UGA were evaluated using the MODFLOW-USG groundwater flow model. The methods used to define the model grid, boundary conditions, and other model inputs are presented for future potential model users to consider when utilizing or altering the groundwater model to serve specific purposes.

The model was calibrated within a reasonable error according to accepted modeling practices (Anderson and others, 2015). The model reproduced field-measured groundwater levels for both low-flow/low-stage conditions and high-flow/high-stage conditions. The model also reproduced measured streamflow gain through the central portion of the model for the low-flow period.

The model highlights the gaining nature of the Gallatin River, and the close interaction between surface water and the UGA. The results also show the importance of MBR from the surrounding catchment areas to the groundwater system.

The model was used to identify potential groundwater flowpaths between septic discharge areas and the Gallatin River. However, the model does not account for any natural attenuation of nutrients between the effluent sources and surface-water discharge. A mass-transport model could account for features such as natural attenuation, dilution, and dispersion, as well as the timing and volume of nitrates expected to reach the Gallatin River or other potential discharge locations.

The model should be considered an approximation of the physical hydrologic system subject to the limitations detailed in this report. Modifications to sensitive input parameters and variables will require reevaluation of the model and likely recalibration. Additional and more highly detailed data on gain/loss conditions in the Gallatin River would be necessary to refine the modeled groundwater/surface-water interaction. Further information on nitrate concentrations and observed inflows and outflows can be found in the Interpretive Report for this study (Meredith and others, 2025).

ACKNOWLEDGMENTS

The authors would like to thank Kristin Gardiner of the Gallatin River Task Force for nominating this project for the GWIP program and providing input regarding development of predictive model scenarios; Ron Edwards and Jim Muscat, formerly of the Big Sky Water and Sewer District, for their assistance with information and data that assisted in model development; and Michelle Pond and Abby Indreland Hunt of WGM Group for providing data for the predictive model scenarios. This project would not be possible without the help of local landowners, who allowed access to their wells and springs and provided their knowledge of the area. Additional thanks are extended to Mike Richter and the MBMG Ground Water Assessment Program for assistance in establishing the monitoring network used for model calibration. The authors would also like to acknowledge the diligent work of Jenna Dohman and Ann Hanson, who were instrumental in assembling this report, and Carly Peach and James Rose, who collected much of the field data.

REFERENCES

Abatzoglou, J.T., 2013, Development of gridded surface meteorological data for ecological applications and modelling: International Journal of Climatology, v. 33, p. 121–131, available at https://www.climatologylab.org/gridmet.html [Accessed 11/14/2024].

Allen, R.G., Pereira, L.S., Raes, D., and Smith, M., 1998, Crop evapotranspiration—Guidelines for computing crop water requirements: Rome, Food and Agriculture Organization of the United Nations, Irrigation and Drainage Paper 56: Food and Agriculture Organization of the United Nations Rome, 174 p., available at https://www.fao.org/3/X0490E/x0490e00.htm [Accessed March 2025].

Anderson, M.P., Woessner, W.W., and Hunt, R.J., 2015, Applied groundwater modeling: Simulation of flow and advective transport: San Diego, Calif., Academic Press, 564 p., https://doi.org/10.1111/gwat.12464

Aquaveo, 2019, GMS User Manual 10.4: Salt Lake City, UT, available at https://www.xmswiki.com/wiki/GMS:GMS_User_Manual_10.4 [Accessed 8/20/2022]

Big Sky County Water and Sewer District (BSCWSD), 2024, WRRF Expansion—Big Sky Water Sewer Project, available at https://bigskywatersewer.com/wrrf-expansion-project/ [Accessed January 9, 2025].

Boggs, S. 2001, Principles of sedimentology and stratigraphy: Upper Saddle River, NJ, Prentice Hall, 3rd ed., 726 p.

Craig, J.R., Ramadhan, M., and Muffels, C., 2019, A particle tracking algorithm for arbitrary unstructured grids: Groundwater, v. 58, no. 1, p. 19–26, https://doi.org/10.1111/gwat.12894

Department of Natural Resources and Conservation (DNRC), 2011, General water use requirements: water resources: Water Policy Interim Committee, September 13, 2011.

Domenico, P.A., and Schwartz, F.W., 1990, Physical and Chemical Hydrogeology: New York, John Wiley & Sons, 824 p.

Environmental Simulations, Inc. (ESI), 2020, Groundwater Vistas version 8, available at https://groundwatermodels.com/Groundwater_Vistas.php [Accessed March 2025].

Fetter, C.W., 2010, Applied hydrogeology, 4th ed.: Upper Saddle River, N.J., Prentice Hall, 598 p.

Gallatin City–County Health Department (GCCHD), 2022, Wastewater Treatment Systems, Gallatin County, Montana, available at https://gis.gallatin.mt.gov/webmaps/?map=ehs [Accessed 8/29/2022]

Gardner, K., Marchisin, E., and Olson, J., 2021, Upper Gallatin River watershed monitoring report: Gallatin River Task Force, Big Sky, Mont., 24 p., available at https://gallatinrivertaskforce.org/wp-content/uploads/2022/06/2021-Annual-GRTF-WQ-Report-FINAL.pdf [Accessed March 2025].

Gotkowitz, M.B., ed., 2023, Standard procedures and guidelines for field activities, Montana Bureau of Mines and Geology, Version 2: Montana Bureau of Mines and Geology Open-File Report 758, 99 p., https://doi.org/10.59691/UUYM4848

Healy, R.W., 2010, Estimating groundwater recharge: Cambridge, UK, Cambridge University Press, 256 p., https://doi.org/10.1017/CBO9780511780745

Horton, R.E., 1919, Rainfall interception: American Meteorological Society, Monthly Weather review, v. 47, no. 9, p. 603–623, https://doi.org/10.1175/1520-0493(1919)47<603:RI>2.0.CO;2

Langevin, C.D., Hughes, J.D., Provost, A.M., Russcher, M.J., Morway, E.D., Reno, M.J., Bonelli, W.P., Panday, S., Merrick, D., Niswonger, R.G., Boyce, S.E., and Banta, E.R., 2024, MODFLOW 6 Modular Hydrologic Model version 6.6.0: U.S. Geological Survey Software Release, 19 December 2024, https://doi.org/10.5066/P1DXFBUR

Melton, F.S., Huntington, J., Grimm, R., Herring, J., Hall, M., Rollison, D., Erickson, T., Allen, R., Anderson, M., Fisher, J.B. and Kilic, A., 2021, OpenET: Filling a critical data gap in water management for the western united states, Journal of the American Water Resources Association, https://doi.org/10.1111/1752-1688.12956

Meredith, E., Abdo, G., Myse, T., Breitmeyer, R., and Rose, J., 2025, Upper Gallatin River corridor hydrogeologic interpretive report, Big Sky, Montana: Montana Bureau of Mines and Geology Open-File Report 772, https://doi.org/10.59691/YMSG4474

Montana Bureau of Mines and Geology (MBMG), 2025, Ground Water Information Center (GWIC) online database, available at https://mbmggwic.mtech.edu/ [Accessed July 31, 2024].

Montana Department of Environmental Quality (MDEQ), 2023, Final environmental assessment of residential subdivision #2 at the Quarry, issued February 16, 2023.

Montana Department of Environmental Quality (MDEQ), 2024, Draft environmental assessment of residential subdivision #2 at the Quarry, issued November 18, 2024.

Moore, R.B., McKay, L.D., Rea, A.H., Bondelid, T.R., Price, C.V., Dewald, T.G., and Johnston, C.M., 2019, User's guide for the national hydrography dataset plus (NHDPlus) high resolution: U.S. Geological Survey Open-File Report 2019–1096, 66 p., https://doi.org/10.3133/ofr20191096

NSF Unidata, 2023, netCDF-c version 4.9.2 software: Boulder, CO, UCAR/NSF Unidata Program Center, https://doi.org/10.5065/D6H70CW6

NV5 Geospatial, 2021, MT_RAVALLIGRANITE-CUSTERPOWDERRIVER_2019_B19_LIDAR processing report, Work Unit 220298; digital Li-

DAR data prepared for the United States Geological Survey, submitted August 20, 2021, available at https://apps.nationalmap.gov/lidar-explorer/#/ [Accessed March 2025].

NV5 Geospatial, 2024, MT Statewide Phase 3 LiDAR processing report, Work Unit 300374; digital LiDAR data prepared for the United States Geological Survey, submitted March 15, 2024, available at https://apps.nationalmap.gov/lidar-explorer/#/

Panday, S., 2024, MODFLOW USG-Transport: transport and other enhancements to MODFLOW-USG: GSI Environmental, Inc. Software Release, 21 July 2024, available at https://www.gsienv.com/software/modflow-usg/modflow-usg/ [Accessed March 2025].

Panday, S., Langevin, C.D., Niswonger, R.G., Ibaraki, M., and Hughes, J.D., 2019, MODFLOW-USG version 1.5.00: An unstructured grid version of MODFLOW for simulating groundwater flow and tightly coupled processes using a control volume finite-difference formulation: U.S. Geological Survey Software Release, 27 February 2019, https://doi.org/10.3133/tm6A45

Rose, J., 2022, Aquifer tests completed in the Upper Gallatin River Valley, Big Sky, Montana: Montana Bureau of Mines and Geology Open-File Report 750, 18 p., https://doi.org/10.59691/XMEB6222

Rose, J., and Waren, K., 2022, Hydrogeology and groundwater availability at Big Sky, Montana: Montana Bureau of Mines and Geology Open-File Report 747, 90 p., https://doi.org/10.59691/OMMP9599

Sauer, V.B., and Meyer, R.W., 1992, Determination of error in individual discharge measurements: U.S. Geological Survey Open-File Report 92–144.

S.S. Papadopulos and Assoc. Inc., 2024, User's guide for mod-PATH3DU, a groundwater path and travel-time simulator, available at mp3du.sspa.com/man [Accessed December 9, 2024].

Thornthwaite, C.W., and Mather, J.R., 1957, Instructions and tables for computing potential evapotranspiration and the water balance: Publications in Climatology, v. 10, no. 3, p. 1–104, available at https://www.wrc.udel.edu/wp-content/publications/ThornthwaiteandMather1957Instructions_Tables_ComputingPotentialEvapotranspiration_Water%20Balance.pdf [Accessed October 2024].

United States Department of Agriculture (USDA) National Agricultural Statistics Service (NASS), 2025, 20240131, Cropland Data Layer: USDA NASS, USDA NASS Marketing and Information Services Office, Washington, D.C., available at https://croplandcros.scinet.usda.gov/ [Accessed March 2025].

United States Department of Agriculture (USDA), Natural Resource Conservation Service (NRCS), National Water and Climate Center, 2024, Water and climate information system, report generator: Air and Water Database, available at https://nwcc-apps.sc.egov.usda.gov/ [Accessed December 19, 2024].

United States Department of Agriculture (USDA), Natural Resource Conservation Service (NRCS), 2009a, Part 630 Hydrology national engineering handbook, ch. 7: Hydrologic soil groups, available at https://www.hydrocad.net/neh/630ch7.pdf [Accessed March 2025].

United States Department of Agriculture (USDA), Natural Resource Conservation Service (NRCS), 2009b, Part 630 Hydrology national engineering handbook, ch. 9: Hydrologic soil-cover complexes, available at https://irrigationtoolbox.com/NEH/Part630_Hydrology/H_210_630_09.pdf [Accessed March 2025].

Watermark Numerical Computing, 2024, PEST_HP - PEST for highly parallelized computing environments: Watermark Numerical Computing, Manual for version 18, 90 p., available at https://pesthomepage.org/documentation [Accessed March 2025].

Westenbroek, S.M., Engott, J.A., Kelson, V.A., and Hunt, R.J., 2018, SWB version 2.0—A soil-water-balance code for estimating net infiltration and other water-budget components: U.S. Geological Survey Techniques and Methods, book 6, ch. A59, 118 p., https://doi.org/10.3133/ tm6A59

WGM Group, 2020, Canyon Area feasibility study, Technical Memorandum, 200 p, available at https://www.gallatinrivertaskforce.org/wp-content/uploads/2020/05/Canyon-Feasibility-Study_FINAL_05-15-20.pdf [Accessed March 2025].

APPENDIX A
SWB MODEL/RECHARGE METHODS

INTRODUCTION

A soil–water balance (SWB) model was constructed to provide estimates of groundwater recharge to the Upper Gallatin Aquifer (UGA) groundwater flow model. The U.S. Geological Survey (USGS) SWB model code version 2.0 calculates input and output terms for the soil–zone water balance using a daily time step using a Thornthwaite–Mather-based water-balance approach (Westenbroek and others, 2018; Thornthwaite and Mather, 1957). Many of the input data sets for the SWB model rely on geographic information systems (GIS) data. The SWB model uses gridded daily climate data and landscape/vegetation properties to calculate net precipitation as both rainfall and snowmelt, and then partition and redistribute that water across the landscape as outputs of overland runoff, evapotranspiration, infiltration into the soil zone, and net infiltration past the root zone. The net infiltration past the root zone is potential groundwater recharge.

The SWB model was used to provide two input datasets to the groundwater flow model:

1. areal vertical recharge over the footprint of the groundwater flow model domain as the calculated output net infiltration over the footprint, and

2. mountain-block recharge (MBR) as 6-yr (2018 through 2023) average values of net infiltration in the mountain block watersheds draining to the groundwater flow model domain, with that water simulated to flow into the groundwater flow model along its east and west perimeters.

The active SWB model domain covers approximately 60.4 mi^2 and extends beyond the groundwater flow model domain (fig. 1). The SWB model grid has 397 rows and 710 columns with a constant grid cell size of 100 ft (30.48 m) on each side. The active area of the SWB model grid was developed from the USGS National Hydrography Dataset Plus (NHDPlus) High Resolution (HR) (Moore and others, 2019) Hydrologic Unit Code 12 (HUC12) watershed GIS feature class and includes 168,318 active model cells. The SWB model grid was partitioned into those SWB grid cells overlying the groundwater flow model, and the mountain-block watersheds draining to the model domain. At the southern end of the model, the upstream mountain-block watershed area was divided into the central area of the watershed where MBR would have discharged to the alluvium and then the Gallatin River upstream outside of the groundwater flow model, and those mountain block areas to the east and west that would be expected to potentially deliver MBR to the southwest and southeast areas of the model domain (fig. A1). SWB model inputs at each model cell include climate (daily precipitation and minimum/maximum temperatures, overland runoff flow direction, soil properties, and land cover, plus lookup tables containing parameter values for calculating water-balance terms in each grid cell).

SWB MODEL INPUTS

Spatially gridded daily climate inputs for precipitation and minimum/maximum temperature were obtained from gridMET (Abatzoglou, 2013). The gridMET datasets are gridded on a 1/24th degree (~4 km) spacing over the contiguous U.S. and are available as individual files of daily data for each climate variable for each calendar year. Figure A2 shows the average 2018–2023 average annual precipitation for the gridMET data grid cells covering the SWB model domain.

Overland flow routing directions for the SWB model cells were developed using the recently released (October 2024) digital elevation model (DEM) covering the bulk of the groundwater flow model and SWB model domains based on light detection and ranging (lidar) methods (NV5 Geospatial, 2024), as well as the previously available lidar DEMs available for small areas of the northern portion of the model domains (NV5 Geospatial, 2021). These lidar-based DEM datasets are released at a 1-m resolution distributed in multiple tiles, and the tiles covering the SWB model domain were obtained, merged, and further processed in two ways to ensure continuous routing of overland flow across the SWB model domain. First, bridges across Beaver Creek and Michener Creek were noted to not be processed to be removed from the “bare earth” elevation, and elevations were linearly interpolated through the bridge decks from upstream to downstream to allow simulation of flow through these areas. Second, a process was undertaken to “burn” drainageways into the dataset through a GIS-based multistep process to ensure spurious sinks would be filled in the final dataset (Brett Oliver, oral commun., October 24, 2024) to be used as inputs to the SWB model, as follows:

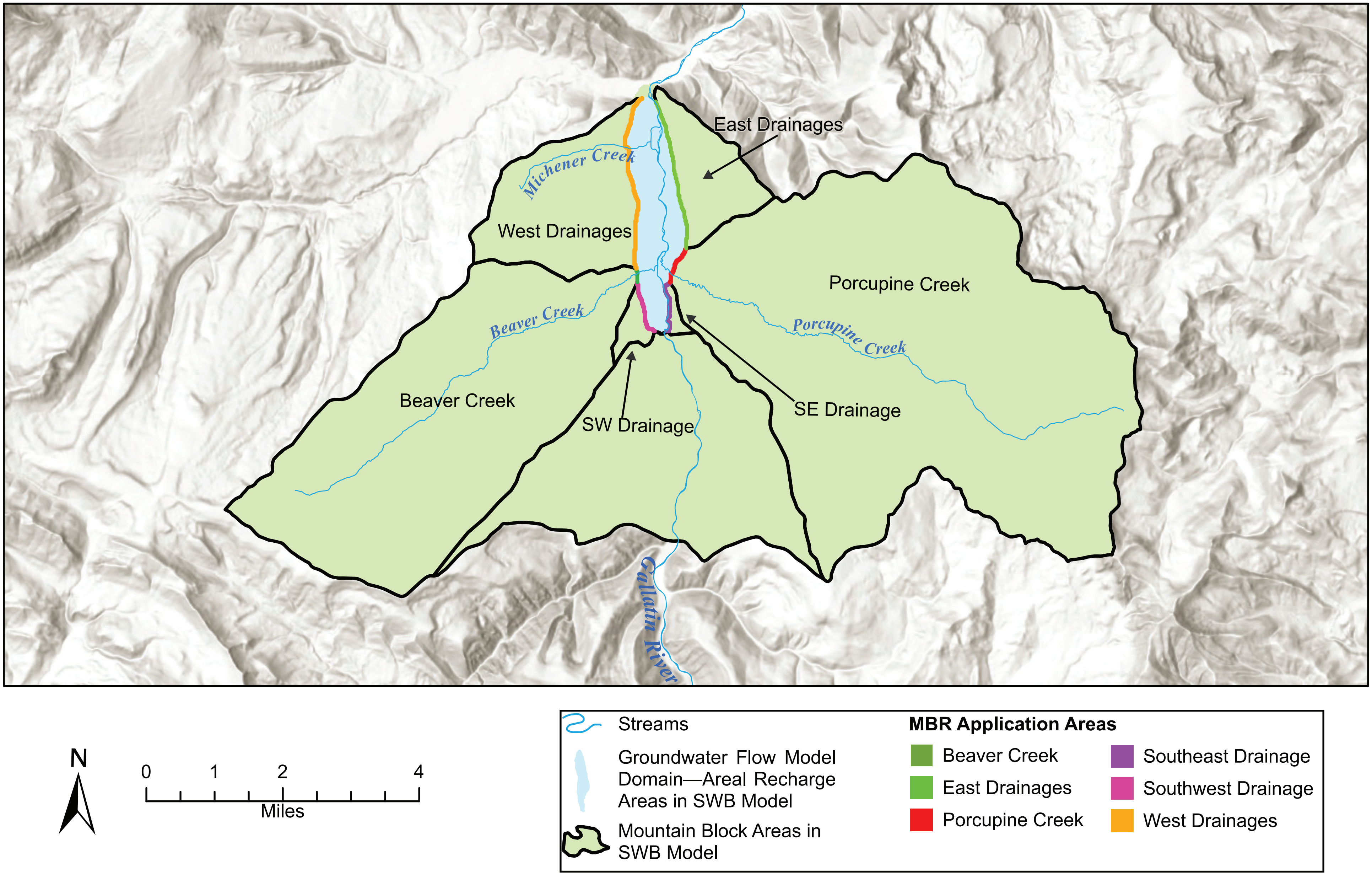

Figure A1. Active SWB model domain as applied to mountain block areas to estimate and apply MBR in the groundwater flow model and footprint of groundwater flow model to estimate and apply vertical areal recharge.

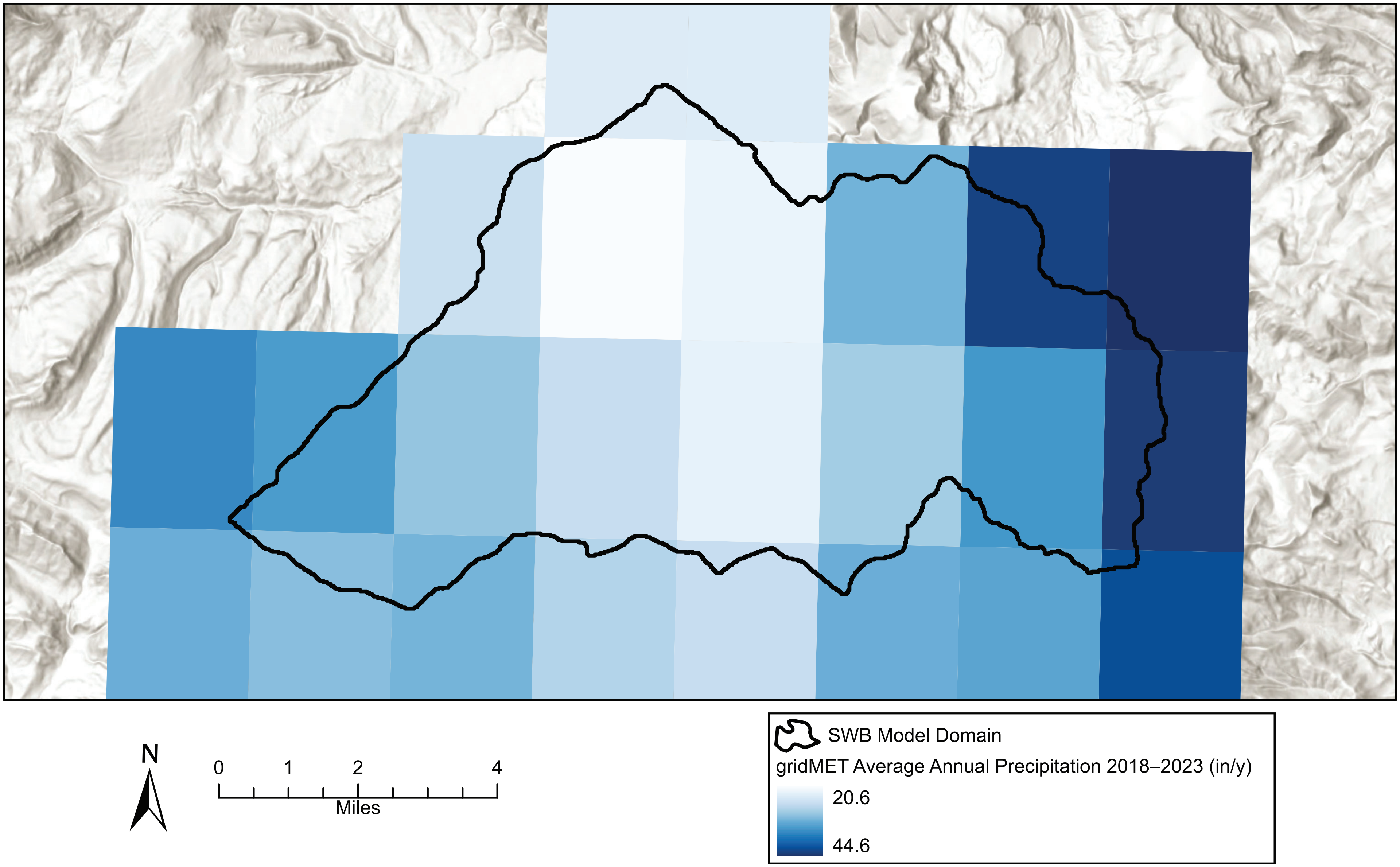

Figure A2. Average annual gridMET precipitation rates 2018 through 2023 over the area of the SWB model domain, derived from daily gridMET data used in the SWB model.

1. perform an initial pass of generating flow directions from the 1-m lidar DEM,
2. identify and fill spurious sinks in the 1-m DEM,
3. develop dataset of drainageways from the filled 1-m DEM,
4. resample the filled 1-m DEM to the 100-ft SWB model grid cells as mean values,
5. perform an initial pass of generating flow directions from the resampled DEM,
6. fill spurious sinks in the resampled DEM,
7. "burn" the drainageways from step 3 into the filled and resampled DEM by reducing those raster pixel elevations by an additional 1-foot (30.48-cm) depth,
8. fill spurious sinks in the resampled DEM, if any, and
9. generate flow directions from the resampled, fill/burn/fill DEM.

The final flow direction raster from the steps above was used as the input for the SWB model. Figure A3 shows the drainageways delineated from the lidar-based DEM.

The U.S. Department of Agriculture (USDA) Natural Resources Conservation Service (NRCS) gridded national soil survey geographic database (gSSURGO) for Montana provided the basis for the hydrologic soil groups (HSG) and the available water capacity (AWC) input data for the SWB model (Soil Survey Staff, 2023). The HSG and AWC data in gSSURGO are gridded representations of mapped soil unit polygons, and the data values assigned by lookup tables relate the soil unit properties to the soil unit polygon spatial distribution. Note that soils mapping has been completed and updated at different times with different interpretations, and not all soil unit polygons have been edge-matched and made consistent between soils mapping areas, so there may be visible contrasts in soils properties at boundaries between mapped areas. The native gSSURGO dataset is gridded at a 10-m resolution that was then resampled to the 100-ft SWB model grid cells for this study. The HSGs (U.S. Department of Agriculture NRCS, 2009a) used in the study include the four basic HSGs (A, B, C, and D) and one dual HSGs (B/D) modified to better represent the surficial soil units in the study area (fig. A4). The NRCS AWC data for the top 150 cm were used for this study because many of the land uses/land covers have rooting zones that extend to that depth and beyond. The AWC data for the upper 150 cm were converted to units of inches per foot (in/ft) of soil thickness as required by the SWB model code (fig. A5).

The SWB model also requires inputs of land use/land cover categories to parameterize phenomena such as precipitation interception, overland runoff, and ET from vegetation. The USDA Cropland Data Layer (CDL) was the source for land use/land cover categories (USDA NASS, 2024). The CDL is a crop/vegetation-specific land cover raster-based GIS data layer created annually for the continental U.S. based on moderate resolution satellite imagery as well as ground-truthing. The CDL data are released at a 30-m resolution that was then resampled to the 100-ft SWB model grid cells for this study. Because the CDL data are produced primarily from automated processing of satellite imagery, some raster pixels of spurious crop/land use types appear in the dataset. The spurious crop/land use categories primarily appeared within treed areas of the mountains of the SWB model domain, and as such were remapped to the evergreen forest category. The maximum number of remapped CDL pixels was approximately 0.13% of the total number of pixels in the SWB model domain for calendar year 2023. Figure A6 shows the resampled and remapped land use/land cover category raster input dataset for year 2023.

In addition to the GIS-based spatial input datasets, the SWB model for the study area used two lookup tables to calculate various terms of the water balance: a primary land-use lookup table, and a secondary vegetation water-use lookup table, which was used to calculate the evapotranspiration part of the water balance using the FAO56 method (Allen and others, 1998; Westenbroek and others, 2018). The primary land-use lookup table contains values for precipitation interception (Horton, 1919), runoff curve numbers (USDA NRCS, 2009b), maximum daily recharge (Allen and others, 1998), and rooting depths (Allen and others, 1998) for each combination of land use/land cover category and HSG in the model. With 10 land-use classes and 5 hydrologic soil groups, the SWB model potentially has 50 different values for each of these categories (although many combinations of land

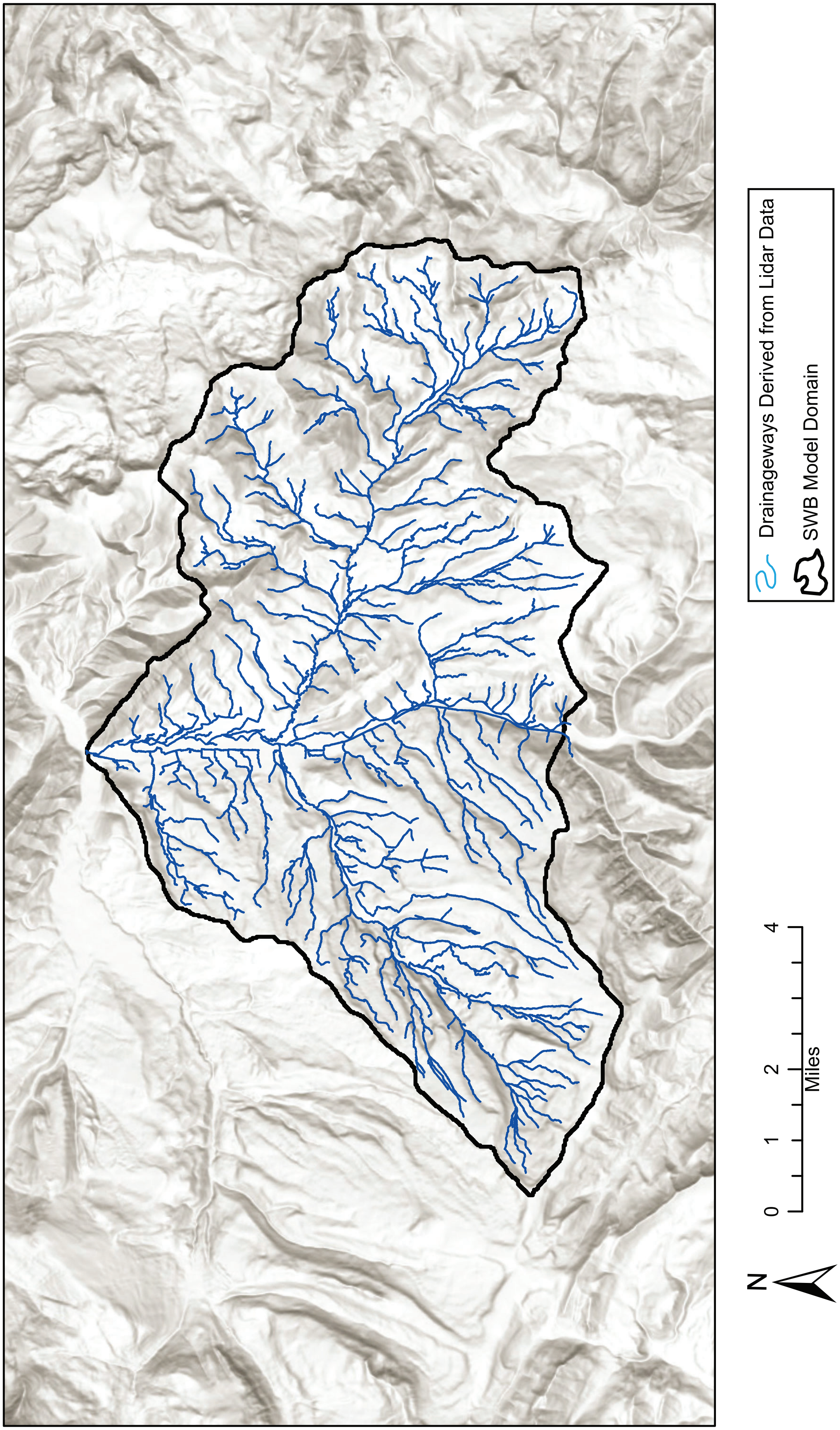

Figure A3. Drainageways derived from the lidar-based DEM and used to enforce downstream flow routing of overland runoff in the SWB model.

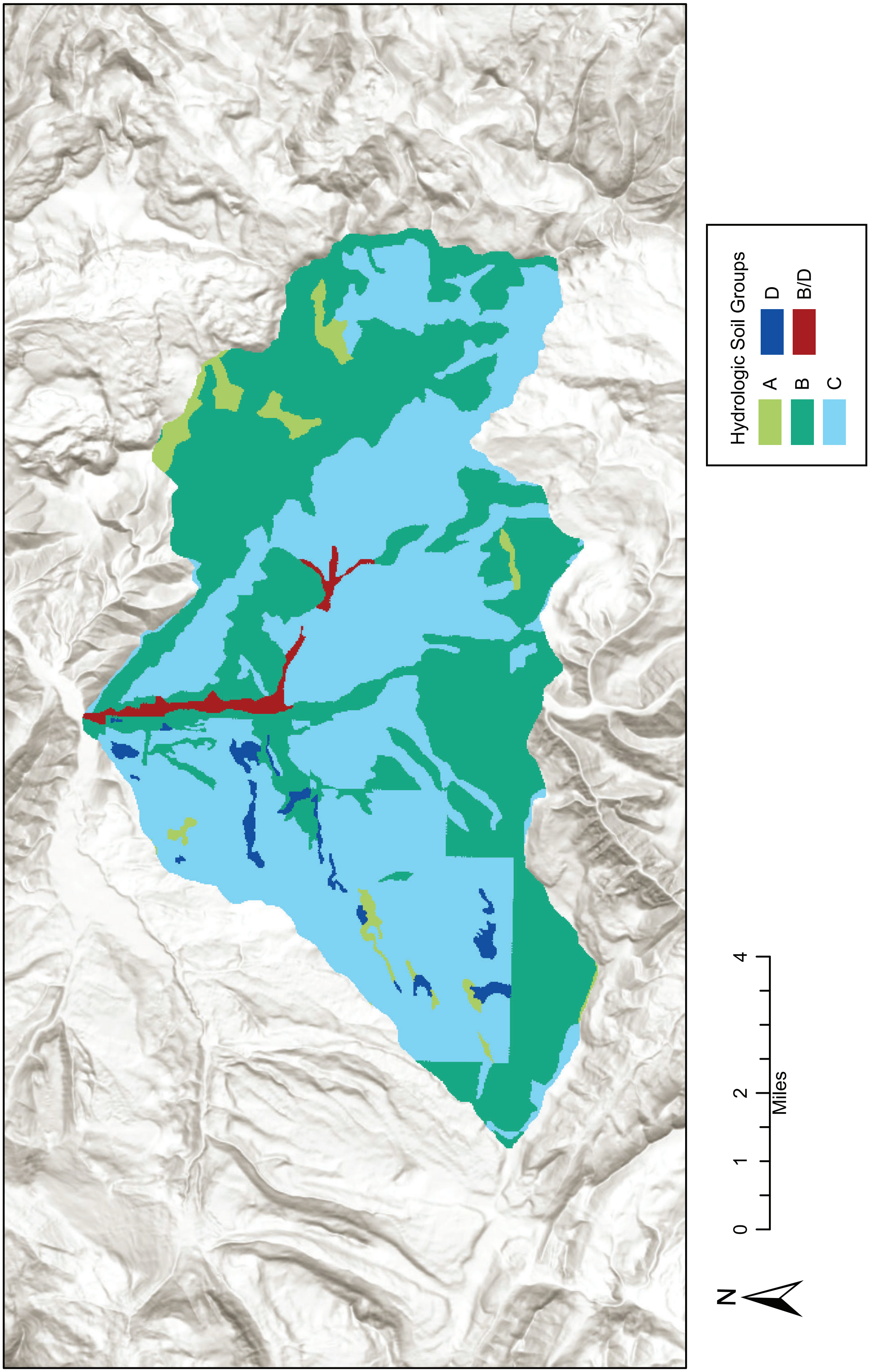

Figure A4. Active SWB model domain hydrologic soil group spatial distribution, mapped from gSSURGO.

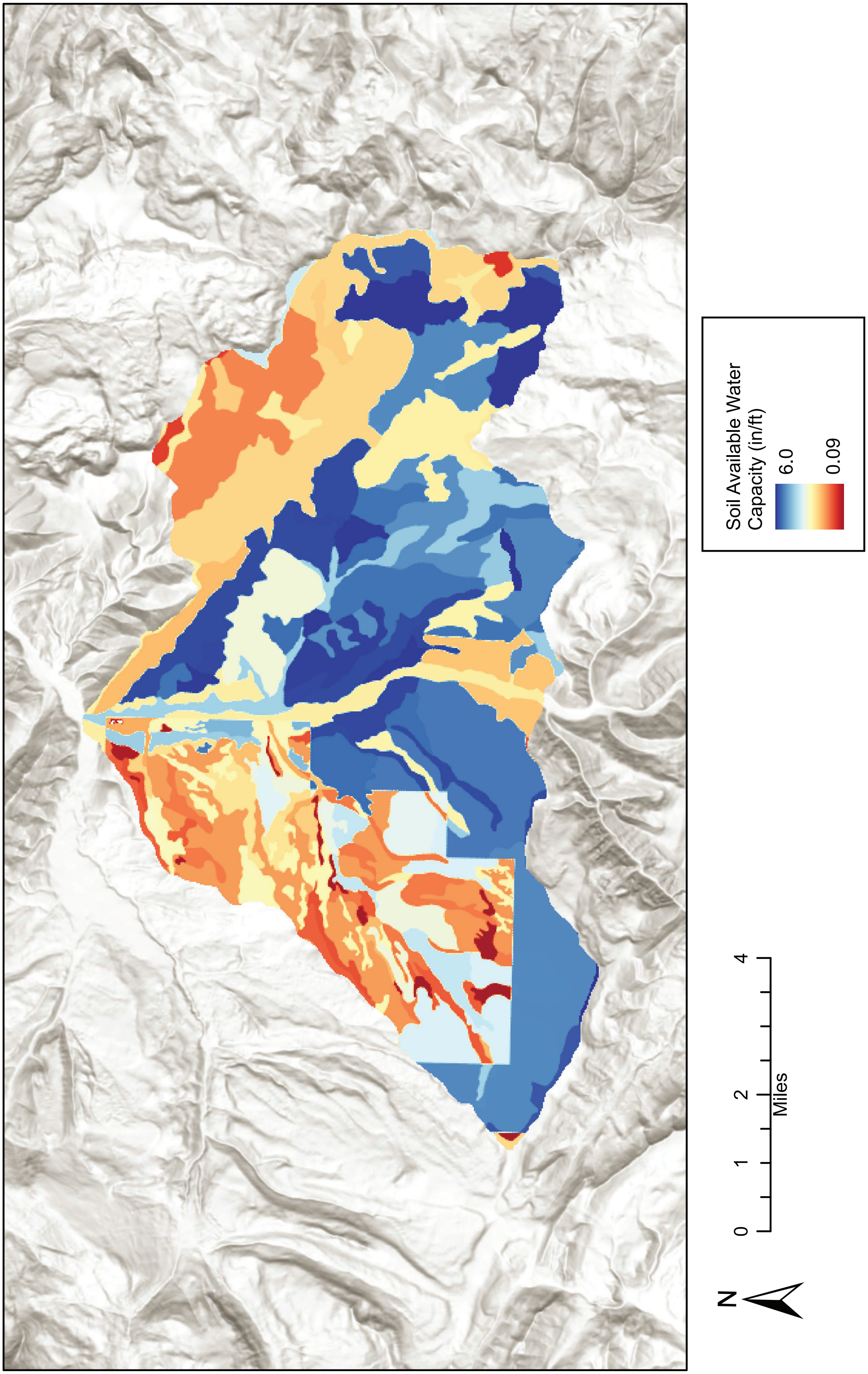

Figure A5. Active SWB model domain available water capacity spatial distribution, mapped from gSSURGO.

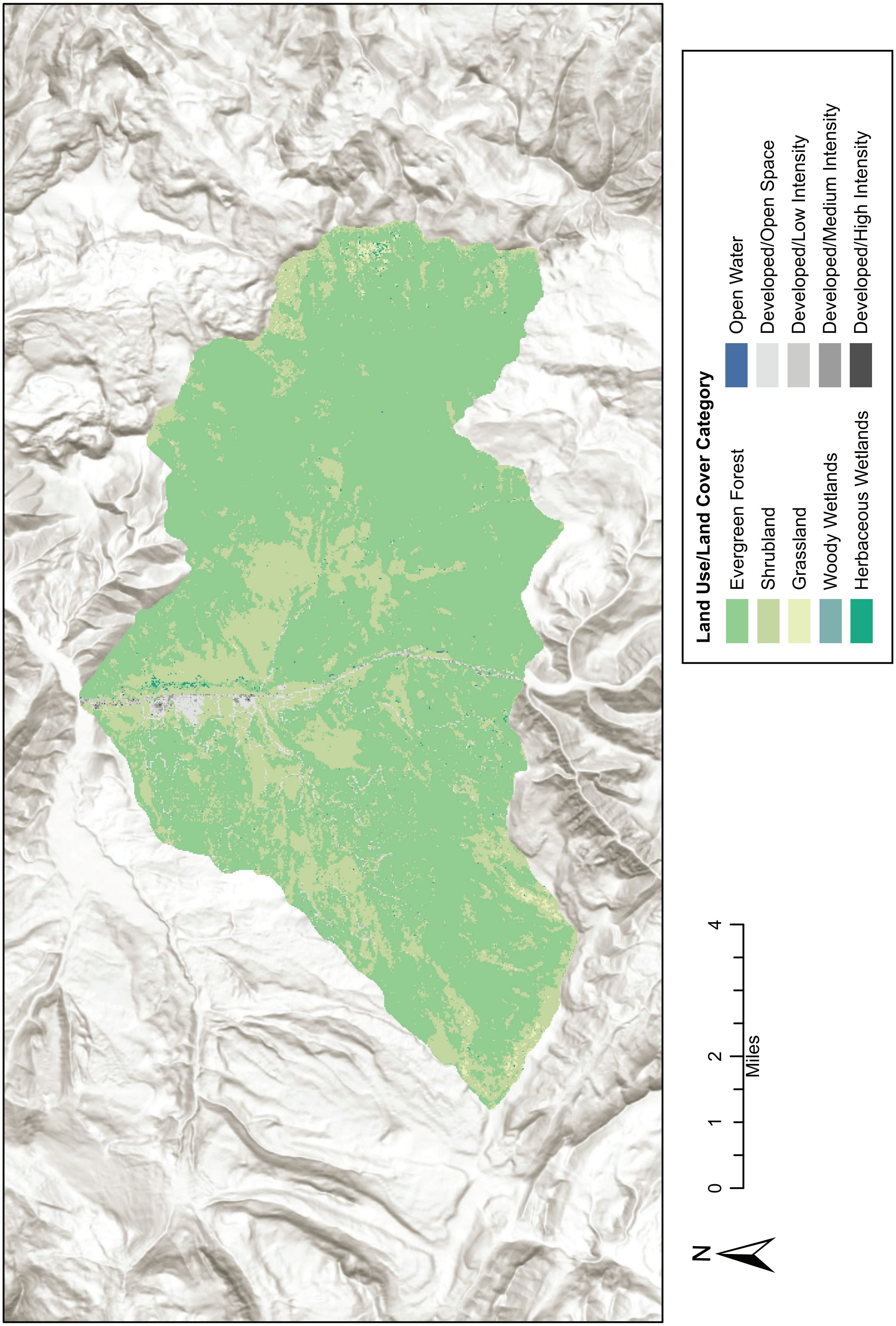

Figure A6. Active SWB model domain land use/land cover categories, mapped from the 2023 Cropland Data Layer.

use and HSG do not occur in the study area).

The vegetation water usage table includes plant growth settings such as basal crop coefficients (K_{cb}; K_{cb} values for onset of growth, plant maturity, and dormancy), growing season lengths, and bare soil evaporation settings for every land use/land cover category (Allen and others, 1998).

SWB MODEL EXECUTION

The SWB model code was executed for the years 2017 through 2023, inclusive. Because determining antecedent soil moisture conditions *a priori* for all model cells would be difficult if not impossible, the initial soil moisture percent condition was set to be 100% throughout the SWB model domain. Setting the initial soil moisture percent condition to 100% allows the SWB model code to deplete the soil moisture storage in each model cell due to ET and vertical downward drainage past the root zone (net infiltration or potential recharge). The year 2017 was then considered a model "warmup" period to determine reasonable antecedent soil moisture conditions for the period 2018–2023. SWB model outputs for 2018–2023 were considered for processing and developing the estimates for groundwater recharge in the groundwater flow model.

SWB MODEL OUTPUTS

The SWB model code produces daily gridded outputs for each of the calculated water balance terms in Network Common Data Format (netCDF; NSF Unidata, 2023). Python-based scripts were developed to read the netCDF file for net infiltration (potential recharge) produce the data needed for the groundwater flow model. These scripts aggregated the daily output potential recharge values to averaged values to be used in the groundwater flow model.

For each of the mountain block areas shown in figure A1, output potential recharge values were averaged as volumetric rates for the 2018–2023 period as estimates of longer term MBR. (Note that for the mountain block south of the groundwater flow model domain, the MBR generated would be expected to discharge to the alluvium and the Gallatin River itself upstream of the model domain and thus would be implemented in the groundwater flow model as alluvial groundwater inflow through the MODFLOW General Head Boundary Package.) Also, Beaver Creek and Porcupine Creek were observed to produce perennial streamflow outside the groundwater flow model domain throughout the year, and this streamflow represents MBR that has discharged to each of these streams. The volumetric streamflow discharge rates measured at each of these streams in late August 2020 (Beaver Creek at 1.67 cfs and Beaver Creek at 5.75 cfs) were subtracted from the corresponding averaged MBR volumetric rates to account for MBR that had already discharged to surface water. For each block, these average MBR volumetric rate values were distributed evenly to the MODFLOW Recharge Package cells at the perimeter of the groundwater flow model, as shown in figure A7 along with the average 2018–2023 net infiltration rates across the SWB model domain.

For the footprint of the groundwater flow model domain, output potential recharge values were averaged as area-weighted areal rates for July–September 2020 and March–May 2021 for the low- and high-flow periods, respectively. Because the groundwater flow model employs an unstructured grid not aligned with the SWB grid, areal potential recharge rates from the SWB outputs were assigned to the groundwater model grid as the area-weighted average value of the SWB outputs from each SWB cell partially overlapping each groundwater model cell. These recharge averaging periods represent the 2 months preceding and the first month of each of the groundwater flow model low- and high-flow stress periods, with the assumption that the groundwater conditions during these flow model conditions are responding to near-term prior recharge inputs as well as the likelihood that there is a lag time of potential infiltration traveling from just beneath the root zone to the water table to become actual (as opposed to potential) recharge. Figure A8 shows the SWB-estimated recharge used as areal recharge in the groundwater flow model. Note that for the low-flow period, the SWB-estimated areal recharge was zero across nearly the entire groundwater flow model domain. High potential recharge rates were estimated within the groundwater model domain beneath both Porcupine and Beaver Creeks for the high-flow period, as would be expected. Non-zero potential recharge rates were estimated over most of the remaining area of the groundwater flow model domain, as also would be expected.

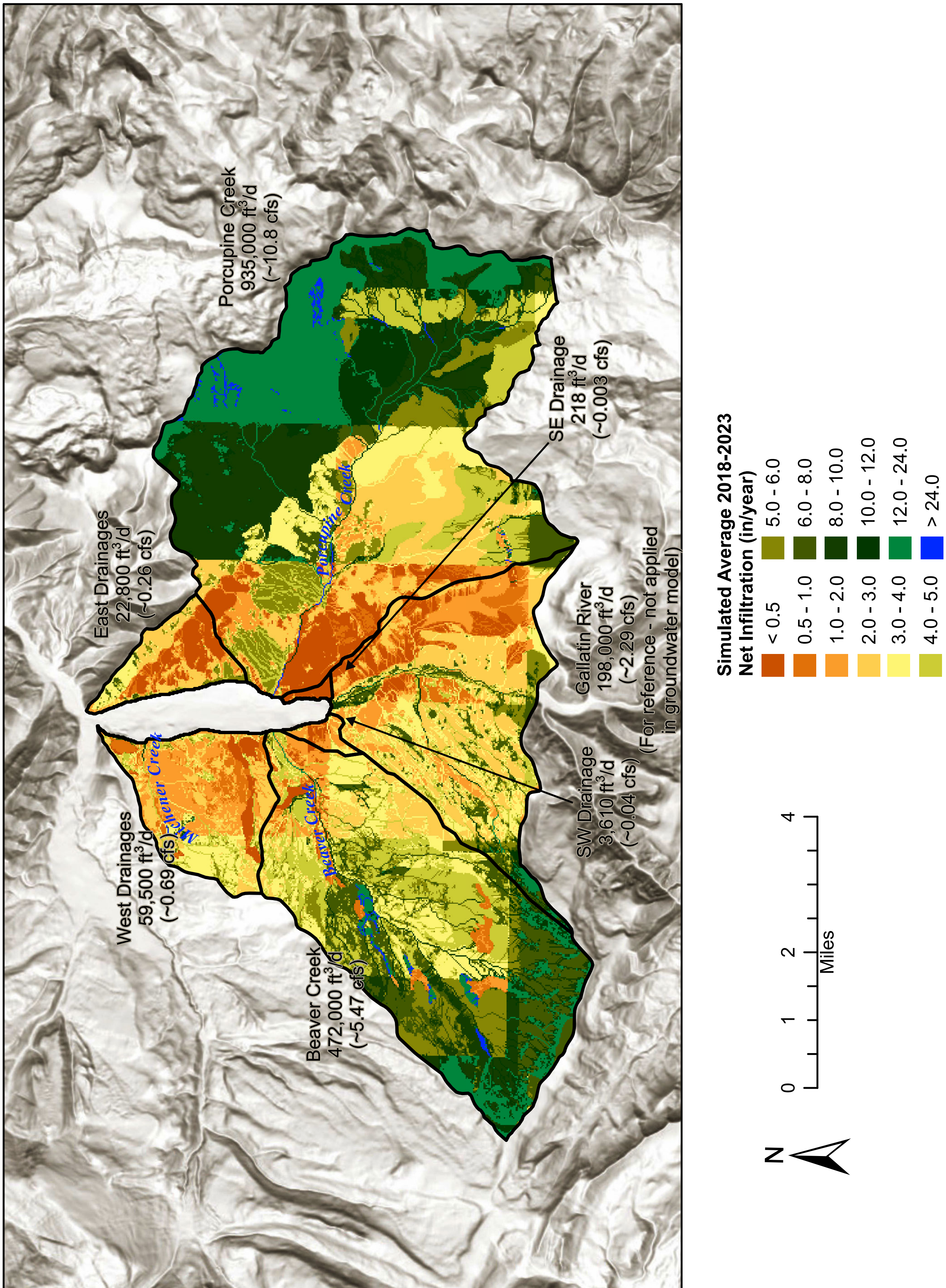

Figure A7. Average 2018 through 2023 SWB-simulated areal net infiltration rates in mountain block areas and resulting estimates of MBR volumetric rates applied in the groundwater flow model at the locations shown on figure A1.

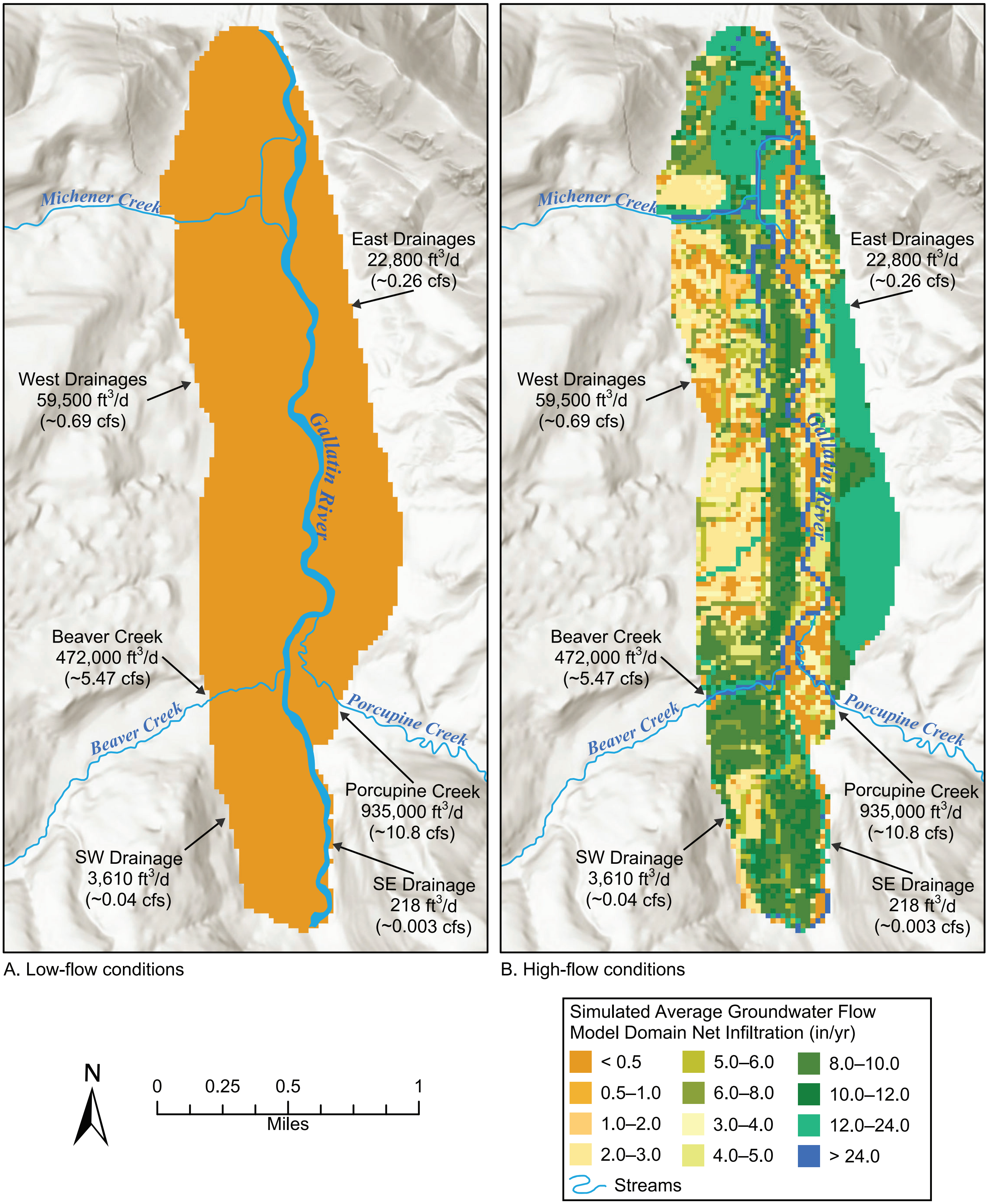

Figure A8. Average SWB-simulated areal net infiltration rates within the area of the groundwater flow model domain for SWB low (July through September 2020) and high-flow (March through May 2021) conditions.

APPENDIX B
MODEL GROUNDWATER-LEVEL CALIBRATION INFORMATION

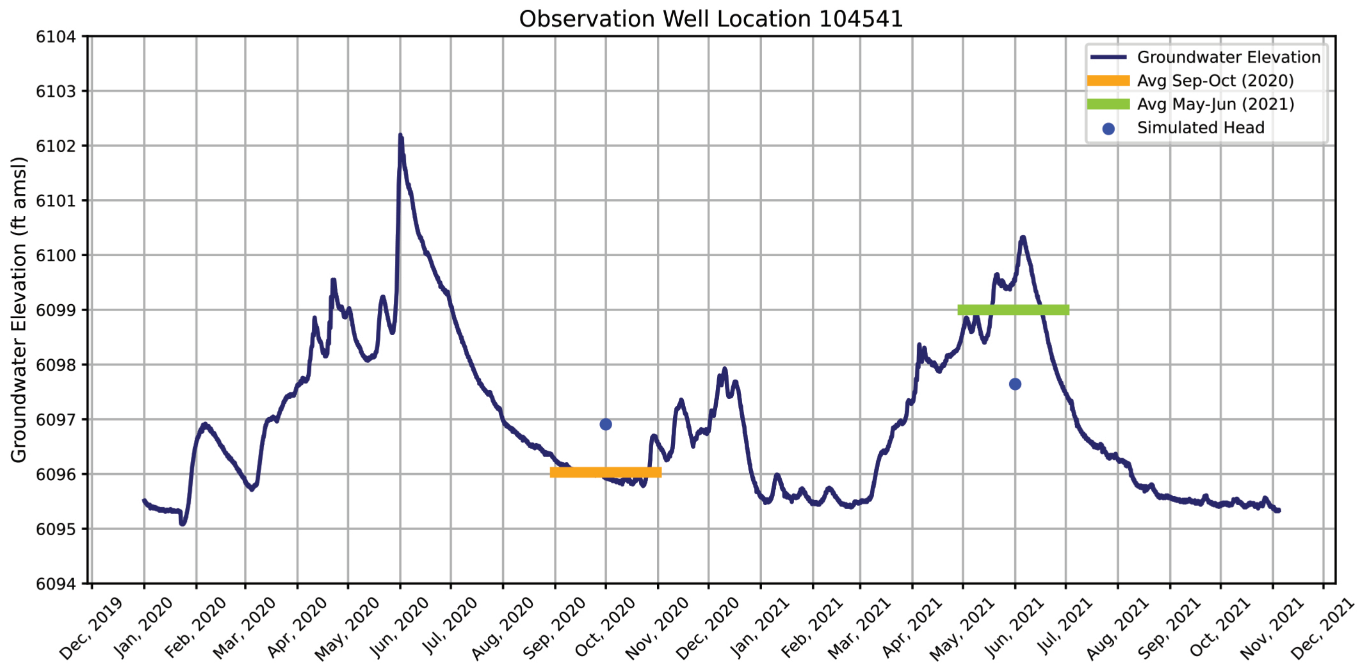
Observation Well Location 104541
Groundwater Elevation
Avg Sep-Oct (2020)
Avg May-Jun (2021)
Simulated Head
Groundwater Elevation (ft amsl)
6094
6095
6096
6097
6098
6099
6100
6101
6102
6103
6104
Dec, 2019
Jan, 2020
Feb, 2020
Mar, 2020
Apr, 2020
May, 2020
Jun, 2020
Jul, 2020
Aug, 2020
Sep, 2020
Oct, 2020
Nov, 2020
Dec, 2020
Jan, 2021
Feb, 2021
Mar, 2021
Apr, 2021
May, 2021
Jun, 2021
Jul, 2021
Aug, 2021
Sep, 2021
Oct, 2021
Nov, 2021
Dec, 2021

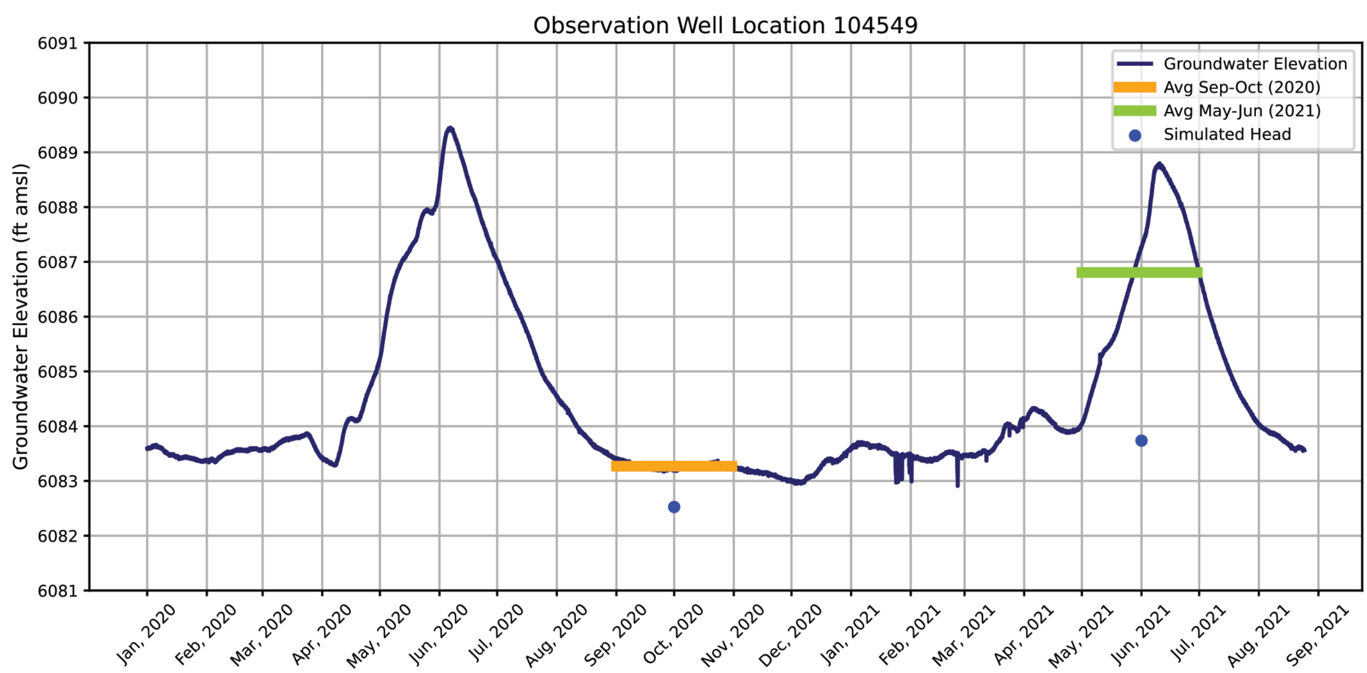
Observation Well Location 104549
Groundwater Elevation
Avg Sep-Oct (2020)
Avg May-Jun (2021)
Simulated Head
Groundwater Elevation (ft amsl)
6081
6082
6083
6084
6085
6086
6087
6088
6089
6090
6091
Jan, 2020
Feb, 2020
Mar, 2020
Apr, 2020
May, 2020
Jun, 2020
Jul, 2020
Aug, 2020
Sep, 2020
Oct, 2020
Nov, 2020
Dec, 2020
Jan, 2021
Feb, 2021
Mar, 2021
Apr, 2021
May, 2021
Jun, 2021
Jul, 2021
Aug, 2021
Sep, 2021

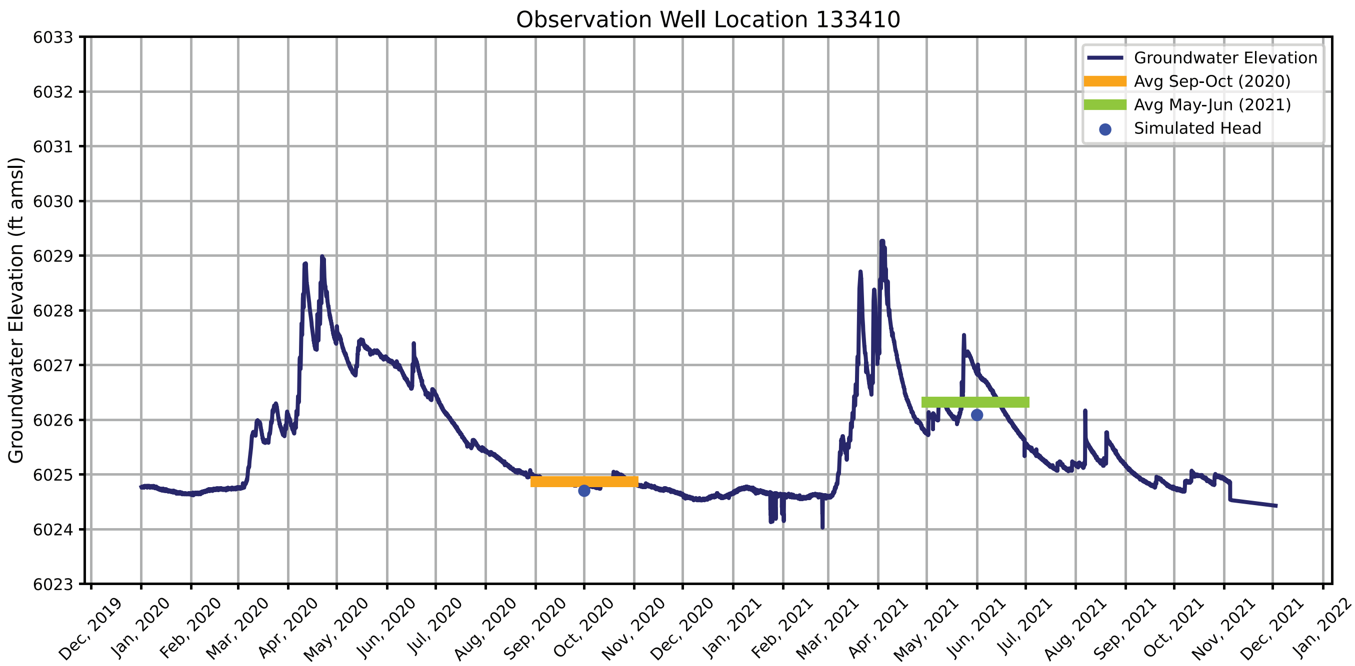
Observation Well Location 133410
Groundwater Elevation
Avg Sep-Oct (2020)
Avg May-Jun (2021)
Simulated Head
Groundwater Elevation (ft amsl)
6023
6024
6025
6026
6027
6028
6029
6030
6031
6032
6033
Dec, 2019
Jan, 2020
Feb, 2020
Mar, 2020
Apr, 2020
May, 2020
Jun, 2020
Jul, 2020
Aug, 2020
Sep, 2020
Oct, 2020
Nov, 2020
Dec, 2020
Jan, 2021
Feb, 2021
Mar, 2021
Apr, 2021
May, 2021
Jun, 2021
Jul, 2021
Aug, 2021
Sep, 2021
Oct, 2021
Nov, 2021
Dec, 2021
Jan, 2022

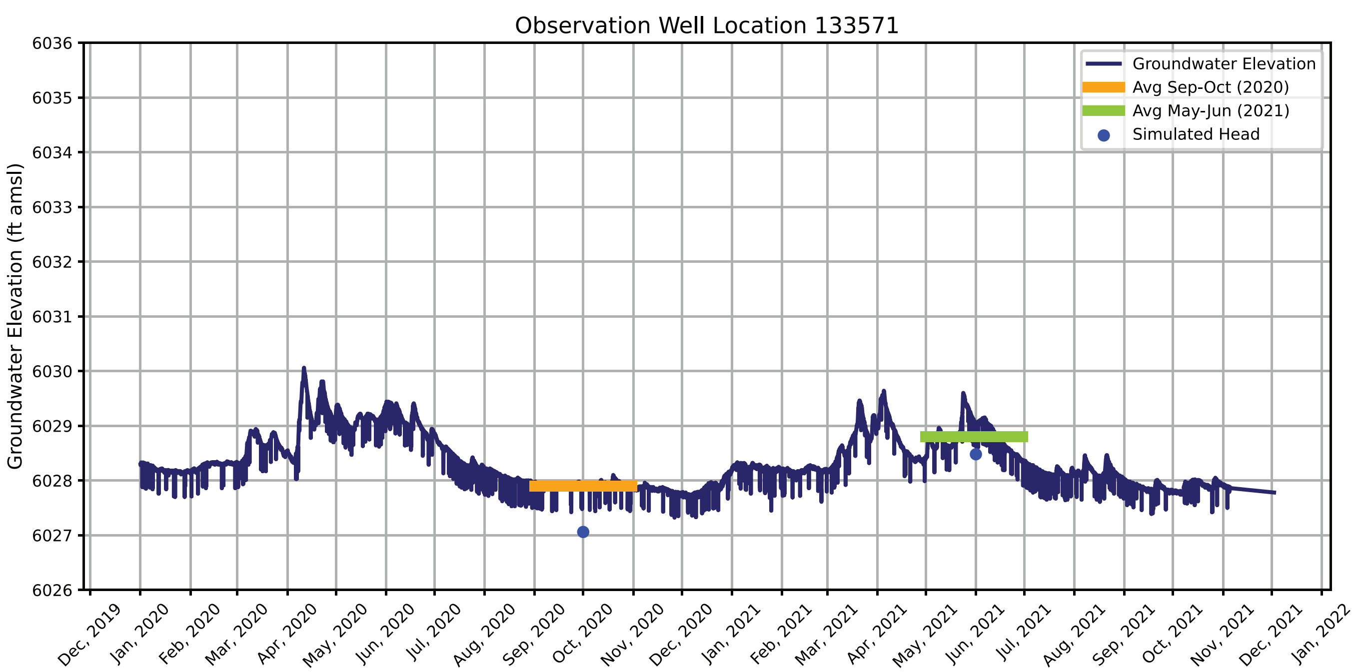
Observation Well Location 133571
Groundwater Elevation
Avg Sep-Oct (2020)
Avg May-Jun (2021)
Simulated Head
Groundwater Elevation (ft amsl)
6026
6027
6028
6029
6030
6031
6032
6033
6034
6035
6036
Dec, 2019
Jan, 2020
Feb, 2020
Mar, 2020
Apr, 2020
May, 2020
Jun, 2020
Jul, 2020
Aug, 2020
Sep, 2020
Oct, 2020
Nov, 2020
Dec, 2020
Jan, 2021
Feb, 2021
Mar, 2021
Apr, 2021
May, 2021
Jun, 2021
Jul, 2021
Aug, 2021
Sep, 2021
Oct, 2021
Nov, 2021
Dec, 2021
Jan, 2022

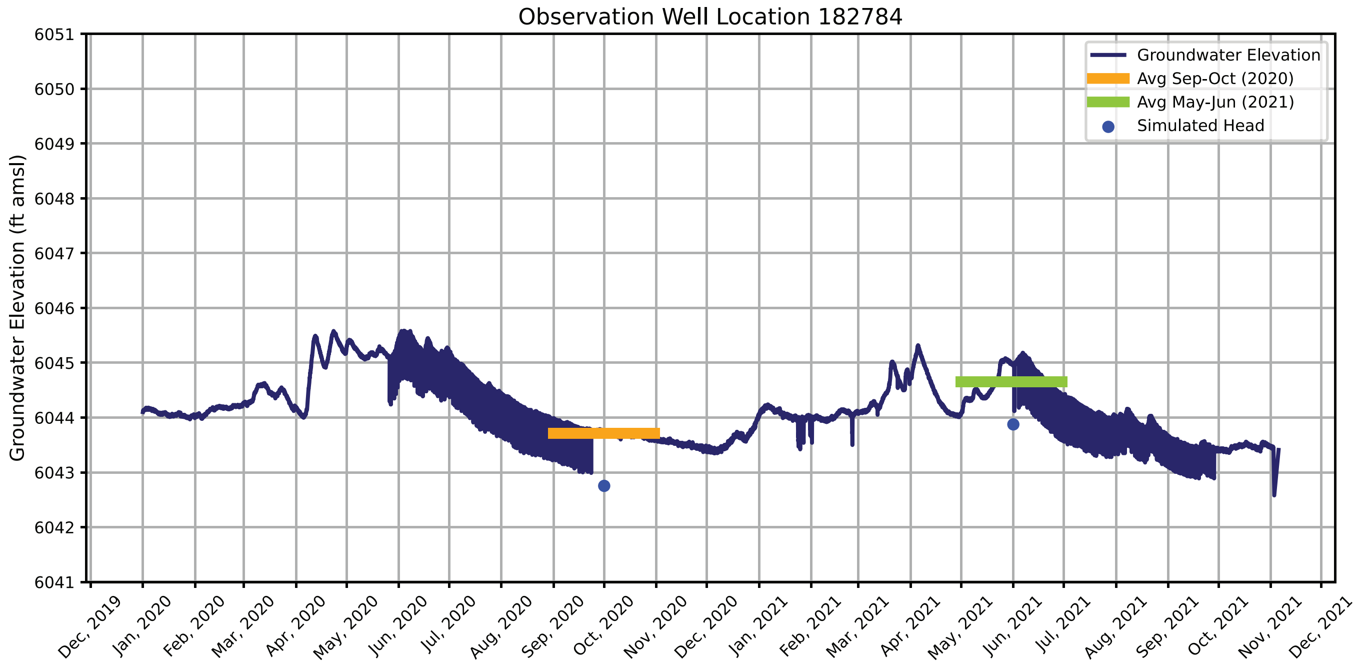
Observation Well Location 182784
Groundwater Elevation
Avg Sep-Oct (2020)
Avg May-Jun (2021)
Simulated Head
Groundwater Elevation (ft amsl)
6051
6050
6049
6048
6047
6046
6045
6044
6043
6042
6041
Dec, 2019
Jan, 2020
Feb, 2020
Mar, 2020
Apr, 2020
May, 2020
Jun, 2020
Jul, 2020
Aug, 2020
Sep, 2020
Oct, 2020
Nov, 2020
Dec, 2020
Jan, 2021
Feb, 2021
Mar, 2021
Apr, 2021
May, 2021
Jun, 2021
Jul, 2021
Aug, 2021
Sep, 2021
Oct, 2021
Nov, 2021
Dec, 2021

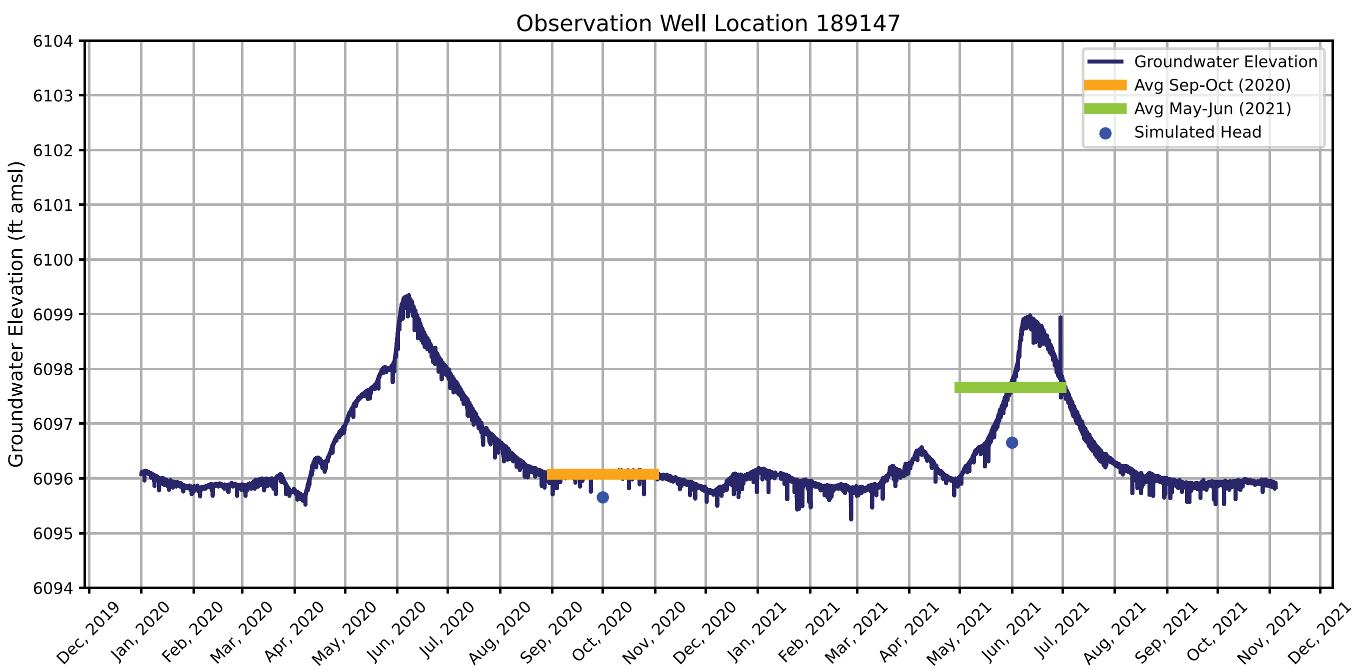
Observation Well Location 189147
Groundwater Elevation
Avg Sep-Oct (2020)
Avg May-Jun (2021)
Simulated Head
Groundwater Elevation (ft amsl)
6104
6103
6102
6101
6100
6099
6098
6097
6096
6095
6094
Dec, 2019
Jan, 2020
Feb, 2020
Mar, 2020
Apr, 2020
May, 2020
Jun, 2020
Jul, 2020
Aug, 2020
Sep, 2020
Oct, 2020
Nov, 2020
Dec, 2020
Jan, 2021
Feb, 2021
Mar, 2021
Apr, 2021
May, 2021
Jun, 2021
Jul, 2021
Aug, 2021
Sep, 2021
Oct, 2021
Nov, 2021
Dec, 2021

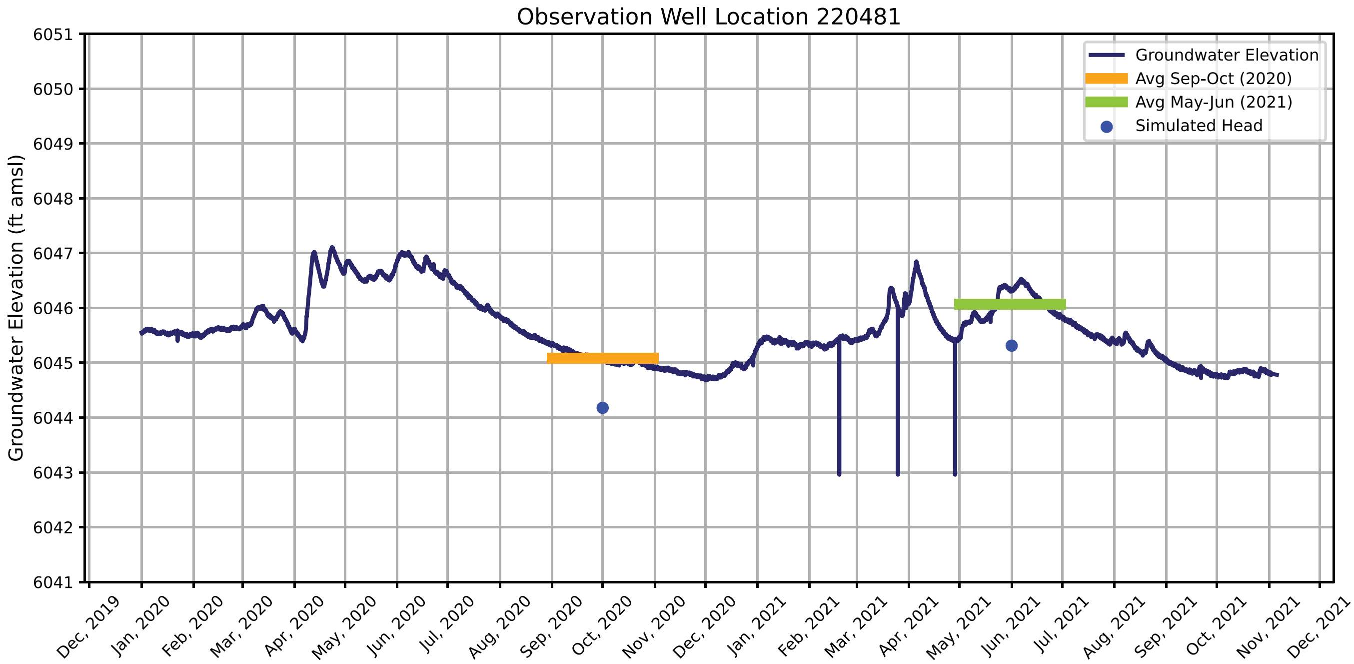
Observation Well Location 220481
Groundwater Elevation
Avg Sep-Oct (2020)
Avg May-Jun (2021)
Simulated Head
Groundwater Elevation (ft amsl)
6051
6050
6049
6048
6047
6046
6045
6044
6043
6042
6041
Dec, 2019
Jan, 2020
Feb, 2020
Mar, 2020
Apr, 2020
May, 2020
Jun, 2020
Jul, 2020
Aug, 2020
Sep, 2020
Oct, 2020
Nov, 2020
Dec, 2020
Jan, 2021
Feb, 2021
Mar, 2021
Apr, 2021
May, 2021
Jun, 2021
Jul, 2021
Aug, 2021
Sep, 2021
Oct, 2021
Nov, 2021
Dec, 2021

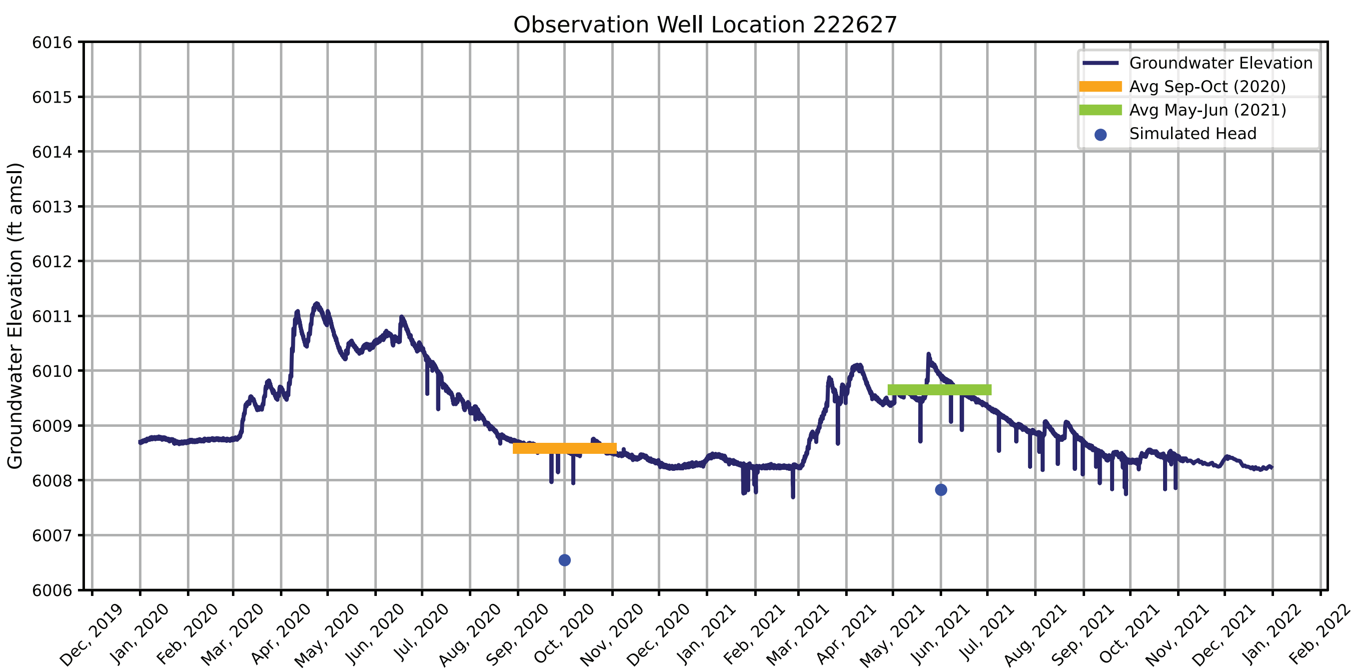
Observation Well Location 222627
Groundwater Elevation
Avg Sep-Oct (2020)
Avg May-Jun (2021)
Simulated Head
Groundwater Elevation (ft amsl)
6016
6015
6014
6013
6012
6011
6010
6009
6008
6007
6006
Dec, 2019
Jan, 2020
Feb, 2020
Mar, 2020
Apr, 2020
May, 2020
Jun, 2020
Jul, 2020
Aug, 2020
Sep, 2020
Oct, 2020
Nov, 2020
Dec, 2020
Jan, 2021
Feb, 2021
Mar, 2021
Apr, 2021
May, 2021
Jun, 2021
Jul, 2021
Aug, 2021
Sep, 2021
Oct, 2021
Nov, 2021
Dec, 2021
Jan, 2022
Feb, 2022

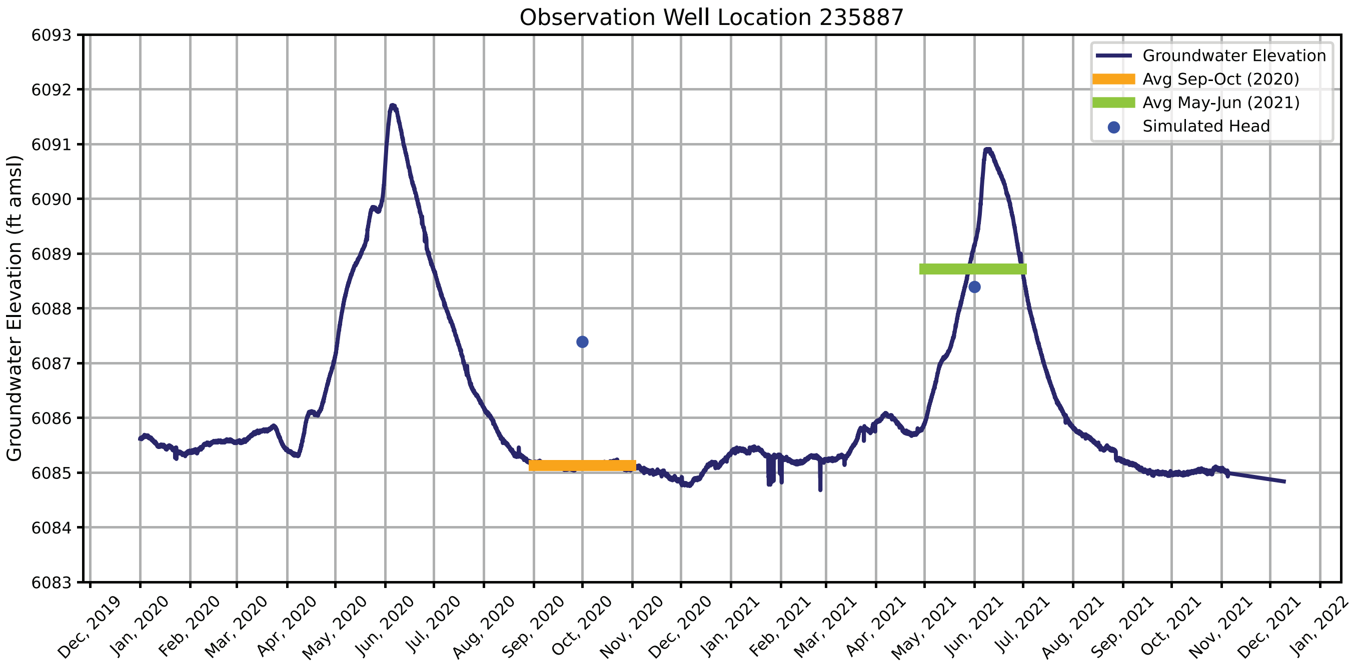
Observation Well Location 235887
Groundwater Elevation (ft amsl)
6093
6092
6091
6090
6089
6088
6087
6086
6085
6084
6083
Groundwater Elevation
Avg Sep-Oct (2020)
Avg May-Jun (2021)
Simulated Head
Dec, 2019
Jan, 2020
Feb, 2020
Mar, 2020
Apr, 2020
May, 2020
Jun, 2020
Jul, 2020
Aug, 2020
Sep, 2020
Oct, 2020
Nov, 2020
Dec, 2020
Jan, 2021
Feb, 2021
Mar, 2021
Apr, 2021
May, 2021
Jun, 2021
Jul, 2021
Aug, 2021
Sep, 2021
Oct, 2021
Nov, 2021
Dec, 2021
Jan, 2022

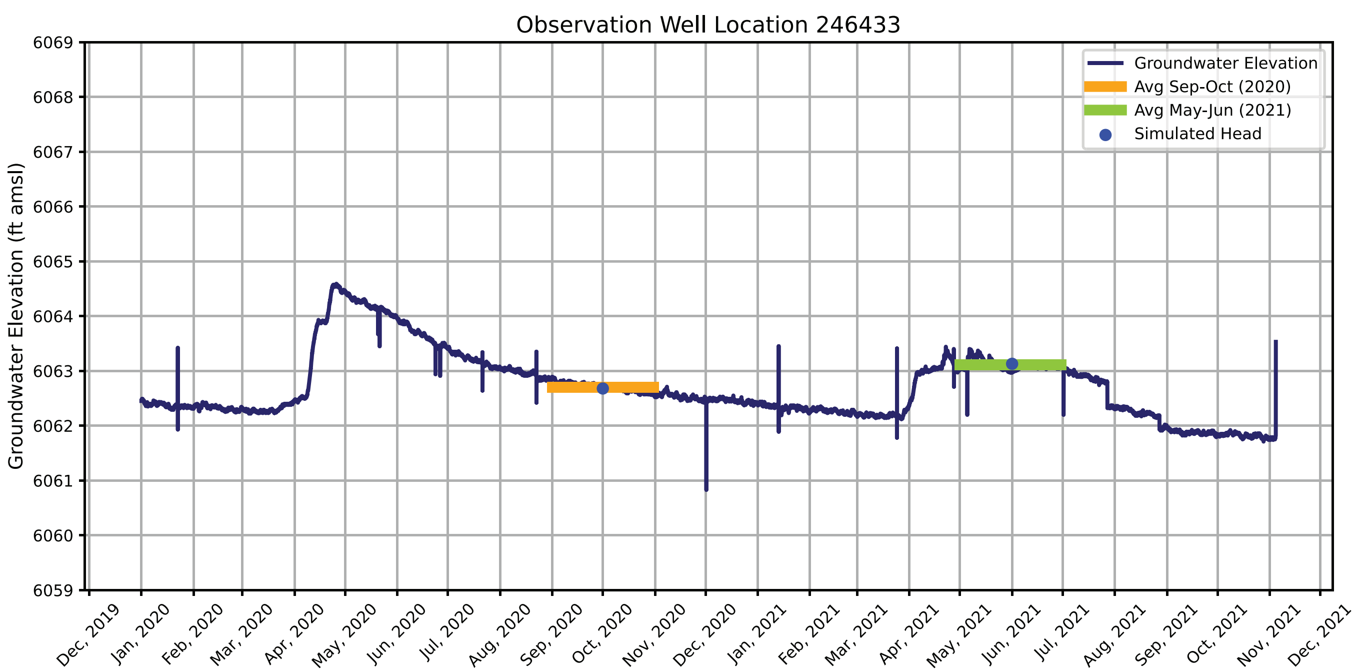
Observation Well Location 246433
Groundwater Elevation (ft amsl)
6069
6068
6067
6066
6065
6064
6063
6062
6061
6060
6059
Groundwater Elevation
Avg Sep-Oct (2020)
Avg May-Jun (2021)
Simulated Head
Dec, 2019
Jan, 2020
Feb, 2020
Mar, 2020
Apr, 2020
May, 2020
Jun, 2020
Jul, 2020
Aug, 2020
Sep, 2020
Oct, 2020
Nov, 2020
Dec, 2020
Jan, 2021
Feb, 2021
Mar, 2021
Apr, 2021
May, 2021
Jun, 2021
Jul, 2021
Aug, 2021
Sep, 2021
Oct, 2021
Nov, 2021
Dec, 2021

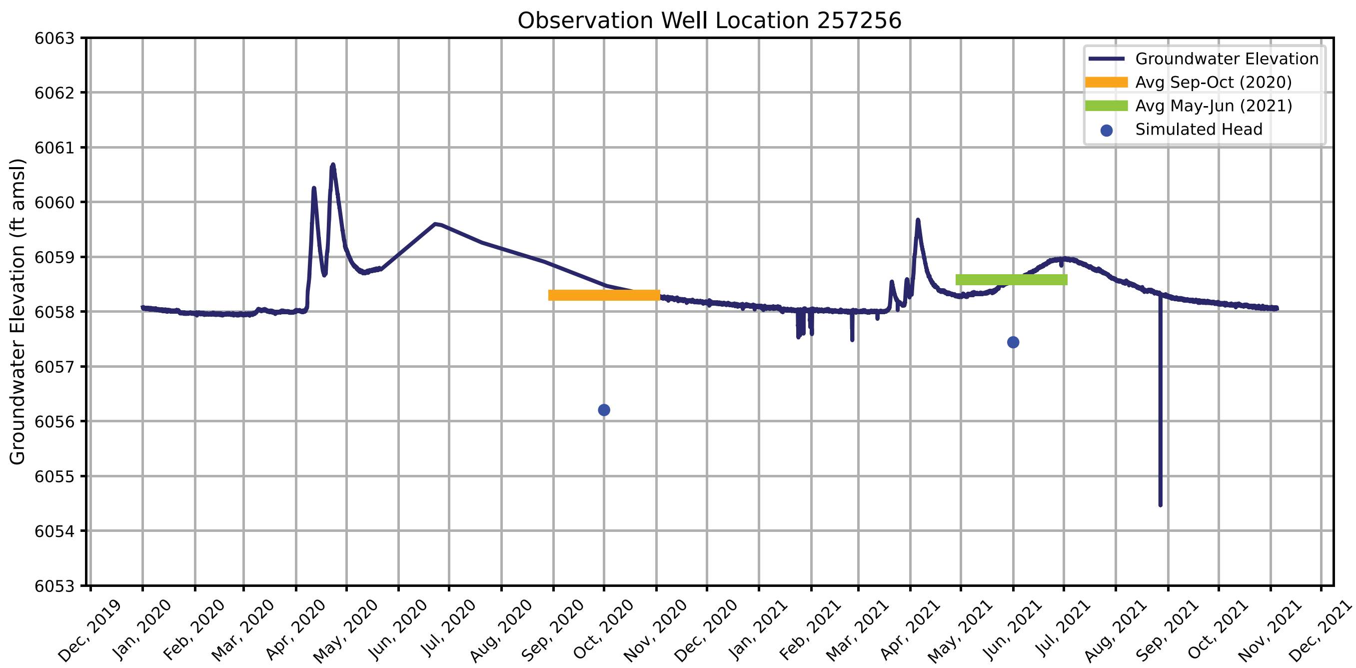
Observation Well Location 257256
Groundwater Elevation
Avg Sep-Oct (2020)
Avg May-Jun (2021)
Simulated Head
Groundwater Elevation (ft amsl)
6063
6062
6061
6060
6059
6058
6057
6056
6055
6054
6053
Dec, 2019
Jan, 2020
Feb, 2020
Mar, 2020
Apr, 2020
May, 2020
Jun, 2020
Jul, 2020
Aug, 2020
Sep, 2020
Oct, 2020
Nov, 2020
Dec, 2020
Jan, 2021
Feb, 2021
Mar, 2021
Apr, 2021
May, 2021
Jun, 2021
Jul, 2021
Aug, 2021
Sep, 2021
Oct, 2021
Nov, 2021
Dec, 2021

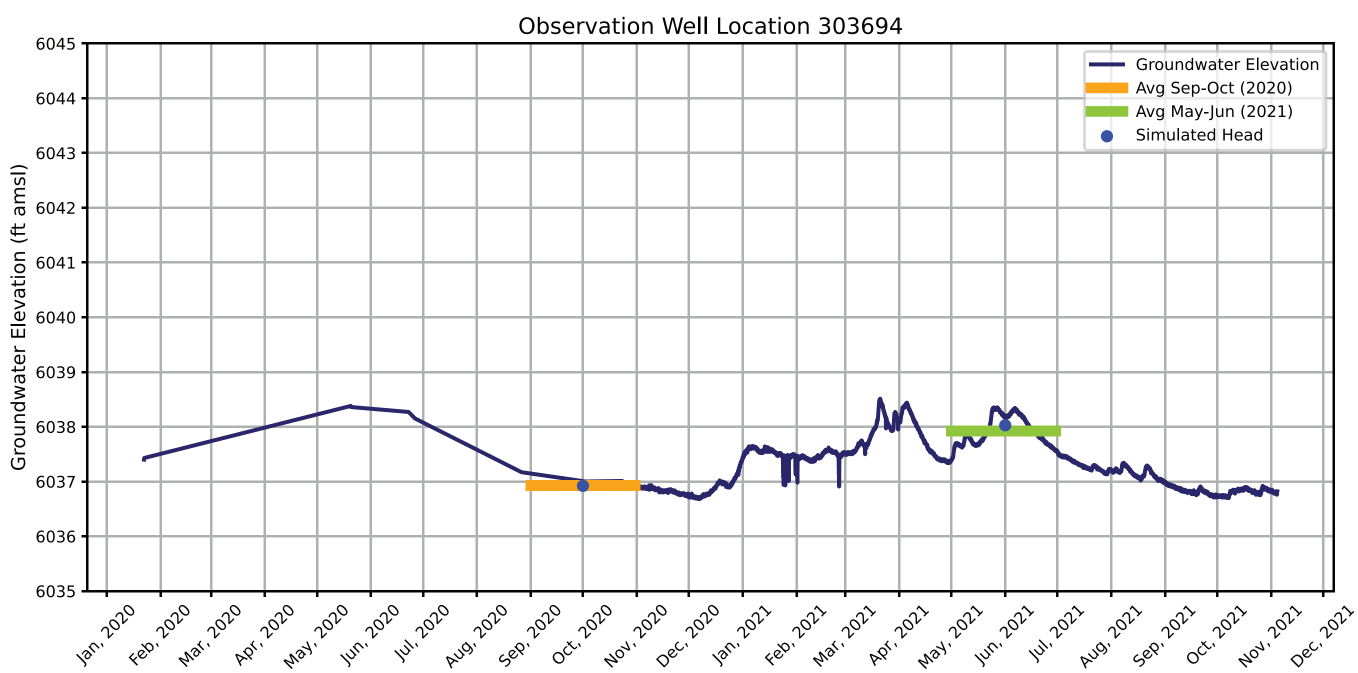
Observation Well Location 303694
Groundwater Elevation
Avg Sep-Oct (2020)
Avg May-Jun (2021)
Simulated Head
Groundwater Elevation (ft amsl)
6045
6044
6043
6042
6041
6040
6039
6038
6037
6036
6035
Jan, 2020
Feb, 2020
Mar, 2020
Apr, 2020
May, 2020
Jun, 2020
Jul, 2020
Aug, 2020
Sep, 2020
Oct, 2020
Nov, 2020
Dec, 2020
Jan, 2021
Feb, 2021
Mar, 2021
Apr, 2021
May, 2021
Jun, 2021
Jul, 2021
Aug, 2021
Sep, 2021
Oct, 2021
Nov, 2021
Dec, 2021

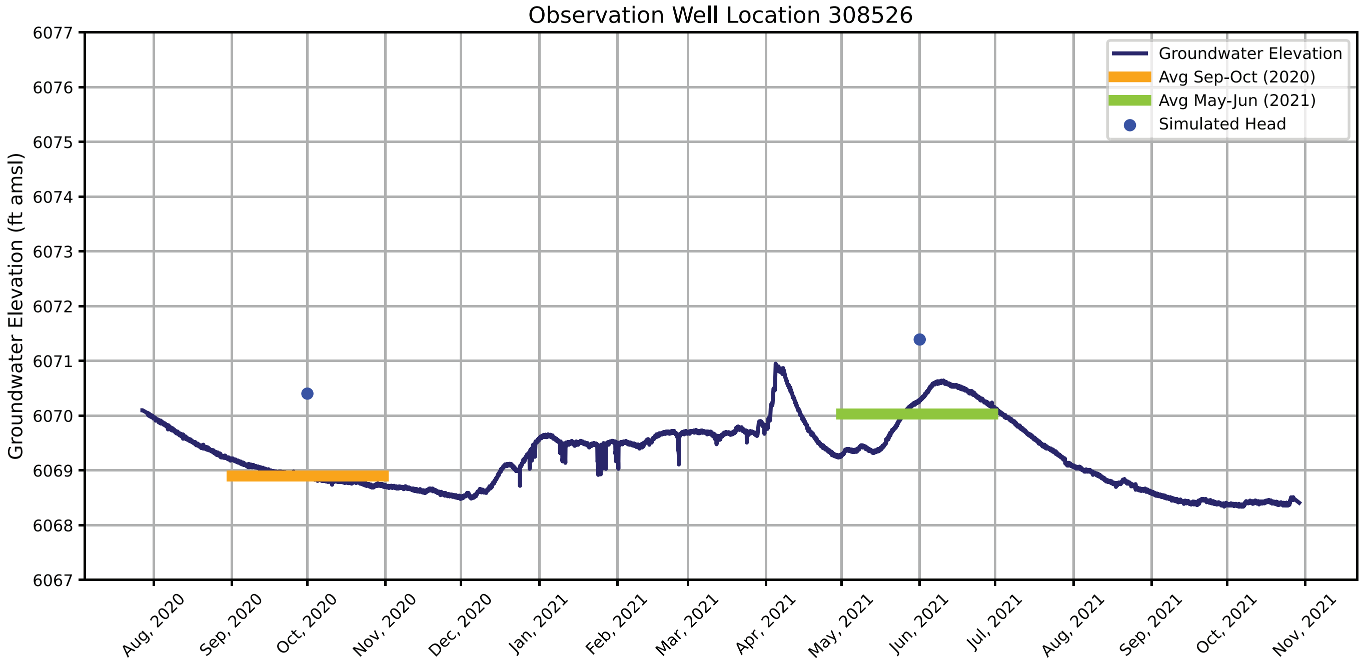
Observation Well Location 308526
Groundwater Elevation
Avg Sep-Oct (2020)
Avg May-Jun (2021)
Simulated Head
Groundwater Elevation (ft amsl)
6077
6076
6075
6074
6073
6072
6071
6070
6069
6068
6067
Aug, 2020
Sep, 2020
Oct, 2020
Nov, 2020
Dec, 2020
Jan, 2021
Feb, 2021
Mar, 2021
Apr, 2021
May, 2021
Jun, 2021
Jul, 2021
Aug, 2021
Sep, 2021
Oct, 2021
Nov, 2021

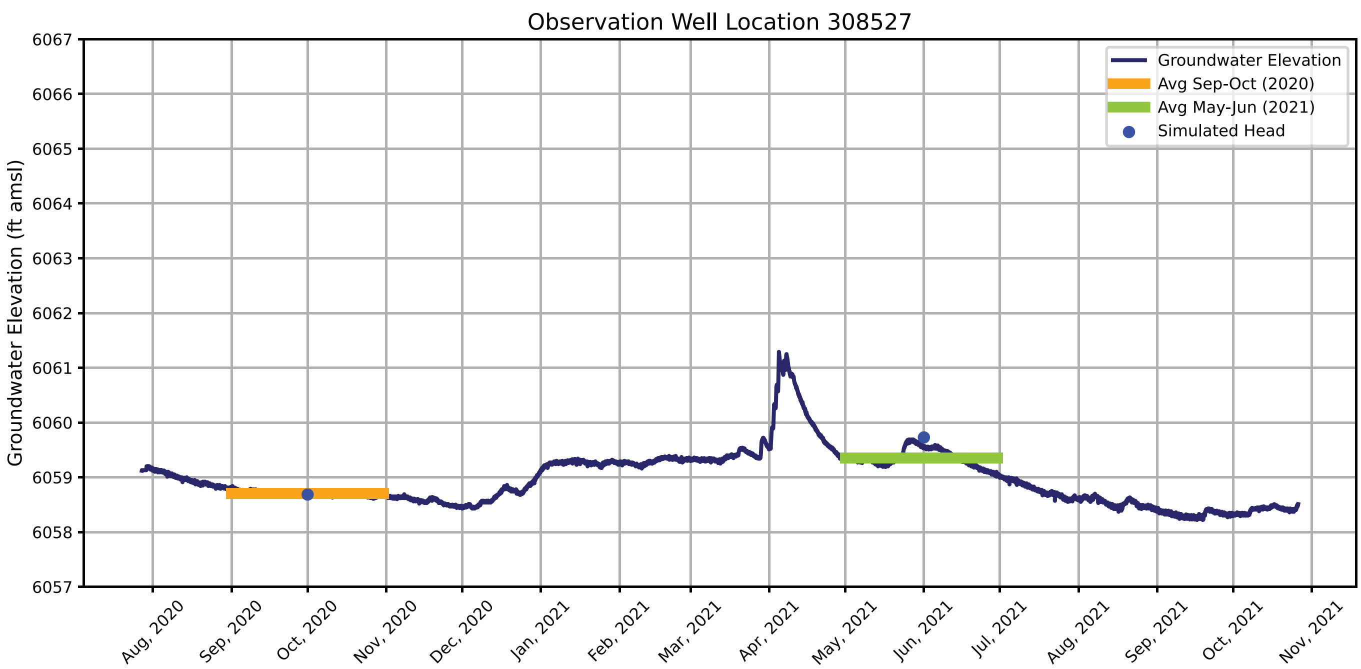
Observation Well Location 308527
Groundwater Elevation
Avg Sep-Oct (2020)
Avg May-Jun (2021)
Simulated Head
Groundwater Elevation (ft amsl)
6067
6066
6065
6064
6063
6062
6061
6060
6059
6058
6057
Aug, 2020
Sep, 2020
Oct, 2020
Nov, 2020
Dec, 2020
Jan, 2021
Feb, 2021
Mar, 2021
Apr, 2021
May, 2021
Jun, 2021
Jul, 2021
Aug, 2021
Sep, 2021
Oct, 2021
Nov, 2021

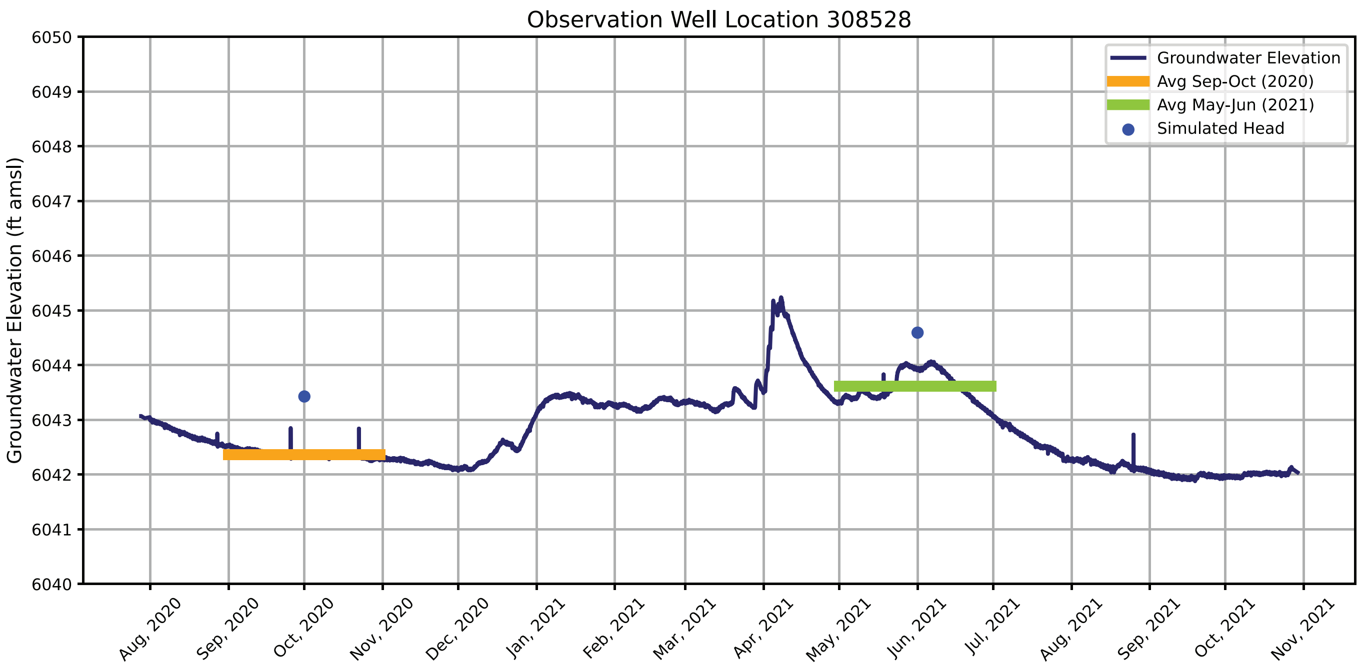
Observation Well Location 308528
Groundwater Elevation
Avg Sep-Oct (2020)
Avg May-Jun (2021)
Simulated Head
Groundwater Elevation (ft amsl)
6040
6041
6042
6043
6044
6045
6046
6047
6048
6049
6050
Aug, 2020
Sep, 2020
Oct, 2020
Nov, 2020
Dec, 2020
Jan, 2021
Feb, 2021
Mar, 2021
Apr, 2021
May, 2021
Jun, 2021
Jul, 2021
Aug, 2021
Sep, 2021
Oct, 2021
Nov, 2021

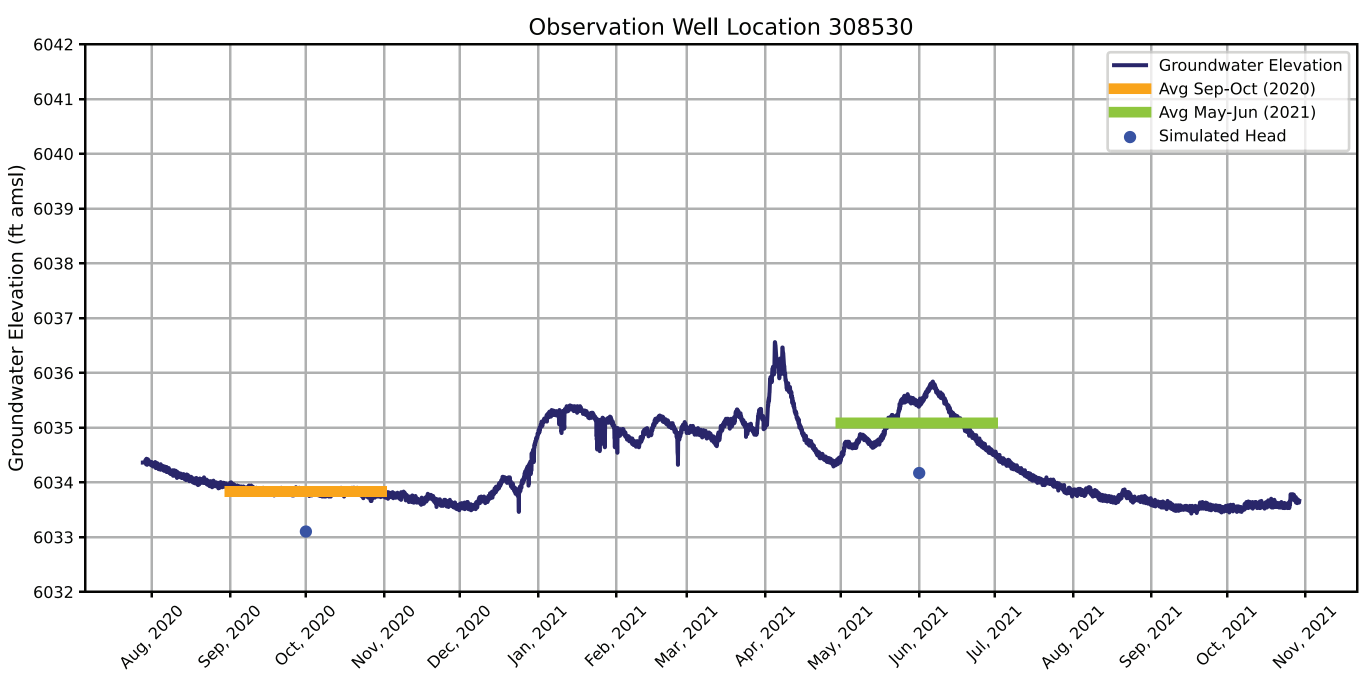
Observation Well Location 308530
Groundwater Elevation
Avg Sep-Oct (2020)
Avg May-Jun (2021)
Simulated Head
Groundwater Elevation (ft amsl)
6032
6033
6034
6035
6036
6037
6038
6039
6040
6041
6042
Aug, 2020
Sep, 2020
Oct, 2020
Nov, 2020
Dec, 2020
Jan, 2021
Feb, 2021
Mar, 2021
Apr, 2021
May, 2021
Jun, 2021
Jul, 2021
Aug, 2021
Sep, 2021
Oct, 2021
Nov, 2021

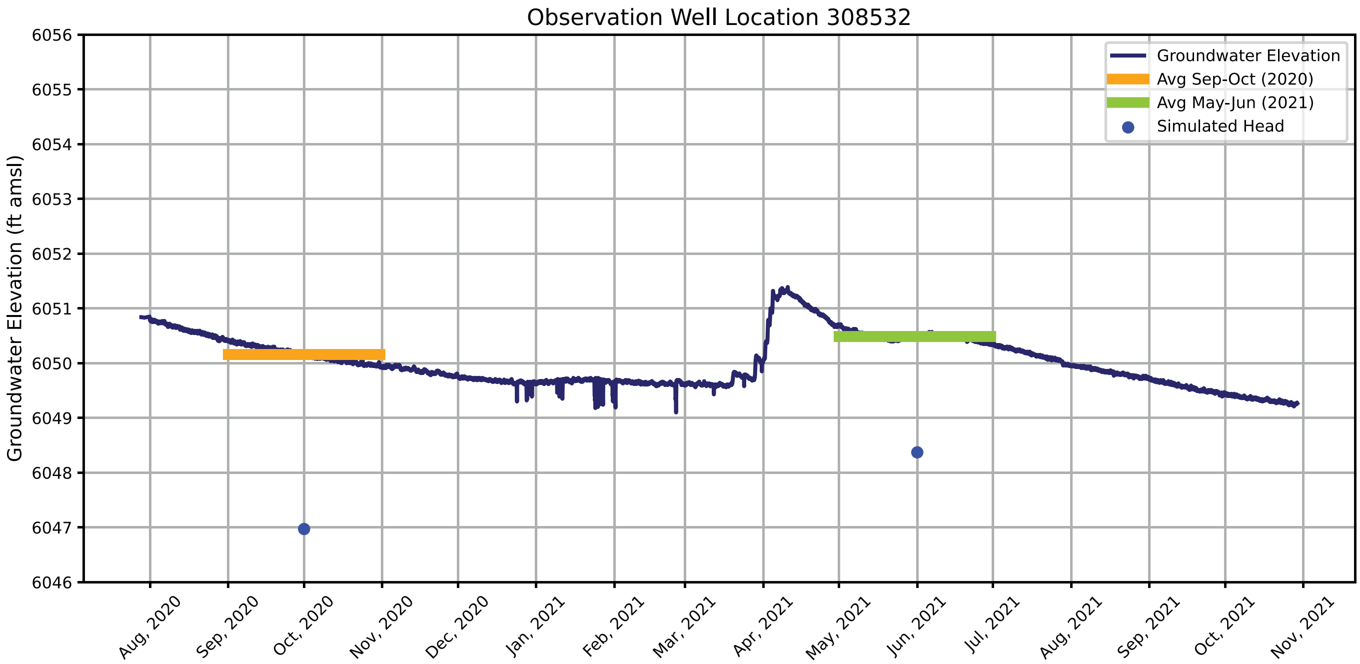
Observation Well Location 308532
Groundwater Elevation
Avg Sep-Oct (2020)
Avg May-Jun (2021)
Simulated Head
Groundwater Elevation (ft amsl)
6056
6055
6054
6053
6052
6051
6050
6049
6048
6047
6046
Aug, 2020
Sep, 2020
Oct, 2020
Nov, 2020
Dec, 2020
Jan, 2021
Feb, 2021
Mar, 2021
Apr, 2021
May, 2021
Jun, 2021
Jul, 2021
Aug, 2021
Sep, 2021
Oct, 2021
Nov, 2021

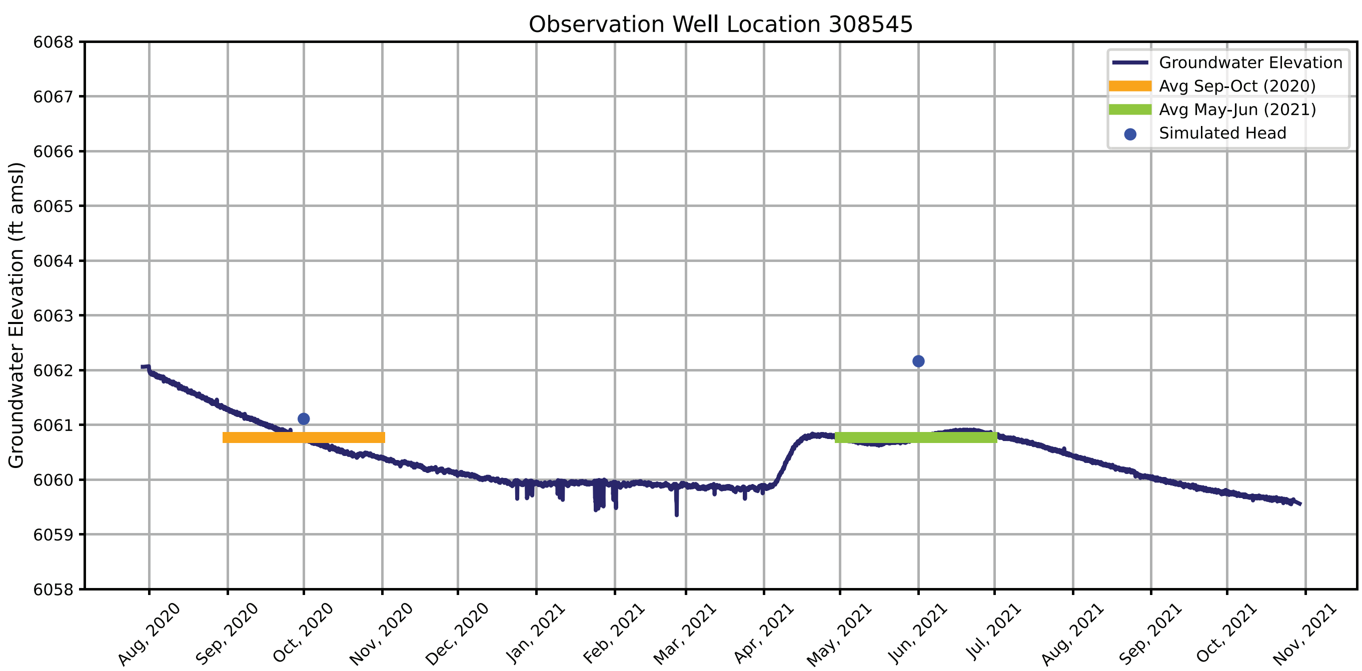
Observation Well Location 308545
Groundwater Elevation
Avg Sep-Oct (2020)
Avg May-Jun (2021)
Simulated Head
Groundwater Elevation (ft amsl)
6068
6067
6066
6065
6064
6063
6062
6061
6060
6059
6058
Aug, 2020
Sep, 2020
Oct, 2020
Nov, 2020
Dec, 2020
Jan, 2021
Feb, 2021
Mar, 2021
Apr, 2021
May, 2021
Jun, 2021
Jul, 2021
Aug, 2021
Sep, 2021
Oct, 2021
Nov, 2021

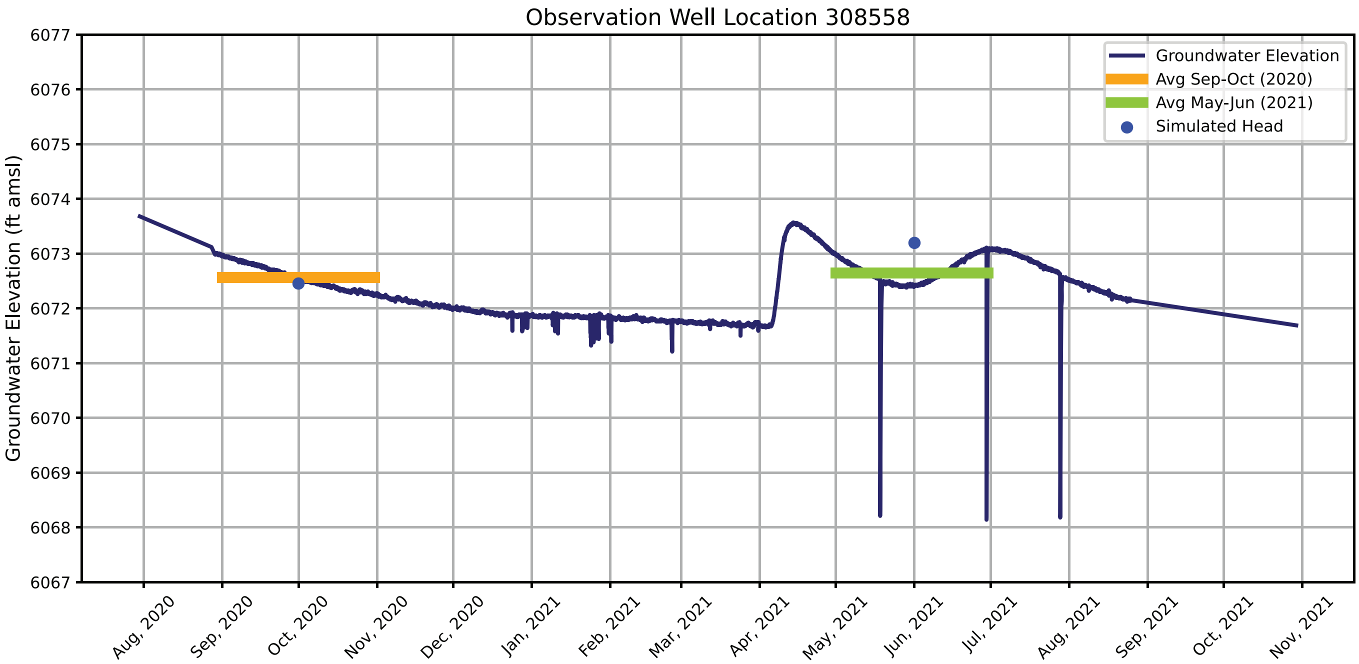

Observation Well Location 308558
Groundwater Elevation
Avg Sep-Oct (2020)
Avg May-Jun (2021)
Simulated Head
Groundwater Elevation (ft amsl)
6077
6076
6075
6074
6073
6072
6071
6070
6069
6068
6067
Aug, 2020
Sep, 2020
Oct, 2020
Nov, 2020
Dec, 2020
Jan, 2021
Feb, 2021
Mar, 2021
Apr, 2021
May, 2021
Jun, 2021
Jul, 2021
Aug, 2021
Sep, 2021
Oct, 2021
Nov, 2021

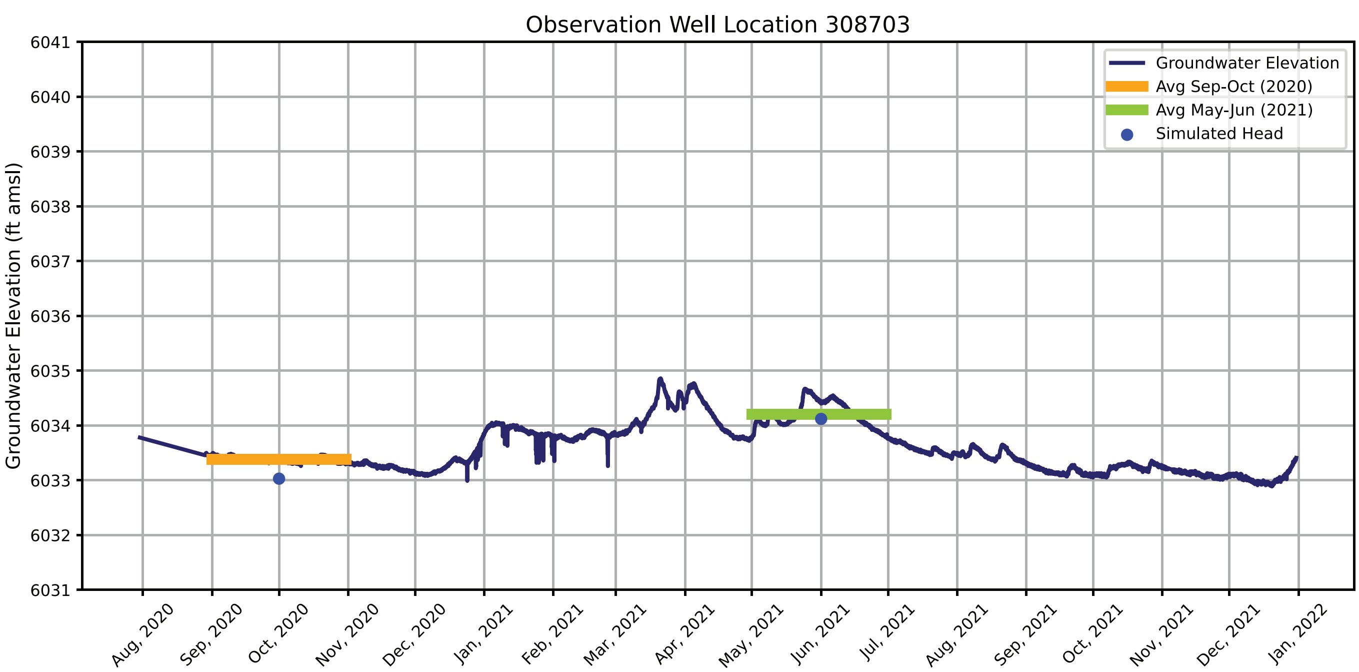

Observation Well Location 308703
Groundwater Elevation
Avg Sep-Oct (2020)
Avg May-Jun (2021)
Simulated Head
Groundwater Elevation (ft amsl)
6041
6040
6039
6038
6037
6036
6035
6034
6033
6032
6031
Aug, 2020
Sep, 2020
Oct, 2020
Nov, 2020
Dec, 2020
Jan, 2021
Feb, 2021
Mar, 2021
Apr, 2021
May, 2021
Jun, 2021
Jul, 2021
Aug, 2021
Sep, 2021
Oct, 2021
Nov, 2021
Dec, 2021
Jan, 2022

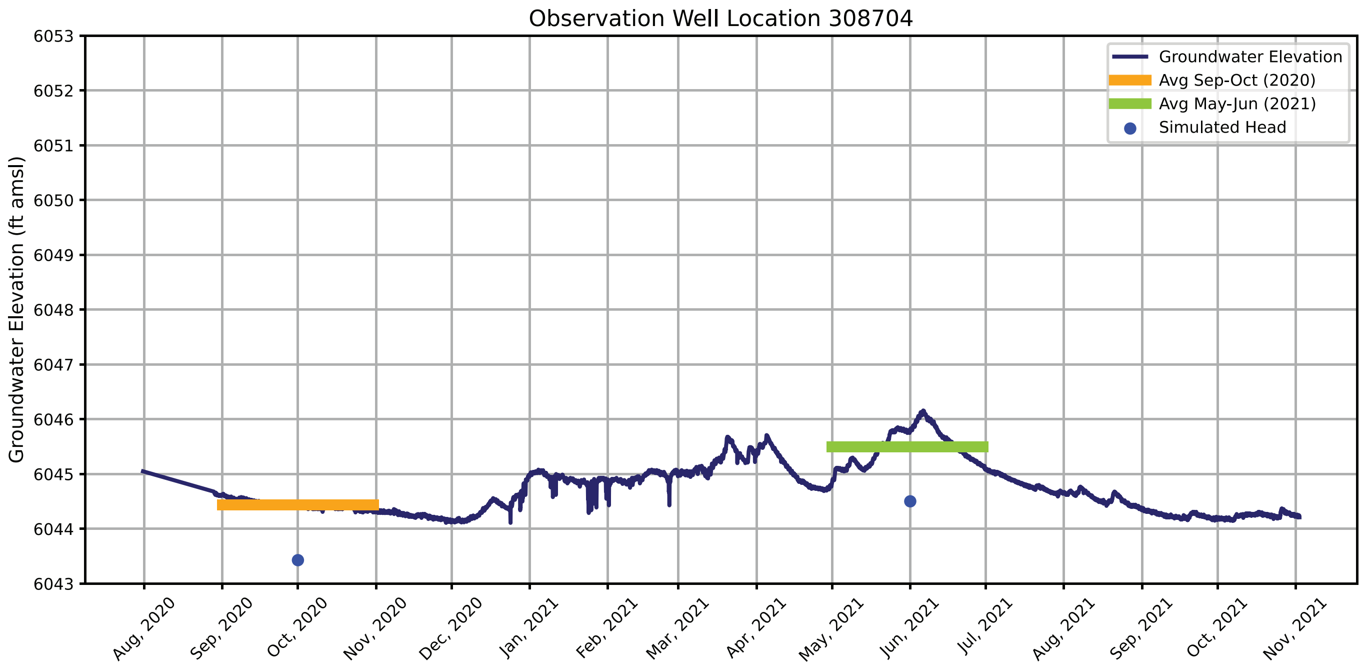
Observation Well Location 308704
Groundwater Elevation
Avg Sep-Oct (2020)
Avg May-Jun (2021)
Simulated Head
Groundwater Elevation (ft amsl)
6053
6052
6051
6050
6049
6048
6047
6046
6045
6044
6043
Aug, 2020
Sep, 2020
Oct, 2020
Nov, 2020
Dec, 2020
Jan, 2021
Feb, 2021
Mar, 2021
Apr, 2021
May, 2021
Jun, 2021
Jul, 2021
Aug, 2021
Sep, 2021
Oct, 2021
Nov, 2021

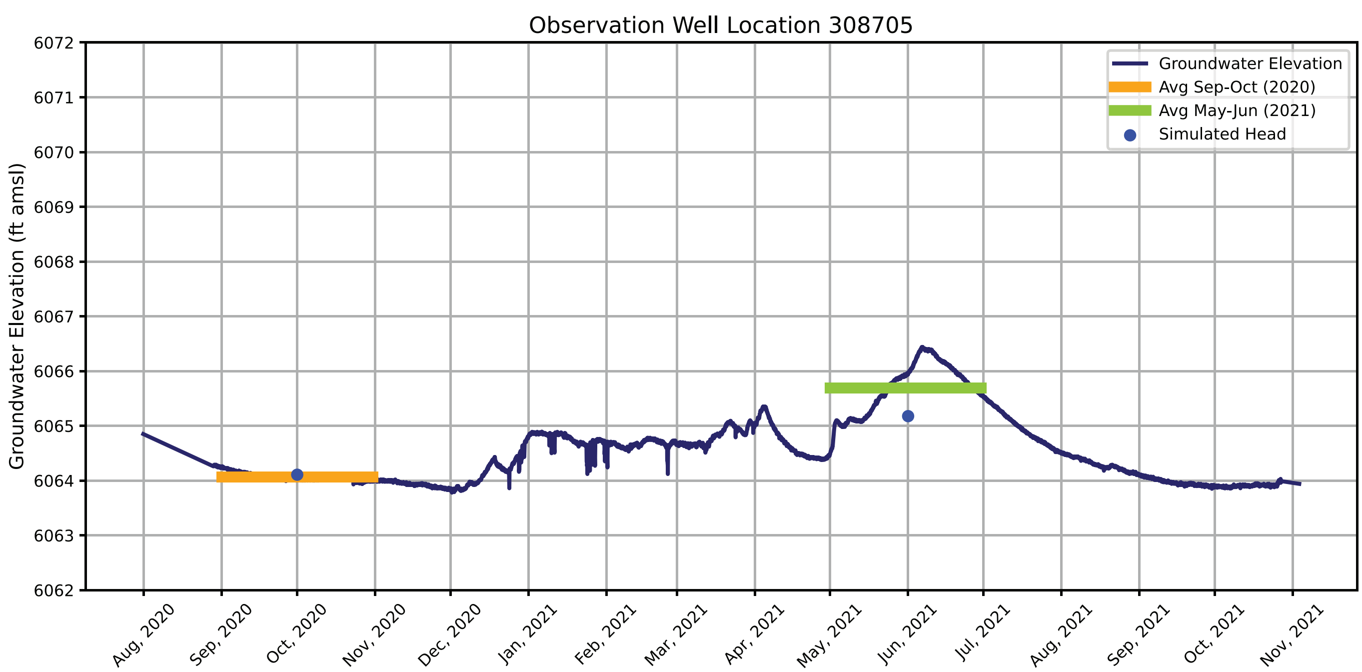
Observation Well Location 308705
Groundwater Elevation
Avg Sep-Oct (2020)
Avg May-Jun (2021)
Simulated Head
Groundwater Elevation (ft amsl)
6072
6071
6070
6069
6068
6067
6066
6065
6064
6063
6062
Aug, 2020
Sep, 2020
Oct, 2020
Nov, 2020
Dec, 2020
Jan, 2021
Feb, 2021
Mar, 2021
Apr, 2021
May, 2021
Jun, 2021
Jul, 2021
Aug, 2021
Sep, 2021
Oct, 2021
Nov, 2021

Table B-1. Simulated vs. observed water levels in the low- and high-flow models.

			Low-Flow Model			High-Flow Model		
GWIC ID	Latitude	Longitude	Observed head (ft)	Simulated head (ft)	Residual (ft)	Observed head (ft)	Simulated head (ft)	Residual (ft)
104541	45.2257168	-111.245399	6,096.03	6,096.91	-0.88	6,099.00	6,097.64	1.36
104549	45.2293047	-111.253528	6,083.27	6,082.52	0.74	6,086.81	6,083.74	3.07
133410	45.249914	-111.253238	6,024.87	6,024.70	0.17	6,026.32	6,026.09	0.23
133571	45.2487358	-111.251668	6,027.90	6,027.06	0.84	6,028.80	6,028.48	0.32
182784	45.2419955	-111.251351	6,043.72	6,042.75	0.96	6,044.65	6,043.88	0.77
189147	45.2235738	-111.250432	6,096.08	6,095.65	0.43	6,097.65	6,096.65	1.00
220481	45.241358	-111.251736	6,045.08	6,044.18	0.91	6,046.07	6,045.31	0.76
222627	45.2568749	-111.253782	6,008.58	6,006.54	2.04	6,009.65	6,007.83	1.82
235887	45.2275716	-111.253227	6,085.13	6,087.39	-2.26	6,088.72	6,088.39	0.33
246433	45.2491043	-111.258242	6,062.70	6,062.68	0.02	6,063.11	6,063.13	-0.02
257256	45.2395629	-111.253974	6,058.30	6,056.21	2.10	6,058.58	6,057.44	1.14
303694	45.2442873	-111.251238	6,036.93	6,036.92	0.00	6,037.92	6,038.03	-0.10
308526	45.2317942	-111.245026	6,068.90	6,070.40	-1.51	6,070.03	6,071.39	-1.36
308527	45.2361621	-111.246221	6,058.70	6,058.68	0.02	6,059.35	6,059.73	-0.38
308528	45.2418238	-111.2467	6,042.37	6,043.43	-1.06	6,043.61	6,044.59	-0.98
308530	45.2454643	-111.246598	6,033.83	6,033.10	0.73	6,035.08	6,034.17	0.91
308532	45.242294	-111.244157	6,050.15	6,046.97	3.18	6,050.49	6,048.37	2.12
308545	45.2362309	-111.242057	6,060.77	6,061.11	-0.34	6,060.77	6,062.16	-1.39
308558	45.2317656	-111.242583	6,072.57	6,072.45	0.11	6,072.64	6,073.20	-0.55
308703	45.2459457	-111.250297	6,033.38	6,033.03	0.35	6,034.20	6,034.12	0.08
308704	45.2415072	-111.250349	6,044.44	6,043.43	1.01	6,045.50	6,044.50	1.00
308705	45.2343184	-111.249754	6,064.06	6,064.11	-0.04	6,065.69	6,065.18	0.52